Development of a novel process for scalable production of baijiu-like alcoholic beverages

by

Thomas William Weiss

B.A., Montana State University, 2019

AN ABSTRACT OF A DISSERTATION

submitted in partial fulfillment of the
requirements for the degree

DOCTOR OF PHILOSOPHY

Carl and Melinda Helwig Department of Biological and Agricultural Engineering
Carl R. Ice College of Engineering

KANSAS STATE UNIVERSITY
Manhattan, Kansas

2026

Abstract

Baijiu, the traditional Chinese distilled spirit, owes its complex flavor to solid-state fermentation in which qu starters, earthen pit mud, and decades-old microbial communities act together in a single, poorly controlled environment. This dissertation proposes that baijiu production is better understood as a series of enrichment stages, each selecting for a distinct metabolic function: hydrolysis, primary fermentation, chain elongation, esterification, and maturation. On this view, the characteristic chemistry of baijiu could be reproduced in a scalable liquid-state process by recreating those selective conditions in sequence. A review of the traditional process (Chapter 1) develops this framework, and the remaining chapters examine its stages experimentally.

The hydrolysis and primary-fermentation stages were first characterized for US grains. Three US sorghum varieties fermented with four commercial yeasts gave alcohol yields of 80.9–90.8%. Waxy sorghum performed best, high-tannin red sorghum performed worst, and Ethanol Red gave the highest average yield, although the yeast effect was not statistically significant (Chapter 2). Among four maize varieties, blue maize gave the highest alcohol concentration (12.4%, v/v), and GR-2 was the most efficient yeast (Chapter 3). In both grains, ease of starch swelling and gelatinization was the property most closely linked to conversion efficiency. Maize variety, yeast strain, and their interaction significantly shaped the volatile ester profile of the spirits. Building on this, a low-energy hydrolysis stage was developed that combines partial starch swelling below the gelatinization temperature with granular starch hydrolyzing enzymes (Chapter 4). Swelling waxy sorghum at 70 °C for 30 min gave the highest ethanol concentration (12.02%, v/v) and yield (92.74%), statistically comparable to conventional 95 °C liquefaction without the high-temperature cooking step. It also produced distillers' grains proteins that remained highly digestible (about 85%) and were markedly lighter in color.

To recreate the chain-elongation function of baijiu pit mud in liquid culture, bovine rumen fluid was adaptively enriched on ethanol, lactate, or glucose (Chapter 5). The productive lineages were dominated by *Clostridium kluyveri*. An ethanol-fed consortium sustained hexanoate production in bioreactors and reached 4.6 g/L hexanoic acid, the precursor of ethyl hexanoate, the key ester of strong-aroma baijiu. Finally, maturation was examined by aging five commercial baijiu styles in small oak barrels under steady and fluctuating conditions (Chapter 6). Oak aging increased compound richness in every baijiu and produced bourbon-like color. However, it did not make the spirits converge chemically with bourbon. Liquor type, set by fermentation, was the dominant determinant of aged composition, and compound volatility acted as a selective filter during aging. Only feng-aroma Xifeng showed net ester synthesis during aging.

Together, these results show that the functional stages of baijiu production can be separated, studied, and engineered individually in liquid state, and that the chemistry established in each stage constrains the outcome of the next. The work provides a foundation for scalable, controllable production of baijiu-style spirits from US grains, together with higher-value coproducts and new product concepts such as oak-aged baijiu.

Development of a novel process for scalable production of baijiu-like alcoholic beverages

by

Thomas William Weiss

B.A., Montana State University, 2019

A DISSERTATION

submitted in partial fulfillment of the
requirements for the degree

DOCTOR OF PHILOSOPHY

Carl and Melinda Helwig Department of Biological and Agricultural Engineering
Carl R. Ice College of Engineering

KANSAS STATE UNIVERSITY
Manhattan, Kansas

2026

Approved by:

Co-Major Professor
Donghai Wang

Approved by:

Co-Major Professor
Shawn Wu

Copyright

© Thomas William Weiss 2026.

Abstract

Baijiu, the traditional Chinese distilled spirit, owes its complex flavor to solid-state fermentation in which qu starters, earthen pit mud, and decades-old microbial communities act together in a single, poorly controlled environment. This dissertation proposes that baijiu production is better understood as a series of enrichment stages, each selecting for a distinct metabolic function: hydrolysis, primary fermentation, chain elongation, esterification, and maturation. On this view, the characteristic chemistry of baijiu could be reproduced in a scalable liquid-state process by recreating those selective conditions in sequence. A review of the traditional process (Chapter 1) develops this framework, and the remaining chapters examine its stages experimentally.

The hydrolysis and primary-fermentation stages were first characterized for US grains. Three US sorghum varieties fermented with four commercial yeasts gave alcohol yields of 80.9–90.8%. Waxy sorghum performed best, high-tannin red sorghum performed worst, and Ethanol Red gave the highest average yield, although the yeast effect was not statistically significant (Chapter 2). Among four maize varieties, blue maize gave the highest alcohol concentration (12.4%, v/v), and GR-2 was the most efficient yeast (Chapter 3). In both grains, ease of starch swelling and gelatinization was the property most closely linked to conversion efficiency. Maize variety, yeast strain, and their interaction significantly shaped the volatile ester profile of the spirits. Building on this, a low-energy hydrolysis stage was developed that combines partial starch swelling below the gelatinization temperature with granular starch hydrolyzing enzymes (Chapter 4). Swelling waxy sorghum at 70 °C for 30 min gave the highest ethanol concentration (12.02%, v/v) and yield (92.74%), statistically comparable to conventional 95 °C liquefaction without the high-temperature cooking step. It also produced distillers' grains proteins that remained highly digestible (about 85%) and were markedly lighter in color.

To recreate the chain-elongation function of baijiu pit mud in liquid culture, bovine rumen fluid was adaptively enriched on ethanol, lactate, or glucose (Chapter 5). The productive lineages were dominated by *Clostridium kluyveri*. An ethanol-fed consortium sustained hexanoate production in bioreactors and reached 4.6 g/L hexanoic acid, the precursor of ethyl hexanoate, the key ester of strong-aroma baijiu. Finally, maturation was examined by aging five commercial baijiu styles in small oak barrels under steady and fluctuating conditions (Chapter 6). Oak aging increased compound richness in every baijiu and produced bourbon-like color. However, it did not make the spirits converge chemically with bourbon. Liquor type, set by fermentation, was the dominant determinant of aged composition, and compound volatility acted as a selective filter during aging. Only feng-aroma Xifeng showed net ester synthesis during aging.

Together, these results show that the functional stages of baijiu production can be separated, studied, and engineered individually in liquid state, and that the chemistry established in each stage constrains the outcome of the next. The work provides a foundation for scalable, controllable production of baijiu-style spirits from US grains, together with higher-value coproducts and new product concepts such as oak-aged baijiu.

Table of Contents

List of Figures xiii

List of Tables xv

List of Nomenclature xvii

Acknowledgements xviii

1 Literature Review: Engineering a Liquid-State Fermentation Framework for Baijiu Production 1

1.1 Introduction 1

1.2 Active Flavor Compounds 3

1.3 The Traditional Process 6

1.4 Daqu 8

1.5 Pit Mud 10

1.6 Grain Fermentation 14

1.7 Distillation 15

1.8 Aging 16

1.9 Sequential Liquid-State Fermentation 19

1.10 Conclusions of the Review 21

1.11 Research Objectives and Dissertation Organization 22

2 Production of Distilled Spirits from Grain Sorghum through Liquid-State Fermentation 24

Chapter Overview 24

2.1 Introduction . . . 25
2.2 Materials and Methods . . . 26
2.2.1 Sorghum samples . . . 26
2.2.2 Chemical, physical, and thermal properties of grain sorghum . . . 27
2.2.3 Selection of yeast strains . . . 27
2.2.4 Liquefaction and simultaneous saccharification and fermentation . . . 28
2.2.5 Analytical methods . . . 29
2.2.6 Statistical analysis . . . 30
2.3 Results and Discussion . . . 30
2.3.1 Physical and chemical properties of grain sorghum . . . 30
2.3.2 Alcohol concentration and yield . . . 31
2.3.3 Fermentation byproducts . . . 34
2.3.4 Volatile compounds . . . 36
2.4 Conclusions . . . 38

3 Blue, Red, and White Maize as Sustainable Resources for Distilled Spirit Production 41
Chapter Overview . . . 41
3.1 Introduction . . . 42
3.2 Materials and Methods . . . 44
3.2.1 Maize samples . . . 44
3.2.2 Chemical, physical, and thermal properties of maize . . . 44
3.2.3 Selection of yeast strains . . . 45
3.2.4 Liquefaction and simultaneous saccharification and fermentation . . . 46
3.2.5 Analytical methods . . . 47
3.2.6 Statistical analysis . . . 47
3.3 Results and Discussion . . . 48
3.3.1 Physical and chemical properties of the maize varieties . . . 48
3.3.2 Alcohol concentration and yield . . . 49

3.3.3 Fermentation byproducts . . . 52
3.3.4 Volatile compounds . . . 53
3.4 Conclusions . . . 61

4 Granular Starch Hydrolyzing Enzymes and Partial Starch Swelling: Ethanol Yield and Distillers' Grains Protein Quality . . . 62
Chapter Overview . . . 62
4.1 Introduction . . . 63
4.2 Materials and Methods . . . 66
4.2.1 Materials . . . 66
4.2.2 Chemical, physical, and thermal properties of grain sorghum . . . 66
4.2.3 Conventional liquefaction and simultaneous saccharification and fermentation . . . 67
4.2.4 Fermentation using GSHE with partial starch swelling . . . 67
4.2.5 Ethanol concentration and yield . . . 68
4.2.6 Protein isolation from wet distillers' grains . . . 68
4.2.7 Protein digestibility . . . 69
4.2.8 Surface hydrophobicity . . . 69
4.2.9 SDS-PAGE . . . 70
4.2.10 Size-exclusion chromatography . . . 70
4.2.11 Color analysis . . . 71
4.2.12 Statistical analysis . . . 71
4.3 Results and Discussion . . . 71
4.3.1 Chemical composition, physical characteristics, and thermal properties of grain sorghum . . . 71
4.3.2 Effect of partial starch swelling on ethanol yield . . . 73
4.3.3 Protein purity, digestibility, and surface hydrophobicity . . . 74
4.3.4 Color . . . 78

4.3.5 Molecular weight distribution by SEC-HPLC . . . 79
4.3.6 SDS-PAGE . . . 80
4.4 Conclusions . . . 82

5 Enrichment of Rumen Fluid toward Chain Elongation Activity for Medium-Chain Fatty Acid Production . . . 85
Chapter Overview . . . 85
5.1 Introduction . . . 86
5.2 Materials and Methods . . . 95
5.2.1 Inoculum Collection and Preparation . . . 95
5.2.2 Media and Reagent Preparation . . . 96
5.2.3 Initial Substrate Enrichment . . . 96
5.2.4 Culture Validation . . . 98
5.2.5 Substrate Optimization . . . 98
5.2.6 HPLC . . . 99
5.2.7 Sibling-Referenced Carbon and Electron Balances . . . 99
5.2.8 Sequencing and Bioinformatic Analysis . . . 99
5.3 Results and Discussion . . . 101
5.3.1 Adaptive Enrichment . . . 101
5.3.2 Lactic Acid Derived Cultures . . . 104
5.3.3 Glucose Derived Culture . . . 110
5.3.4 Ethanol Derived Culture . . . 111
5.3.5 Bottle to Reactor Results and Implications . . . 113
5.3.6 Substrate Optimization . . . 114
5.4 Conclusion . . . 120

6 Small-Barrel Oak Aging of Baijiu: Toward a Chinese-Style Whiskey . . . 122
Chapter Overview . . . 122

6.1 Introduction . . . 123
6.2 Materials and Methods . . . 126
6.2.1 Selection of Chinese baijiu . . . 126
6.2.2 Alcohol content . . . 128
6.2.3 Barrel aging conditions and sampling . . . 128
6.2.4 Volatile compounds and flavor analysis . . . 128
6.2.5 Color analysis . . . 129
6.2.6 Statistical analysis . . . 129
6.3 Results and Discussion . . . 130
6.3.1 Comparison with traditional bourbon . . . 130
6.3.2 Flavor compound diversity and concentration . . . 133
6.3.3 Compound volatility and aging . . . 136
6.3.4 Flavor chemistry and aging . . . 139
6.3.5 Comparison of barrel-aged baijiu with bourbon . . . 141
6.3.6 Mass loss . . . 143
6.3.7 Color . . . 145
6.4 Conclusions . . . 146

7 Conclusions and Future Work . . . 149
7.1 Summary of Findings . . . 149
7.2 Synthesis . . . 151
7.3 Recommendations for Future Work . . . 152
7.4 Concluding Remarks . . . 153

Bibliography . . . 154

List of Figures

1.1 The traditional method of baijiu production selects for specific metabolic functions crucial to the nature of the final product 7

1.2 Proposed liquid process for baijiu production where each function is strung into a sequence of events rather than occurring simultaneously. 19

2.1 Rapid Visco Analyser pasting profiles of the three sorghum flours. 33

2.2 Effects of yeast strain and sorghum variety on glycerol formation 35

2.3 Effects of yeast strain and sorghum variety on lactic acid formation 37

2.4 TIC peak areas of the major volatile compounds identified in the fermented sorghum broths 38

3.1 Rapid Visco Analyser pasting profiles of the four maize flours. 52

3.2 Effects of yeast strain and maize variety on glycerol and lactic acid in maize spirit distillates. 54

3.3 Mean concentration of volatile flavor compounds by maize variety and by yeast strain 59

3.4 Cluster analysis of yeast, maize, and flavor compound interactions 60

4.1 SEC-HPLC chromatograms of sorghum proteins extracted from wet distillers' grains 81

4.2 SDS-PAGE of kafirins extracted from wet distillers' grains 83

5.1 Overview of the rumen fluid enrichment scheme 87

5.2 HPLC results for the serum-bottle enrichments 103

5.3 Bray–Curtis PCoA of community trajectories 105

5.4 Community composition of serum bottle enrichments. 107
5.5 Community composition of T4 serum bottles and validation reactors 109
5.6 Substrate use and products in the validation reactors 112
5.7 Community composition of the substrate-dose reactors 117
5.8 Substrate use and products in the substrate-optimization reactors 118

6.1 Concentrations of major compound classes in unaged and aged samples . . . 131
6.2 Gain and loss of compound classes during aging 135
6.3 Normalized compound concentrations across samples 142
6.4 Mass loss during barrel aging in the validation trial 144

List of Tables

2.1 Commercial yeast strains used for spirit production in this chapter. 28

2.2 Physical properties of the grain sorghum varieties. 31

2.3 Chemical composition of the grain sorghum varieties. 31

2.4 Effect of sorghum variety and yeast strain on alcohol concentration and alcohol yield. 32

2.5 Analysis of variance for the effects of sorghum variety, yeast strain, and their interaction on final ethanol concentration and ethanol yield. 32

2.6 ANOVA of the effects of sorghum variety and yeast strain on volatile compound peak areas 39

2.7 Tukey's test for the effect of yeast strain on volatile compound peak areas . . 39

3.1 Commercial yeast strains used for maize spirit production. 46

3.2 Physical properties of the maize varieties. 48

3.3 Chemical composition of the maize varieties. 49

3.4 Effect of maize variety and yeast strain on alcohol concentration and alcohol yield. 50

3.5 Analysis of variance for the effects of maize variety, yeast strain, and their interaction on final ethanol concentration and ethanol yield. 50

3.6 Starch gelatinization properties of the maize varieties measured by differential scanning calorimetry. 51

3.7 Fermentation completion (%) over time as affected by yeast strain and maize variety. 52

3.8 Volatile compounds in spirits from white and yellow maize 56

3.9 Volatile compounds in spirits from red and blue maize 57
3.10 ANOVA of the effects of maize variety and yeast strain on volatile compounds 58

4.1 Chemical composition, physical characteristics, and thermal properties of the waxy and normal sorghums 72
4.2 Ethanol concentration and yield after 72 h under conventional and GSHE processing with partial starch swelling. 74
4.3 Properties of proteins extracted from sorghum flour and wet distillers' grains (WDG). 75
4.4 Color of proteins extracted from sorghum flour and wet distillers' grains (WDG). 78

5.1 Weekly feed added at each enrichment transfer 97
5.2 Cumulative theoretical concentrations in the validation reactors 98
5.3 Shannon diversity index after enrichment. 102
5.4 Final product concentrations and characteristics of the initial enrichment cultures 106

6.1 Baijiu brands, aroma types, sensory characteristics, and sample codes 127
6.2 Richness and Shannon diversity of volatile compounds in the unaged and aged samples. 130
6.3 Total concentration and richness of flavor compounds in unaged and aged samples 132
6.4 PERMANOVA and PERMDISP results for volatile composition (Aitchison distance). 133
6.5 Compounds responding significantly to experimental factors (LME) 137

Nomenclature

Abbreviation	Definition
AUG	Amyloglucosidase units
CLR	Centered log-ratio (transformation)
DADY	Red Star Distillers Active Dry Yeast
db	Dry basis
DDG(S)	Distillers' dried grains (with solubles)
DG	Distillers' grains
DSC	Differential scanning calorimetry
FDR	False discovery rate
GAU	Glucoamylase units
GC–MS	Gas chromatography–mass spectrometry
GSHE	Granular starch hydrolyzing enzyme
HPLC	High-performance liquid chromatography
HS-SPME	Headspace solid-phase microextraction
KNU	Kilo Novo units (α-amylase activity)
LME	Linear mixed-effects (model)
LR	Likelihood ratio
LSD	Least significant difference
MCFA	Medium-chain fatty acid
NS / WS	Normal sorghum / waxy sorghum
OD_{600}	Optical density at 600 nm
PCoA	Principal coordinates analysis
PERMANOVA	Permutational multivariate analysis of variance
PERMDISP	Permutational analysis of multivariate dispersions
rBOX	Reverse β-oxidation
RH	Relative humidity
RID	Refractive index detector
RVA	Rapid Visco Analyser
SDS-PAGE	Sodium dodecyl sulfate–polyacrylamide gel electrophoresis
SEC-HPLC	Size-exclusion high-performance liquid chromatography
SKCS	Single Kernel Characterization System
SSF	Simultaneous saccharification and fermentation
TIC	Total ion current
WDG	Wet distillers' grains
L^*, a^*, b^*	CIELAB lightness, red–green, and yellow–blue color coordinates
H'	Shannon diversity index

Acknowledgments

Oh Unbegotten Father, Oh Lord Jesus Christ Son of God, Oh Holy Spirit The Giver of Life, I can do nothing without you, may my work and life bring glory and honor to your kingdom.

Amen

I would also like to thank my committee for their support and advice.

In particular I would like to thank **Dr. Yonghui Li**, *Professor of Grain and Food Science*, for his advice, support, letting me use his equipment, and most of all his encouragement and cheer. His help and expertise was vital for Chapter 4 in particular where he provided the Size-exclusion chromatography, Color analysis, SDS-PAGE, Surface hydrophobicity, and Digestibility data and analysis. Furthermore, he provided the GCMS data that made the flavor compound analysis from Chapters 2, 3, and 6 possible.

I would also like to thank **Dr. Mark Wilkins**, *Head for the Carl and Melinda Helwig Department of Biological and Agricultural Engineering*, for his support, his advice, his advocacy, and for being present to help solve everyday problems. I think I speak for the entire department when I say we could not ask for a better Department Head.

I want to thank both **Dr. Donghai Wang**, *Professor of Biological and Agricultural Engineering*, and **Dr. Xiaorong (Shawn) Wu**, *USDA Research Chemist and Adjunct Faculty for the Department of Grain and Food Science*, for their advice, support, advocacy, and patients. They guided me through the research done for Chapters 2, 3, 4 and 6 as well as advising me for Chapter 5. Dr. Wang provided the lab space, equipment, and initial concepts for this dissertation. Dr. Wu was vital for securing supplies and funding as well as his insightful advice, critiques, and encouragements.

I would not be here without the endless love and support of my family, my father **Scott**, my mother **Kimberly**, and my brother **Taylor**. They put me through school and raised me to be who I am today.

Finally, I must thank my wife **Dori** for her endless love, support, and especially her patients. She gives me a reason to try my hardest.

Chapter 1

Literature Review: Engineering a Liquid-State Fermentation Framework for Baijiu Production

This chapter is based on the review manuscript "From Microbial Communities to Selective Environments: Engineering a Liquid-State Fermentation Framework for Baijiu Production," co-authored by Thomas Weiss, Shan Hong, Yonghui Li, Xiaorong Wu, Mark Wilkins, and Donghai Wang. It has been edited to serve as the introduction and literature review for this dissertation.

1.1 Introduction

Baijiu is a category of Chinese distilled spirits with one of the longest continuous production histories of any fermented beverage, yet its underlying process logic remains poorly understood from an engineering standpoint [1]. The dominant framework in baijiu research treats fermentation outcomes as a product of specific microbial communities; cataloging which organisms are present and which flavor compounds they produce. While this body of work has substantially characterized the chemistry of baijiu, it offers limited guidance for process design, scale-up, or rational improvement of production systems. We propose a complementary framework: baijiu production can be understood not only as a fermentation but as

a staged enrichment process. Under this view, the materials and procedural conditions of each production stage (qu preparation, pit fermentation, and grain fermentation) function as successive environmental filters. Each stage selects for a distinct set of metabolic functions by imposing specific constraints on temperature, oxygen availability, substrate composition, and redox chemistry. The characteristic microbial communities of baijiu are not fixed biological inputs but emergent outcomes of these selection conditions. This distinction has immediate engineering consequences: it means the functional chemistry of baijiu production can, in principle, be reproduced by recreating the selective conditions, without replicating the traditional solid-state format.

Like other spirits, examples are often defined by the region of China in which they are produced. For instance, luzhoulaojiao-jiu comes from Luzhou prefecture in Sichuan, China [2]. Baijiu varieties are also characterized by the specific compounds that define their flavor, aroma, and mouthfeel. For example, luzhoulaojiao is characterized by high concentrations of ethyl hexanoate and ethyl butanoate as well as a variety of other esters, while erguotou is characterized by ethyl lactate and ethyl acetate, and Maotai is characterized by a complex mix of esters and aromatics [1, 3]. These compounds result from the production process and materials used. Most representative examples of baijiu are produced by solid-state fermentation, and all use a type of microbial starter and hydrolytic enzyme source called Qu, similar to the Koji used to make shochu [2, 3]. While the microbial communities, production methods, and resulting flavor compounds are well characterized, less attention has been paid to why traditional baijiu production consistently generates these outcomes [4]. We develop this enrichment argument across the full production pathway. We first examine daqu manufacture, where spatial and thermal gradients generate distinct hydrolytic, fermentative, and esterifying niches. We then turn to pit mud, where strictly anaerobic conditions favor chain-elongating consortia that convert fermentation intermediates into the medium-chain fatty acids underlying strong-aroma baijiu's signature ethyl esters. We next consider grain fermentation, which integrates these functions into a working community, and distillation and aging, which act as further selective stages governing which compounds are recovered and how they mature. Building on this framework, we argue that the functional chemistry of

baijiu can in principle be reproduced in liquid-state fermentation by recreating its sequence of selective environments rather than its solid-state format or microbial inventory. Drawing on a precedent from Grand Arôme rum production, we propose a staged liquid-state fermentation scheme in which discrete reactors replace the spatial heterogeneity of traditional solid-state systems, each reactor optimized to enrich a single metabolic function — hydrolysis, primary fermentation, chain elongation, or esterification — in sequence. This reframing shifts the engineering objective from replicating a traditional microbial ecosystem to designing the environmental conditions that generate it, offering a path toward scalable, controllable baijiu-characteristic fermentation.

1.2 Active Flavor Compounds

While potent brands of baijiu such as Laobaigan baijiu or Maotai baijiu have been documented to contain several hundred potentially flavor-active compounds, only a few have been identified as vital to the quality and flavor of the product. Zhu et al. [5] found that out of the 528 flavor-active compounds in baijiu, 148 were esters, with the most abundant being ethyl hexanoate and ethyl butyrate, which contribute fruity, sweet, and floral aromas. They also found that while shorter-chain alcohols, such as n-butanol, contributed rancid and chemical aromas, medium-chain alcohols, such as n-octanol and n-hexanol, contributed floral aromas. Ma et al. [6] found that out of the 92 aroma-active compounds in Xi baijiu, ethyl 3-methylbutanoate, ethyl hexanoate, ethyl octanoate, and β-damascenone all had very high aroma intensity. Duan et al. [7] found that out of the 66 aroma-active compounds in Langjiu baijiu, ethyl butyrate, ethyl octanoate, ethyl 3-phenylpropionate, methyl 2-methyl-3-furyl disulfide, dimethyl trisulfide, and 2-ethyl-6-methylpyrazine were all detectable by all panelists in an omission experiment. Fan et al. [8] found that out of the 414 volatile compounds in Laobaigan baijiu, ethyl octanoate, ethyl pentanoate, ethyl hexanoate, ethyl butanoate, ethyl lactate, ethyl acetate, hexanoic acid, 3-methylbutanal, and 4-ethylguaiacol were identified as the nine key aroma compounds.

The conclusions we may draw from these studies are clear: among the myriad compounds

that contribute to the various unique varieties of baijiu, short- to medium-chain ethyl esters are among the most important. This distinguishes baijiu from other spirits such as whiskey, which contain only low concentrations of these esters and where wood-derived compounds such as lactones play a comparatively larger role [9]. Strong aroma baijiu, such as Luzhou Laojiao baijiu, has a far higher concentration of ethyl hexanoate, which distinguishes it from other types of baijiu. Ao et al. [10] found a correlation between higher concentrations of ethyl hexanoate and higher grades of raw strong-flavor baijiu, and conversely lower concentrations of ethyl acetate, ethyl butyrate, and ethyl lactate. All grades of strong-flavor baijiu contained 2–2.5 g/L ethyl hexanoate, 1–1.5 g/L ethyl acetate and ethyl lactate, and $<$1 g/L ethyl butanoate [10]. Meanwhile, whiskey and other types of baijiu typically have medium-chain ester levels measured in tens to hundreds of mg/L, with some Langjiu samples containing concentrations as high as 1.2 g/L of ethyl hexanoate [9, 11]. Understanding these key flavor compounds raises an important question: how are these esters produced during fermentation? While liquors such as brandy, wine and other spirits sourced from fruit have high ester contents due to the materials from which they are made, baijiu and other grain-based spirits do not benefit from these readily available compounds [12, 13].

The production of ethyl esters requires two precursor components: excess ethanol and a carboxylic acid. In the case of baijiu, that carboxylic acid is typically a short- to medium-chain fatty acid. Once present, these two compounds may be readily esterified by any number of means, especially by esterases produced by yeast. Two studies by Saerens et al. [14, 15] demonstrate that the addition of medium-chain fatty acids to wort results in esterification with ethanol and that this esterification may be affected by multiple parameters. Significantly, they found that ester production was repressed by the presence of long-chain saturated fatty acids and amplified by the addition of octanoic acid.

Short-chain fatty acids (SCFA) are primarily the product of primary fermentation and are commonly produced in multi-member fermentations such as in kombucha, sauerkraut, sourdough bread, baijiu, and various beers and wines. However, medium-chain fatty acids can only be produced via the following three methods: partial degradation of longer-chain fatty acids via an interrupted β-oxidation cycle, interruption of the fatty acid synthase complex,

or by chain elongation via reverse β-oxidation (rBox) of short-chain acids or alcohols [16].

Chain elongation is considered the most energy-efficient of these routes because reverse β-oxidation uses acetyl-CoA directly as the two-carbon donor, avoiding the ATP-dependent formation of malonyl-CoA required by fatty acid synthesis [16]. This is also considered the most likely source of medium-chain fatty acids produced during baijiu solid-state fermentation, particularly in strong aroma baijiu where pit mud plays a significant role in flavor development. Gao et al. [17] demonstrated that while long-chain fatty acids and esters as well as short-chain fatty acids and esters are produced in the grain directly, almost all of the medium-chain fatty acids are produced in the pit mud during strong-flavor baijiu fermentation. They also found that the pit mud was dominated by *Caproiciproducens*, which is well characterized for its ability to produce hexanoic acid directly from glucose and other substrates via rBox [17–19] Meanwhile, Chai et al. [20] found that as pit mud ages, the diversity within the pit mud decreases, the abundance of *Caproiciproducens* and *Methanosarcina* increases, and the resulting baijiu quality increases. Both Gao et al. [17], Chai et al. [20] found a very high correlation between *Caproiciproducens* and all medium-chain fatty acid ethyl esters [17, 20]. These conclusions are confirmed by the work of Xu et al. [21] who recombined various organisms to recreate strong aroma fermentation and found that the addition of chain-elongating Clostridia such as *Clostridium butyricum* or *Clostridium kluyveri* in addition to *Caproiciproducens sp.* were essential to the production of medium-chain fatty acid ethyl esters. This microbial synergy ultimately explains why strong aroma baijiu achieves its distinctively high concentrations of medium-chain ethyl esters, the compounds responsible for its characteristic flavor profile. From an enrichment perspective, these findings imply that the production of key flavor compounds depends less on the introduction of specific microorganisms and more on the establishment of environmental conditions that favor fermentative, chain-elongating, and esterifying metabolisms. The challenge therefore becomes understanding how traditional production methods consistently generate and maintain these functional communities.

1.3 The Traditional Process

The traditional baijiu production process has been thoroughly reviewed by Zheng and Han [1] as well as by Sun et al. [22] However, we will describe it in brief as well as some variations which result in the production of different brands (Figure 1.1). These differences are illustrative of how differences in the production process result in flavor variation in the final product. The process begins with the production of a starter called Qu or Mold. This stage accounts for the greatest variation in process variables and is thus the most well studied. Daqu, which will be discussed in greater detail in the next section, is the most common type and utilizes large bricks of packed, low moisture wheat dough which can be supplemented with other grains such as barley or peas. These bricks are stacked in a Qu-house which develops mesophilic to thermophilic temperatures over the course of 3 – 6 months depending on the type of daqu being produced and may or may not contain a 'ripening' stage at cooler temperatures for extended periods of time. This type of daqu is used in Strong, Light, Sauce, and other aromas and each has specific material and temperature requirements for the daqu. This is because changes in the daqu manufacturing process have a large effect on the type and quality of the resulting baijiu. Other types of qu include Xiaoqu which is produced using rice balls and sometimes herbs [23]. This type of qu is typically used in feng and rice aroma baijiu. Finally, the starter fuqu is produced from piling wheat bran and often supplementing it with pure cultures of organisms such as *Aspergillus oryzae*, *Bacillus*, or *Wickerhamomyces* [24]. This type of qu is used in Erguotou and sesame aroma baijiu.

After the qu is finished it is ground and stored as a powder for future use. The qu will be mixed with steeped or steamed grain and sometimes a material such as rice hulls or straw is added for structure. Most of this grain will be sorghum [8, 11]. Corn is used in some lower quality types of baijiu and can account for up to 50% of material in some cases [25]. Whether this grain is ground or not is dependent on the variety of baijiu being produced, however, it is typically kept whole. This mix is buried in a fired clay or mud pit and sealed with clay [26]. Often, a given process involves multiple stages of fermentation, distillation, and recycling of the distilled grain. In some cases, it also includes a stacking phase, during which the

grains are piled to allow alcohol-producing microorganisms that prefer cooler temperatures to colonize before pit fermentation resumes. This step is particularly important when using high temperature daqu, as the thermophilic conditions used during its production are not favorable for ethanol producing microbes [27]. After pit fermentation takes place, the grain is mixed with more rice hulls or other bran and loaded into a type of pot-still similar to a sealed steam basket. The water from the pit is placed under the grain in a boiling pan and the vapors pass through the grain, pulling out the volatiles.

The raw baijiu must then be aged to "smooth it out". This may occur in a variety of containers from porcelain jars to more oxygen permeable clay to large and continually renewed vessels of paper [28]. This occurs over a period of time ranging from two years to multiple decades. Upon the completion of aging, the baijiu must then be blended for consistency, checked for final quality and then bottled for sale [29].

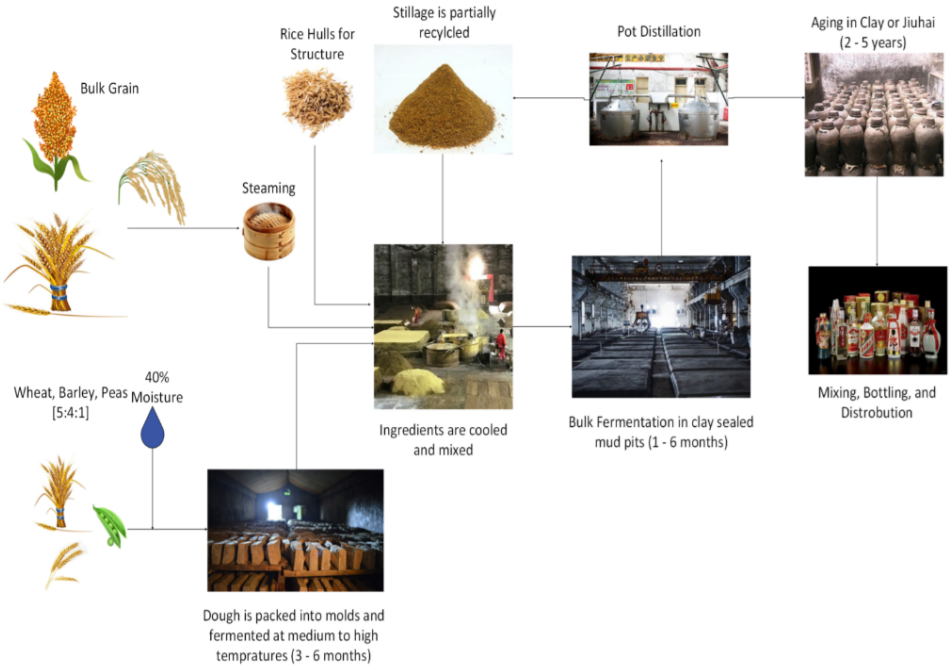


Figure 1.1: The traditional method of baijiu production selects for specific metabolic functions crucial to the nature of the final product

1.4 Daqu

The first major enrichment stage in baijiu production is the manufacture of Qu, a starter culture used throughout Chinese fermentation industries. Daqu is a type of wheat based qu packed into a brick and fermented at mesophilic to thermophilic temperatures and is almost exclusively used for the production of baijiu. Daqu begins with a 40% (dry basis) hydrated dough which may be supplemented with 40% barley flour and 10% pea flour for strong aroma daqu [30]. For Sauce Aroma baijiu the daqu consists of 85 – 90% wheat and 10 – 15% sorghum flour [31]. Both of these types of daqu operate at low thermophilic temperatures of 50 – 60 °C while higher thermophilic temperatures of 60 - 70 °C are used for the pure wheat daqu used to make Maotai [32]. These bricks range in size from 2420 cm^3 for light aroma daqu to 5531 cm^3 for Maotai [33].

The daqu fermentation process is partially aerobic and the portion of the substrate which is exposed to oxygen is controlled which makes it a unique process. Typically, solid-state fermentation is difficult to model and control due to uneven distribution of heat, moisture, and oxygen [34]. However, daqu is shaped into controlled sizes and stacked in insulated rooms called qu-rooms in such a way as to control air flow. This allows for greater control of heat and air distribution by controlling the size of the qu and the way in which they are stacked. A stack of daqu will only have a variation of about 5 °C between the center and the exterior. However, there are significant differences between bricks from the center and the exterior of the stack. The center comprises of black and red daqu which is rich in flavor compounds while the exterior is white and is richer in enzymatic activity and yellow is between them with properties also being middling [35]. The saccharification power of medium temperature daqu is about 700 U/g and high temperature daqu is about 200 U/g [36]. However, this differs amongst the positions in the qu pile. For example, in high temperature daqu, white daqu has the highest protease activity and liquefaction capacity while red daqu has the highest esterification activity and black has the highest fermentation capacity [37]. This spatial differentiation is significant because it demonstrates that a single daqu stack contains multiple selective environments operating simultaneously. Rather than producing a uniform

microbial community, the temperature, oxygen, and moisture gradients generate distinct functional niches enriched for different enzymatic activities. In effect, the qu room functions as a distributed enrichment system capable of selecting for complementary metabolic functions within the same production batch. For both medium- and high-temperature daqu, alcohol acyltransferase (AAT) activity has been found to be the main contributor to ester synthesis, peaking at 10 days of daqu production at about 1200 U/g [38]. The esterification capacity of finished medium-temperature daqu has been reported as about 3.5 mg ethyl caproate synthesized per day per gram [38, 39].

The incubation temperature of daqu is not strictly controlled during the fermentation period and is governed by the bioheat produced by the bricks themselves. Temperature control is accomplished by the stacking regime, the qu-house, and brick size and is not uniform throughout the stack [40]. Meanwhile humidity has an inverse relationship to temperature, first falling then rising [41]. There is no existing consensus on the microbial succession of organisms. However, generally lactic acid bacteria and various yeasts dominate initially which trends towards filamentous fungi and thermophilic bacteria including lactic acid bacteria. However, several genera appear consistently including *Bacillus*, *Aspergillus*, *Rhizomucor*, *Weissella*, *Lactobacillus*, *Thermoactinomyces*, *Thermomyces*, *Kroppenstedtia*, *Pichia*, *Candida*, and *Saccharopolyspora* occurring regularly in various studies [39–44]. While these genera are consistently found in the daqu microcosm, it does not imply a core functional microbiome. Xu et al. [45] demonstrated that there are both positive and negative correlations among these organisms and that they contribute differently or negatively towards the desired outcome of baijiu, namely the production of ethyl hexanoate. Furthermore, it has been found that specific species and even strains contribute disproportionately to flavor development. Specifically, a strain of *Aspergillus niger* was found to catalyze esterification far more effectively than any other strain of the same species harvested from daqu, causing 85% of hexanoic acid to be converted to ethyl hexanoate under optimized conditions [45]. At first glance, the existence of such specialized strains appears to challenge an enrichment-based interpretation of fermentation. However, it may instead represent the long-term consequence of enrichment. Repeated cultivation under conditions favoring ester production can progres-

sively reduce stochastic community dynamics, enrich organisms possessing advantageous traits, and ultimately lead to the emergence of domesticated strains. Thus, microbial identity should not be disregarded; rather, microbial domestication and environmental selection should be viewed as complementary processes operating on different timescales. Environmental conditions initially select for desired functions, while prolonged maintenance of those conditions may eventually produce highly specialized organisms optimized for those functions.

1.5 Pit Mud

Rather than isolating organisms in pure culture, producers repeatedly apply environmental filters that favor desired traits while suppressing competing metabolisms. The resulting community is therefore an emergent property of the process rather than a fixed biological ingredient. The significance of this distinction extends beyond daqu itself. If daqu can be understood as an enrichment stage that selects for hydrolysis, fermentation, and esterification, then the subsequent fermentation and pit-mud environments may likewise be viewed as enrichment stages selecting for progressively more specialized metabolic functions. Under this framework, strong-aroma baijiu production emerges as a sequence of ecological enrichments culminating in the establishment of chain-elongating consortia responsible for medium-chain fatty acid production. Pit mud, thus, represents a second ecological reactor distinct from daqu. Whereas daqu primarily selects for hydrolytic, fermentative, and ester-producing functions under partially aerobic thermophilic conditions, pit mud selects for strictly anaerobic metabolisms capable of converting fermentation intermediates into medium-chain fatty acids. The transition from daqu to pit mud therefore represents a transition between enrichment stages, each favoring a different set of metabolic capabilities.

Medium-chain fatty acids such as hexanoic and octanoic acid are increasingly recognized as valuable biogenic platform molecules with applications spanning renewable chemicals, food fermentation, and flavor production. In distilled spirits and fermented foods, medium-chain fatty acids serve as critical precursors for ethyl esters that impart fruity, floral, and sweet

aroma characteristics [46]. Strong-aroma baijiu in particular is distinguished by exceptionally high concentrations of ethyl hexanoate, a compound strongly associated with product quality and sensory complexity [47, 48]. Unlike many Western distilled spirits, which rely primarily on barrel aging and thermal reactions for flavor development, strong-aroma baijiu derives much of its characteristic profile directly from microbial metabolism during fermentation [49, 50]. These metabolic activities occur in the fermentation vessel itself which acts as a microbial reservoir for the mutualistic and strictly anaerobic consortiums which produce these compounds [51]. These vessels are called mud pits and are large holes in the ground lined in red clay mud. During production, cooked grain is mixed with qu and buried in one of these mud pits where fermentation takes place [52]. The mud in these pits is extremely effective for the production of medium-chain fatty acids, however, they can take decades to centuries to sufficiently enrich [20].

The organisms in pit mud which significantly contribute to the production of flavor compounds in baijiu are commonly referred to as chain elongators [8, 17, 19, 20, 50] These organisms are capable of producing butyric, hexanoic, and octanoic acid, or longer carbon chains from hexose, lactate, ethanol and/or acetic acid via the reverse β-oxidation (rBox) pathway [20, 52]. The rBox pathway functions as an electron sink, consolidating short-chain fermentation products into longer-chain fatty acids while simultaneously preferentially altering environmental toxicity and redox balance. In each cycle, an electron donor such as ethanol is oxidized to acetyl-CoA, which condenses with an acyl-CoA primer (initially acetyl-CoA itself) to form a 3-ketoacyl-CoA. This intermediate is reduced, dehydrated, and reduced again to give an acyl-CoA two carbons longer, so that acetyl-CoA is extended to butyryl-CoA and then to hexanoyl-CoA. The cycle terminates when the acyl-CoA is converted to the free carboxylate by a CoA transferase or thioesterase and released from the cell [18]. The energetic yield of this reaction is dependent on the substrates, for example:

$$2\,\text{Ethanol} + \text{Acetic acid} \rightarrow n\text{-Caproic acid} + 2\,H_2O \qquad \Delta G = -79\ \text{kJ mol}^{-1} \tag{1.1}$$

whereas with hydrogen as the electron donor:

$$3\,\text{Acetic acid} + 4\,H_2 \rightarrow n\text{-Caproic acid} + 4\,H_2O \qquad \Delta G = -177\ \text{kJ mol}^{-1} \tag{1.2}$$

However, this metabolic strategy is in competition with methanogenesis, which supports a diverse community and thus forms more mutualistic relationships [53]. This is partially since methanogens can eliminate reduced carbon waste by allowing it to escape the environment as a gas and thus increasing the thermodynamic ceiling. To support this activity, various organisms will adapt to the presence of specific methanogens by tailoring their output to the preferred input of that methanogen [20]. Chain elongating bacteria also benefit from existing in a consortium, but these should be more limited [52, 54]. As an example, *Candidatus Geobacter eutrophica* can syntrophically transfer electrons to chain elongating organisms or methanogens which sink them into chain elongation or methanogenesis, thereby improving the efficiency of fermentation [55]. The importance of methanogens further illustrates that pit mud functions as an ecological selection system rather than a simple microbial reservoir. Methanogenesis, chain elongation, sulfate reduction, and other anaerobic processes compete for common substrates. The long-term physical and chemical conditions of the pit therefore determine which metabolic strategies are favored and ultimately which flavor compounds accumulate in the final product.

As stated above, chain elongating bacteria can utilize a wide variety of substrates including lactate, ethanol, butyrate, glucose and acetate [52, 54]. All benefit from the addition of acetate as a co-substrate [56] Among these organisms *Clostridium kluyveri* is among the best-characterized and most productive chain-elongating organisms, primarily consumes ethanol, and was found to be present in pit mud and bovine rumen fluid [57]. *Caproiciproducens galactitolivorans* is also present in rumen fluid and consumes hexose, fructose, lactate, or galactitol [19]. *Megasphaera elsdenii* is also known to consume both fructose, glucose, and sucrose and is present in pit mud and rumen fluid [58]. *Ruminococcaceae* is a rumen associated bacteria which performs chain elongation from lactic acid [59]. All of the above organisms thrive in neutral to mildly acidic pH and a 30 – 40 °C temperature range. Notably, these

substrate preferences provide a mechanistic explanation for why traditional pit fermentation consistently enriches chain elongators. The grain hydrolyzing and then fermenting in the pit produces the compounds that serve as preferred substrates for reverse β-oxidation. Thus, the preceding stages of baijiu production create the conditions necessary for the subsequent enrichment of chain-elongating consortia.

As with other functional microbial communities, chain-elongating communities can be enriched to adjust or improve production. Changing substrates, pH, or temperature changes the ratios of abundances of different organisms, bringing different syntrophic and mutualistic relationships to bear [60]. However, the potential of these cultures can only be realized if methanogenic activity is inhibited [61]. There are several ways to accomplish this. The first is to add 2-bromoethanesulfonic acid (BESA) or another brominated compound [62]. Another is adjusting pH, however, *Megasphaera sp.* is less tolerant of low pH than *Clostridium kluyveri* [63]. Therefore, while pH other than 7 is progressively inhibitory to acetoclastic methanogens it does not completely suppress them and can also suppress desired chain elongation activity [64]. The final method available to suppress methanogens is adding ferric iron (Fe III) [65]. The advantage of this final method is that ferric iron is beneficial to chain elongation since coupling reduced and oxidized iron can facilitate the reaction [66]. An ideal system would not have acetoclastic methanogens and need minimal inhibition of methanogenesis, which beneficially simplifies requirements and ingredient lists. There is an opportunity for fermentation systems capable of selectively producing high-value flavor compounds and other renewable chemicals directly from biomass-derived substrates. As modern fermentation industries favor liquid-state processing due to advantages in process control, scalability, and substrate utilization efficiency, there is growing interest in developing controllable microbial consortia capable of reproducing the functional chemistry traditionally associated with complex solid-state fermentation such as baijiu pit mud.

1.6 Grain Fermentation

The product of the cultivation of both daqu and pit mud is a functional community which exists within the fermenting grain. Baijiu is produced from grain, primarily sorghum, barley, and wheat, which is steamed and mixed with rice hulls for structure and daqu as a starter. Hydrolysis has been demonstrated to be carried out primarily by the thermophilic fungal genera *Lichtheimia*, *Aspergillus*, *Rhizomucor*, and *Saccharomycopsis* [67]. These organisms are all well known for their hydrolytic capability and are used independently for the production of α-amylase and gluco-amylase [68–70]. These fungi dominate initially but are soon outcompeted by primary fermenters such as *Lactobacillus* [4, 67]. The four main products of primary fermentation are lactic acid, acetic acid, butyric acid, and ethanol. Lactic acid is a vital compound for the production of longer chain acids but also for maintaining the pH balance of the environment and selecting for acid tolerant organisms. However, preventing the takeover of lactic acid bacteria is crucial since lactate metal complexes can inhibit chain elongation [71]. The hydrolytic genus *Bacillus* appears particularly suitable for this task, consistently demonstrating negative correlations between populations as well as facilitating inter-species hydrogen transfer which supports chain elongation and methanogenesis [72, 73]. The genus *Bacillus* also produces butyrate via fermentation but not as much as *Clostridium* via chain elongation [74]. Given that baijiu is an alcoholic beverage, it is notable that *Saccharomyces cerevisiae* makes up a relatively small fraction of the community in many of the cited studies. Ethanol production in the fermented grains is therefore likely shared among yeasts, including non-*Saccharomyces* species, and heterofermentative lactic acid bacteria, which produce ethanol and lactic acid in roughly equimolar amounts from glucose when citrate and pyruvate are absent [30, 75]. The community within the pit is a gradient from fungal activity at the surface to primary fermenters in the center and finally chain elongators near the bottom which forms as the temporal succession follows from the daqu communities to the fermented grain communities under new conditions and with the addition of the pit mud communities [51, 75]. This is a key difference between solid and liquid state fermentation, solid fermentation is inhomogeneous and notoriously difficult to regu-

late and control, whereas liquid fermentation is comparatively easy to mix, monitor, and control [34, 76]. However, this seeming disadvantage of the solid-state fermentation scheme can allow for dedicated clades existing in separate regions of the vessel while still allowing the exchange of material via diffusion, evaporation, and condensation. Consequently, reproducing baijiu chemistry in liquid-state fermentation may require replacing spatial separation with temporal or reactor-level separation. Rather than recreating the exact microbial community present in solid-state systems, a liquid-state process must reproduce the sequence of selective environments that support hydrolysis, primary fermentation, chain elongation, and esterification. One more advantage of solid-state fermentation is that there is not a concern about off-gas stripping of ethyl-esters which will volatilize out of a water matrix even at low concentrations [77, 78].

1.7 Distillation

The preceding enrichment stages generate a complex mixture of alcohols, organic acids, esters, sulfur compounds, and other volatile metabolites. However, only a subset of these compounds is recovered in the final distillate. Distillation therefore represents a final chemical selection stage in baijiu production, where compounds are transferred from the fermented matrix into the spirit according to their partitioning behavior, volatility, solubility, and interactions with the fermentation substrate. Importantly, recovery is not determined by boiling point alone. The ability of a compound to enter the vapor phase is strongly influenced by its solubility in the aqueous fermentation environment and its affinity for the liquid, solid, and vapor phases during distillation.

Traditional baijiu distillation utilizes a solid-state apparatus (zhengtong), where fermented grains are placed above a liquid collection chamber. Heat generates steam from the liquid phase, and the rising vapor extracts volatile compounds from the solid grain bed before condensation. As a result, flavor recovery depends on mass transfer through a complex porous matrix containing solids, residual water, microorganisms, and fermentation products [22].

Studies on bio-based ester recovery demonstrate that aqueous solubility is a major factor controlling ester transfer during distillation. Ethyl esters with greater water solubility are more readily recovered, while less soluble compounds exhibit altered partitioning behavior that affects their enrichment in the vapor phase [77].Recovery is also influenced by temperature, residence time, and molecular structure, with longer-chain esters generally requiring greater thermal input for efficient vaporization. This is especially relevant for strong-aroma baijiu, where medium-chain ethyl esters such as ethyl hexanoate are major contributors to aroma but possess lower volatility compared with shorter-chain compounds.

Distillation conditions also influence the separation of desirable and undesirable compounds. Research on fruit spirits and distilled sugarcane spirits shows that different fractions contain distinct chemical profiles, with highly volatile aroma compounds often appearing in early distillate fractions while a larger proportion of ethanol is recovered in the heart fraction [79, 80]

From an engineering perspective, reproducing baijiu flavor chemistry requires both biological generation of precursor compounds and effective recovery of those compounds during distillation. A liquid-state fermentation system may successfully reproduce microbial activity and metabolite production, but it may still produce a different flavor profile if the physical environment of distillation changes compound partitioning and recovery. Failure to generate sufficient medium-chain fatty acids during fermentation, convert them into ethyl esters, or recover those esters efficiently from the fermentation matrix can result in a spirit that differs substantially from traditional strong-aroma baijiu despite similar fermentation microbiology.

1.8 Aging

After distillation, the raw spirit enters the last selective stage of production: aging. The role of oxygen transfer is one of the primary differences between aging systems. In whiskey, maturation is strongly influenced by interaction with wooden barrels, where oxygen penetration, evaporation, and extraction of wood-derived compounds collectively drive flavor

development. Environmental conditions, including temperature and humidity, influence the rate of these processes by affecting spirit movement within the wood matrix and the transfer of volatile compounds [81].Smaller barrels accelerate these reactions by increasing the surface area-to-volume ratio, resulting in faster extraction of phenolic compounds and increased oxygen exposure compared with traditional barrel systems [81].These principles have motivated alternative aging methods, including controlled temperature cycling and other approaches intended to accelerate maturation reactions.

Baijiu aging differs fundamentally because traditional aging vessels are typically chemically inert compared with oak and are selected primarily for their influence on oxygen permeability rather than extraction of wood-derived compounds. Historically, clay vessels have been widely used for baijiu maturation, although porcelain vessels have become increasingly common due to their durability and lower permeability [22]. While porcelain minimizes oxygen transfer, it also limits the catalytic effects associated with metallic containers sometimes used for lower-quality products [22]. More recently, specialized aging vessels such as Jiuhai have demonstrated the importance of controlled oxygen exposure in baijiu maturation. Jiuhai vessels are constructed from paper treated with a mixture of beeswax, lime, and pig blood, producing a material with controlled oxygen permeability and minimal evaporation losses. Their large size moderates oxygen transfer over extended aging periods, allowing gradual chemical transformation while preserving the original spirit volume [82].

The relationship between vessel permeability and spirit development is consistent with observations from other fermented beverages. In wine production, oxygen transfer through oak barrels has been shown to strongly influence maturation chemistry, although oxygen permeability decreases over time as the wood becomes saturated with liquid components [81]. Modern ceramic amphora systems have attempted to replicate this controlled oxygen transfer by engineering clay porosity during firing, allowing predictable and prolonged oxygen exposure without the degradation of the vessel over repeated use [83].

The chemical consequences of oxygen exposure during baijiu aging are primarily related to changes in ester balance and the formation of increasingly complex flavor compounds. Oxygen promotes oxidation reactions that convert alcohols into corresponding acids and other

reactive intermediates, which can subsequently participate in esterification reactions [28]. Since esters are among the most important aroma compounds in baijiu, particularly short- and medium-chain ethyl esters, these reactions can significantly influence aroma intensity and balance. However, aging does not simply increase ester concentration indefinitely. Deng et al. [84] demonstrated that straight-chain ester concentrations in aged baijiu follow a nonlinear pattern, initially increasing before declining over approximately a decade of aging. This trend corresponds with changes in pH, suggesting that acidification and oxidation gradually alter the equilibrium between ester formation and degradation.

In addition to ester transformations, aging promotes the development of more complex aromatic compounds through oxidation and condensation pathways. Oxidation reactions can facilitate the formation of carbon-carbon bonds when reactive methyl groups are adjacent to carboxylic acid groups, contributing to the formation of lactones and other increasingly complex flavor compounds [28]. These reactions contribute to the transition from younger baijiu profiles, which are often characterized by stronger fruity and sharper aromas, toward older spirits with greater herbal, woody, and mature characteristics. Jiuhai-aged baijiu has been shown to contain increased concentrations of aromatic compounds and esters associated with spicy, herbal, and woody sensory attributes compared with unaged product [82].

Other aging-associated compounds follow similarly complex trajectories. Maillard reaction intermediates and related compounds, including furfurals and ketones, can undergo changes during long-term maturation. In baijiu varieties where these compounds are significant contributors to aroma, their concentrations may initially decline before increasing over extended aging periods, forming a nonlinear pattern over decades of maturation [85]. This suggests that aging is not a simple accumulation process but a dynamic chemical succession in which early-stage degradation reactions may create intermediates that later contribute to new flavor compounds.

From an engineering perspective, aging represents the final selective environment in the baijiu production pathway. Fermentation establishes the precursor pool of alcohols, acids, esters, and other metabolites, while aging determines how those compounds are transformed and balanced over time. Therefore, a scalable liquid-state baijiu production process must

consider not only the reproduction of microbial enrichment stages but also the physical aging environment required to guide post-distillation chemistry. Controlled oxygen transfer, vessel composition, and maturation conditions may ultimately provide a pathway to reproduce traditional aging effects without relying on centuries-old storage practices.

1.9 Sequential Liquid-State Fermentation

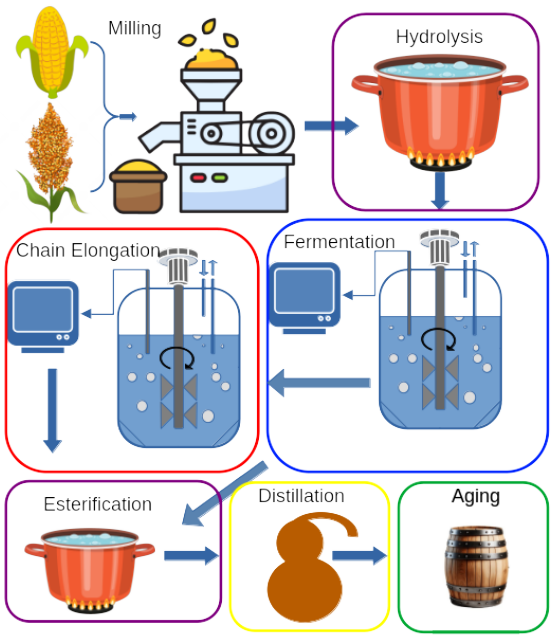


Figure 1.2: Proposed liquid process for baijiu production where each function is strung into a sequence of events rather than occurring simultaneously.

The primary challenge in adapting baijiu production to liquid-state fermentation is not the inability of microorganisms to produce desired metabolites, but the difficulty of maintaining the sequence of selective environments that occurs naturally in solid-state fermentation. Traditional baijiu production achieves this through spatial and temporal heterogeneity. Hydrolytic fungi, primary fermenters, chain elongators, and ester-producing organisms occupy partially separated ecological niches within the grain and pit environment. In a liquid-state system, these gradients collapse, creating competition between organisms with different metabolic objectives. One potential solution is to replace spatial organization with sequential

fermentation stages, allowing each reactor to function as a controlled enrichment environment. A similar principle is demonstrated in the production of Grand Arôme rum, a style of rum characterized by exceptionally high concentrations of esters and volatile compounds. Unlike conventional rum production, which typically relies on relatively simple sugar fermentation followed by distillation, Grand Arôme production utilizes extended fermentation strategies designed to promote the accumulation of organic acids and ester precursors [86]. Historically, this process involved long fermentations, recycling of acidic stillage, and the deliberate creation of conditions favorable for complex microbial interactions. Rather than maximizing ethanol production, the process prioritizes the generation of secondary metabolites responsible for aroma complexity.

The relevance of Grand Arôme rum to baijiu production is the concept of staged microbial succession. Instead of requiring all metabolic functions to occur simultaneously within one fermentation vessel, liquid systems can be designed as a series of reactors, each optimized for a specific function. An initial hydrolysis stage could maximize conversion of complex grain carbohydrates into fermentable sugars. A subsequent fermentation stage could promote ethanol and organic acid production. A third stage could enrich chain-elongating organisms capable of converting lactate, ethanol, and acetate into medium-chain fatty acids.

Finally, an esterification stage could promote conversion of these acids into ethyl esters prior to distillation. This final step need not depend on microbial esterase activity; direct acid-catalyzed esterification of medium-chain fatty acids with ethanol is a well-established industrial reaction, and both homogeneous acid catalysts and heterogeneous catalysts such as sulfonated ion-exchange resins have been shown to drive high-conversion esterification of fatty acids with ethanol under moderate temperatures [87, 88]. Incorporating a chemically catalyzed esterification stage, rather than relying solely on microbial esterases, could offer a more controllable and scalable endpoint for the proposed reactor sequence.

This approach mirrors the ecological succession observed in traditional baijiu production but replaces uncontrolled gradients with engineered process control. Importantly, this does not require recreating the complete microbial diversity of a pit mud ecosystem. Instead, each reactor can be treated as an enrichment step designed to favor a desired metabolic

function (Figure 1.2). This reduces competition between incompatible metabolisms while allowing the overall process to reproduce the chemical progression responsible for baijiu flavor development. The Grand Arôme model therefore provides a practical framework for translating the enrichment concept into a scalable liquid-state process. Traditional baijiu relies on a single vessel containing multiple overlapping ecological niches, while a liquid-state alternative could achieve the same functional succession by connecting multiple specialized fermentation environments. This represents a shift from attempting to imitate the traditional microbial community toward engineering the environmental conditions that generate the desired chemistry.

1.10 Conclusions of the Review

Traditional baijiu production represents one of the most complex examples of industrial microbial ecology, yet its complexity has often been interpreted primarily through the identification of microbial species and flavor compounds rather than through the environmental conditions that produce them. This chapter proposes an alternative framework: baijiu production is best understood as a sequence of enrichment processes in which each stage establishes selective pressures that favor specific metabolic functions. Daqu enriches hydrolytic, fermentative, and ester-producing capabilities under aerobic thermophilic conditions. Pit mud establishes anaerobic environments that favor syntrophic interactions and chain elongation pathways responsible for medium-chain fatty acid production. Grain fermentation integrates these functions, generating the alcohols, acids, and precursors required for ester formation. Distillation and aging then act as additional selection stages, determining which compounds are recovered and how they are chemically transformed into the final spirit profile. This perspective changes the engineering challenge of baijiu production. The goal is not to recreate the complete microbial community of traditional fermentation systems, which is both unnecessary and impractical, but rather to reproduce the sequence of chemical and ecological conditions that generates the desired metabolites. Solid-state fermentation achieves this naturally through spatial gradients, substrate heterogeneity, and long-term microbial

adaptation. A liquid-state alternative must therefore replace spatial separation with controlled temporal separation, using sequential reactors or enrichment stages to guide microbial succession.

The production strategy used in Grand Arôme rum provides a relevant precedent for this approach. By extending and separating fermentation stages to encourage the accumulation of specific flavor precursors, Grand Arôme production demonstrates that complex spirit chemistry can emerge from intentionally structured liquid fermentation systems. Applying this principle to baijiu could enable the development of a scalable process in which hydrolysis, primary fermentation, chain elongation, esterification, and maturation are each optimized independently rather than occurring simultaneously within a single heterogeneous environment. Such an approach would represent a shift from traditional fermentation replication toward process-based engineering. The future of baijiu production may not depend on reproducing centuries-old microbial ecosystems but on understanding and controlling the selective environments that created them. By treating traditional methods as ecological engineering systems rather than fixed recipes, it becomes possible to design liquid-state processes capable of producing baijiu-characteristic chemistry with improved control, scalability, and reproducibility.

1.11 Research Objectives and Dissertation Organization

The framework developed in this chapter divides a liquid-state baijiu-style process into a sequence of stages: hydrolysis, primary fermentation, chain elongation, esterification, and maturation. Each stage can be studied and optimized on its own. The overall objective of this dissertation is to build the experimental foundation for such a process by examining the individual stages in turn, using the grains, microbial communities, and aging practices most relevant to the United States. The specific objectives, and the chapters that address them, are:

1. To evaluate US grain sorghum, the traditional baijiu grain, for liquid-state spirit fer-

mentation. This includes determining how sorghum variety and commercial yeast strain affect alcohol yield, fermentation byproducts, and volatile compounds (Chapter 2).

2. To extend this evaluation to maize, the grain most widely used in liquid-state baijiu and American whiskey, including specialty blue, red, and white varieties. The aim is to identify the starch properties and yeast–substrate interactions that govern yield and flavor (Chapter 3).

3. To develop a lower-energy hydrolysis stage based on partial starch swelling and granular starch hydrolyzing enzymes, and to determine its effects on ethanol yield and on the protein quality of the distillers' grains coproduct (Chapter 4).

4. To recreate the chain-elongation function of baijiu pit mud in liquid culture by adaptively enriching bovine rumen fluid toward medium-chain fatty acid production (Chapter 5).

5. To examine maturation as the final selective stage by aging commercial baijiu in small oak barrels, and to determine how the fermentation-derived starting chemistry and the aging environment together shape the final spirit (Chapter 6).

Chapter 7 summarizes the findings across these chapters, relates them back to the staged-process framework, and outlines directions for future work.

Chapter 2

Production of Distilled Spirits from Grain Sorghum through Liquid-State Fermentation

This chapter is adapted from the following published article: Weiss, T., Zhao, J., Hu, R., Liu, M., Li, Y., Zheng, Y., Smith, G., and Wang, D. (2022). Production of distilled spirits using grain sorghum through liquid fermentation. Journal of Agriculture and Food Research, 9, 100314. https://doi.org/10.1016/j.jafr.2022.100314. *The article is published open access under a CC BY-NC-ND license, and it is included here under the author rights retained by the author for use in a thesis or dissertation.* *The text has been edited for consistency with the rest of this dissertation.*

Chapter Overview

Chapter 1 argued that a liquid-state route to baijiu-style spirits should be built as a sequence of controlled stages, starting with starch hydrolysis and primary alcoholic fermentation. Before later stages such as chain elongation or esterification can be engineered, this first stage has to be characterized for the raw materials and yeasts that a liquid process would actually use. Sorghum is the traditional grain for high-quality baijiu, so it is the logical place to start. This chapter evaluates three US sorghum varieties (red, white, and waxy)

fermented with four commercial *Saccharomyces cerevisiae* strains (DADY, Ethanol Red, GR-2, and 71B). Grain chemistry, starch pasting behavior, ethanol yield, the major fermentation byproducts (glycerol and lactic acid), and the volatile profile of the fermented broth (the precursor to the spirit) are reported.

Sorghum variety significantly affected alcohol concentration and yield; the effect of yeast strain was not statistically significant ($p \approx 0.15$), although clear numerical differences among strains were observed. Final alcohol concentration ranged from 10.26 to 11.34% (v/v), and alcohol yield ranged from 80.93 to 90.77% of theoretical. Ethanol Red gave the highest average alcohol concentration (11.10%, v/v) and yield (87.33%) across all three sorghums. Waxy sorghum gave a significantly higher average alcohol concentration (11.20%, v/v) and yield (89.65%) than white sorghum (10.74% and 84.74%) or red sorghum (10.28% and 82.27%). Glycerol and lactic acid were the main fermentation byproducts. Glycerol formation depended mainly on yeast strain: DADY produced the most (about 0.11–0.12%, v/v; 1.4–1.5 g/L) and GR-2 the least (0.07–0.09%, v/v; 0.9–1.1 g/L). Lactic acid stayed below about 0.10% (v/v; 1.2 g/L) under all conditions. Eight major volatile compounds were identified in the fermented broths, and they are associated mainly with fruity, sour, sweet, floral, buttery, and creamy notes.

2.1 Introduction

Distilled spirits are alcoholic beverages made by distilling a fermented grain, fruit, or other carbohydrate source. The category includes brandy, gin, rum, tequila, whiskey, vodka, baijiu, and a wide range of flavored liqueurs. The global alcoholic beverage market was valued at roughly $1475 billion in 2021. It was projected to grow about 9.1% per year and reach approximately $2797 billion by 2028 [89]. In the United States, spirits account for more than 30% of total alcohol sales, which is close to 97 billion U.S. dollars [90]. By volume, vodka is the best-selling spirit, followed by whiskey and rum. Most whiskey, vodka, and gin is produced from corn, wheat, and rye, although some vodkas are made from potatoes.

Spirits made from sorghum are not new. Sorghum has been used in rum, vodka, and beer,

and several small craft producers in the United States offer sorghum-based whiskeys and spirits. In China, sorghum is the main, and often the only, grain used for high-quality baijiu, which is sometimes called "sorghum spirit." As described in Chapter 1, the best-known baijiu styles are produced by solid-state fermentation, in which the microbial community grows on a moist solid grain matrix. Liquid-state fermentation is also practiced in China, but it has generally used corn rather than sorghum as the raw material [91].

Many sorghum grains contain appreciable amounts of phenolic compounds, including condensed tannins, and these are considered one of the main factors shaping the aroma of sorghum spirits [92–94]. Han et al. [95] compared baijiu made from sorghum with baijiu made from wheat, corn, rice, and barley. They ranked sorghum baijiu highest in flavor and quality, followed by wheat, and recommended sorghum, optionally blended with wheat, as the primary raw material. Xu et al. [96] evaluated five Australian sorghum varieties for solid-state baijiu production. Szambelan et al. [97] studied sorghum distillates from Poland produced by liquid fermentation and focused on the volatile compounds formed during fermentation. Despite these studies and the availability of a few craft sorghum spirits, there was no published information on how US sorghum varieties perform in distilled-spirit fermentation.

The objectives of the work described in this chapter were therefore to (1) evaluate the fermentation performance of US sorghum varieties for distilled spirit production, including the associated coproducts, and (2) characterize the formation of volatile compounds related to the flavor quality of the resulting spirits.

2.2 Materials and Methods

2.2.1 Sorghum samples

Three grain sorghum varieties (red, white, and waxy) were obtained from Nu Life Market (Scott City, KS, USA). Each sample was cleaned on a Gamet sieve shaker (Dean Gamet Mfg. Co., Minneapolis, MN) fitted with a 1.98-mm (5/64-in) triangular-hole sieve to remove

broken kernels and fine foreign material. Larger broken kernels and foreign material were then picked out by hand. Clean grain was milled to flour in an Udy cyclone mill (Udy, Fort Collins, CO) with a 1.0-mm screen. The flour was sealed in plastic bags and kept in a closed plastic container at 25°C until use.

2.2.2 Chemical, physical, and thermal properties of grain sorghum

Moisture was measured by AOAC method 930.15. Starch was measured with a Megazyme kit (Bray, Ireland) following AACC approved method 76-12. Crude protein was measured by combustion nitrogen analysis (AOAC 990.03), and nitrogen was converted to protein with a factor of 6.25. Crude fat and ash were measured by AOAC methods 920.39 and 942.05, respectively. Crude fiber was measured with the filter bag technique (ANKOM Technology, Macedon, NY). Condensed tannin was measured with a modified vanillin assay [98]. Kernel hardness, kernel weight, and kernel diameter were measured with a Single Kernel Characterization System (SKCS 4100, Perten Instruments, Inc., Reno, NV, USA).

Pasting properties of the sorghum flours were measured with a Rapid Visco Analyser (RVA-3c, Newport Scientific Ltd., Warriewood, Australia). Flour (4.0 g at 14% moisture) was mixed with 25 mL of water at 50°C. The slurry was held at 50°C for 1 min, heated to 95°C, held at 95°C for 2.5 min, cooled to 50°C, and held for 2 min, for a total run time of 13 min.

2.2.3 Selection of yeast strains

Four commercial *S. cerevisiae* strains marketed for vodka and fuel-alcohol production were used: Lalvin 71B (71B; Lallemand, Australia), SafSpirit GR-2 (GR-2; Fermentis, Marcq-en-Barœul, France), Red Star Distillers Active Dry Yeast (DADY; Fermentis, Milwaukee, WI, USA), and Ethanol Red (Lesaffre, Milwaukee, WI, USA). These strains are considered well suited to vodka and high-concentration alcohol fermentation [99]. 71B is an active dry yeast intended for neutral spirits, vodka, and gin. GR-2 is marketed for very neutral alcohol, especially vodka. DADY was selected for distillers' grain-mash fermentations and has been

used for light whiskey and neutral spirits. Ethanol Red is a high-ethanol-tolerance strain developed for the fuel ethanol industry and is suitable for very-high-gravity fermentation. The properties of the four strains are summarized in Table 2.1.

Table 2.1: Commercial yeast strains used for spirit production in this chapter.

Supplier	Strain	Fermentation temperature	Intended products
Lallemand, Australia	Lalvin 71B	15–30°C	Neutral spirits, vodka, and gin
Fermentis, France	SafSpirit GR-2	20–32°C	Very neutral alcohol, especially vodka
Fermentis, United States	Red Star Distillers Active Dry Yeast (DADY)	32°C	Ethanol, light spirits, and whiskeys
Lesaffre, United States	Ethanol Red	30–40°C	Fuel ethanol

2.2.4 Liquefaction and simultaneous saccharification and fermentation

Sorghum flour was liquefied before fermentation. Slurries containing 30% sorghum flour (dry basis) were prepared in flasks, and α-amylase (240 KNU/g starch, approximately 1.26 g/mL; Novozymes, New York, NY) was added. The flasks were placed in a rotary water-bath shaker at 70°C. The bath was then heated to 90°C and held there for a few minutes with shaking at 180 rpm. It was then lowered to 85°C and held for 60 min. At the end of liquefaction, the flasks were removed from the bath.

Once the mashes had cooled to room temperature, their pH was adjusted to about 4.2 with 2 M HCl. Each dry yeast was rehydrated before inoculation by adding 1.0 g of yeast to 19 mL of preculture medium. The medium contained, per liter, 20 g glucose, 5.0 g peptone, 3.0 g yeast extract (omitted for 71B), 1.0 g KH_2PO_4, and 0.5 g $MgSO_4 \cdot 7H_2O$. The cultures were incubated at 38°C and 200 rpm for about 30 min, except 71B, which was activated at 35°C for 20 min. Each flask then received 1.0 mL of activated culture (approximately 2.8×10^8 cells/mL), 100 µL of Spirizyme glucoamylase (Novozymes, Franklinton, NC), and

0.30 g of yeast extract. The flasks were closed with S-type airlocks filled with mineral oil and incubated at 30°C and 150 rpm for 72 h. At 72 h, the broth was sampled for chemical analysis, and the remaining mash was distilled to determine alcohol yield.

For distillation, the entire contents of each 250-mL flask were transferred to a 500-mL distillation flask, and the fermentation flask was rinsed four times with 25 mL of distilled water (100 mL total). The distillate was collected in a 100-mL volumetric flask held in ice water. Distillation was stopped when the distillate was within 0.5 mL of the mark. The volumetric flask was equilibrated in a 25°C water bath for a few hours and then made up to volume with distilled water. Ethanol in the distillate was quantified by HPLC on a Rezex RCM column (Phenomenex, Torrance, CA) with a refractive index detector [100].

2.2.5 Analytical methods

After fermentation, ethanol, glycerol, lactic acid, and residual sugars (glucose, maltose, and maltotriose) were quantified by HPLC (1260 system, Agilent Technologies Inc., Santa Clara, CA). The system used an Aminex HPX-87H organic acid column (7.8 × 300 mm; Bio-Rad Laboratories, Hercules, CA) at 60°C and a refractive index detector at 45°C. The mobile phase was 5 mM H_2SO_4 at 0.6 mL/min. Glycerol and lactic acid were quantified in g/L; for comparison with other reports they are also given as % (v/v), using densities of 1.26 g/mL for glycerol and 1.21 g/mL for lactic acid. Alcohol yield was expressed as the ratio of the measured ethanol mass to the theoretical ethanol mass, where theoretical ethanol (g) = starch (g) × 1.11 × 0.511 [101].

Volatile compounds in the fermentation broth were analyzed by gas chromatography–mass spectrometry (GC–MS) using a modification of the method of Pinu and Villas-boas [102]. Triplicate 1-mL aliquots of each fermented broth were saturated with anhydrous sodium chloride (about 100–300 mg). Each aliquot was then extracted with 0.5 mL of ethyl acetate containing 0.2 mg/mL phenol as an internal standard (phenol was absent from all samples) by vortexing for 30 s. The ethyl acetate layer was analyzed on an Agilent 6890 GC coupled to a 5973 quadrupole mass selective detector (electron impact ionization, positive

mode, 70 eV; Agilent Technologies, Santa Clara, CA, USA). Separation used a Zebron ZB-1701 column (30 m × 250 µm × 0.25 µm; Phenomenex, Torrance, CA) with a 5-m guard column (7AG-G000-00-GZK, Phenomenex). Injections (1 µL) were made in split mode at 50:1, with helium as the carrier gas at 0.5 mL/min. The oven was held at 50°C for 1 min, ramped at 20°C/min to 200°C, and held for 2 min, for a total run time of 10.5 min. The interface and quadrupole temperatures were 230°C and 150°C, respectively. The detector was switched off from 2.9 to 3.1 min and from 3.3 to 3.5 min to avoid the ethanol and ethyl acetate peaks. Spectra were acquired in scan mode from 30 to 250 amu.

2.2.6 Statistical analysis

Data were compiled in Microsoft Excel (Microsoft Corporation, Redmond, WA), and differences among means were tested by the least significant difference (LSD) method at $p < 0.05$. GC–MS data were analyzed in JMP (JMP Statistical Discovery LLC, Cary, NC). A linear regression model with an interaction term was fitted for each quantified volatile. All models had $p < 0.0001$ and $R^2 > 0.92$ except the model for methyl isobutyrate, for which no factor effect was significant. Analysis of variance (ANOVA) was used to test the effects of sorghum variety, yeast strain, and their interaction on the integrated total ion current (TIC) peak area of each compound.

2.3 Results and Discussion

2.3.1 Physical and chemical properties of grain sorghum

The physical properties of the three sorghum varieties are given in Table 2.2. The varieties differed significantly in kernel hardness index (55.66–74.09), single-kernel weight (23.44–33.39 mg), kernel diameter (2.05–2.81 mm), and test weight (56.67–58.71 lb/bu). White sorghum generally had the highest hardness index and test weight, and red sorghum had the smallest kernels.

The chemical composition of the sorghums is given in Table 2.3. Starch content ranged

Table 2.2: Physical properties of the grain sorghum varieties.

Sorghum	Kernel hardness index	Single kernel weight (mg)	Kernel diameter (mm)	Test weight (lb/bu)
White	74.09 ± 1.29	27.61 ± 0.35	2.57 ± 0.01	58.71 ± 0.01
Waxy	69.31 ± 0.94	33.39 ± 0.63	2.81 ± 0.04	58.64 ± 0.10
Red	55.66 ± 0.96	23.44 ± 0.25	2.05 ± 0.03	56.67 ± 0.06

Values are mean ± standard deviation. Kernel hardness, single kernel weight, and kernel diameter are based on 300 kernels; test weight is based on three replicates.

from 64.50 to 67.83% (db). This is within the range of 61.0–74.8% (db) reported in earlier work [96, 103–106]. White sorghum contained slightly more starch (67.83%, db) than red (66.46%) or waxy sorghum (64.50%). Protein ranged from 9.75 to 11.07% (db) and was highest in white sorghum. Crude fat ranged from 1.95 to 2.68% (db). Crude fiber was similar in all three varieties (about 1.65%, db). Red sorghum contained far more tannin (3.61%, db) than white (0.06%) or waxy sorghum (0.30%) and can be classified as a high-tannin variety.

Table 2.3: Chemical composition of the grain sorghum varieties.

Sorghum	Moisture (%)	Starch (%, db)	Crude protein (%, db)	Crude fat (%, db)	Crude fiber (%, db)	Ash (%, db)	Tannin (%, db)
White	11.33 ± 0.08	67.83 ± 1.30	11.07 ± 0.13	2.68 ± 0.07	1.65 ± 0.04	1.64 ± 0.01	0.06 ± 0.009
Waxy	10.17 ± 0.07	64.50 ± 1.40	10.92 ± 0.01	1.95 ± 0.10	1.67 ± 0.01	1.71 ± 0.01	0.30 ± 0.042
Red	11.52 ± 0.04	66.46 ± 0.72	9.75 ± 0.01	2.01 ± 0.06	1.63 ± 0.01	1.75 ± 0.01	3.61 ± 0.041

Values are mean ± standard deviation of two replicates.

2.3.2 Alcohol concentration and yield

Table 2.4 shows how sorghum variety and yeast strain affected alcohol concentration and yield. Alcohol concentration ranged from 10.26 to 11.34% (v/v), and yield ranged from 80.93 to 90.77%, indicating that fermentation performance varied with both factors, although only the effect of sorghum variety was statistically significant. The ANOVA p-values for the yeast effect on concentration and yield were about 0.15 (Table 2.5). Even so, Ethanol Red consistently gave the highest average alcohol concentration (11.10%, v/v) and yield (87.33%) regardless of substrate (Table 2.4). This is expected for a strain bred for high-efficiency

ethanol production and widely used in the fuel ethanol industry. GR-2 and 71B gave similar average yields (85.12% and 85.80%), and DADY gave the lowest (83.94%). Consistent yield is important for producing a spirit of consistent quality. In vodka production, where high alcohol concentration and consistency matter most, Ethanol Red would be a sensible choice.

Table 2.4: Effect of sorghum variety and yeast strain on alcohol concentration and alcohol yield.

Sorghum	DADY	Ethanol Red	GR-2	71B	Average
Alcohol concentration (%, v/v)					
White	10.85 ± 0.16^{ab}	11.16 ± 0.19^{b}	10.87 ± 0.05^{b}	10.09 ± 0.07^{b}	10.74
Waxy	10.90 ± 0.12^{b}	11.34 ± 0.02^{b}	11.29 ± 0.14^{c}	11.27 ± 0.30^{b}	11.20
Red	10.26 ± 0.09^{a}	10.81 ± 0.25^{a}	10.30 ± 0.15^{a}	10.36 ± 0.33^{a}	10.28
Average	10.67	11.10	10.82	10.57	
Alcohol yield (%)					
White	83.63 ± 1.31^{b}	86.00 ± 1.54^{a}	83.78 ± 0.38^{b}	85.47 ± 0.51^{a}	84.74
Waxy	87.25 ± 0.89^{c}	90.77 ± 0.17^{b}	90.35 ± 1.05^{c}	90.22 ± 2.32^{b}	89.65
Red	80.93 ± 0.73^{a}	85.21 ± 2.02^{a}	81.24 ± 1.22^{a}	81.71 ± 2.62^{a}	82.27
Average	83.94	87.33	85.12	85.80	

Values are mean ± standard deviation of three replicates. Within each column, means followed by different letters differ significantly ($p < 0.05$).

Table 2.5: Analysis of variance for the effects of sorghum variety, yeast strain, and their interaction on final ethanol concentration and ethanol yield.

	Ethanol concentration (%, v/v)			Ethanol yield (%)		
Source of variation	df	F	p	df	F	p
Sorghum variety	2	18.1792	0.0002	2	25.9201	0.0001
Yeast strain	3	2.1061	0.1529	3	2.1022	0.1534
Variety × strain	6	1.2968	0.3294	6	1.3121	0.3234

Yeast selection can be used to regulate spirit yield [99], but the fermentation substrate is at least as important. Sorghum variety had a significant effect on both alcohol concentration and yield ($p < 0.05$; Table 2.5). Earlier studies found that waxy sorghums give higher ethanol yields than non-waxy sorghums at equal starch content [107–109], and the present results agree. Waxy sorghum had a significantly higher average alcohol concentration (11.20%, v/v) and yield (89.65%) than white sorghum (10.74% and 84.74%) or red sorghum (10.28% and 82.27%). These differences reflect mainly the properties of the starch. Waxy sorghum starch is rich in amylopectin, which makes it more available for hydrolysis [108]. Amylose

in normal sorghum starch works against this during gelatinization. Waxy sorghum also has lower peak and end gelatinization temperatures than normal sorghum, so its starch is more easily hydrolyzed [107–109]. Waxy sorghum mashes are also usually less viscous during liquefaction, which further improves hydrolysis efficiency.

The pasting profiles in Figure 2.1 support this explanation. The final viscosity of waxy sorghum (2079.0 cP) was much lower than that of red (3154.0 cP) or white sorghum (3413.0 cP), and its setback viscosity was also much lower than that of red (1675.5 cP) or white sorghum (2018.5 cP). Waxy sorghum also reached peak viscosity sooner (5.00 min) than red (5.37 min) or white sorghum (5.80 min). Together, the RVA data show that waxy sorghum starch swells and breaks down more readily than the starch in normal red and white sorghum flours. This difference in swelling behavior is examined further in Chapter 4, where partial starch swelling below the gelatinization temperature is used to improve low-temperature enzymatic hydrolysis.

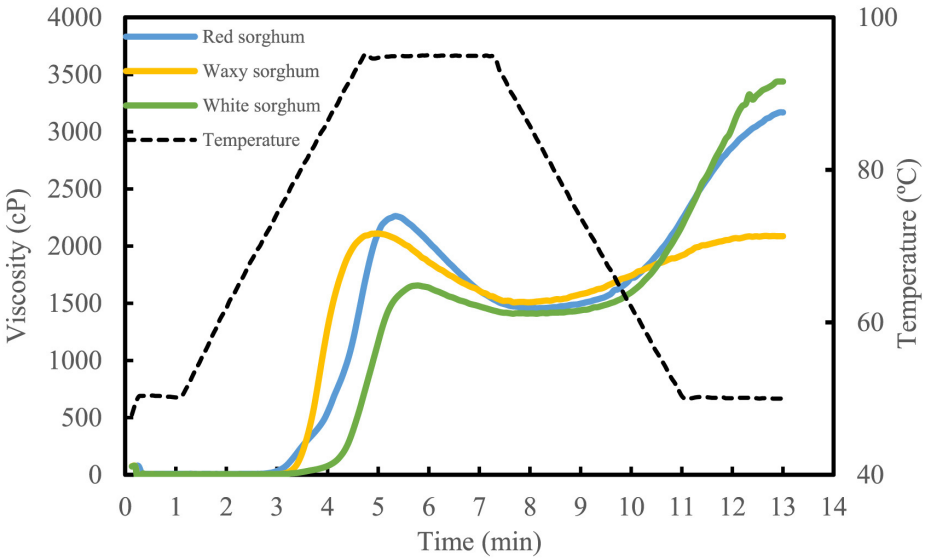


Figure 2.1: Rapid Visco Analyser pasting profiles of the three sorghum flours.

Red sorghum gave the lowest alcohol concentration and yield of the three varieties. The most likely explanation is its high tannin content (3.61%, db). Tannins impair starch digestion because they bind proteins, including hydrolytic enzymes [110]. Mashes of tannin

sorghums are also more viscous than those of waxy or normal sorghum [107–109], and red sorghum here had a higher peak viscosity (2277.5 cP) than waxy (2106.5 cP) or white sorghum (1633.5 cP). For these reasons, high-tannin sorghums generally give lower ethanol yields.

2.3.3 Fermentation byproducts

Alcoholic fermentation converts sugar mainly to ethanol and CO_2, but it also produces a range of other metabolites. Glycerol and lactic acid are the two principal byproducts of spirit fermentation [111, 112]. Figure 2.2 shows how sorghum variety and yeast strain affected glycerol formation. Among the byproducts measured, glycerol was the only one that depended strongly on yeast strain. DADY produced the most glycerol (0.11–0.12%, v/v; 1.4–1.5 g/L), and GR-2 produced the least (0.07–0.09%, v/v; 0.9–1.1 g/L). Glycerol levels within each strain were tightly grouped, and the only notable deviations were two outlying values from Ethanol Red. Sorghum variety did not significantly affect glycerol formation, although red sorghum gave a wider range (0.07–0.13%, v/v; 0.9–1.65 g/L) and a slightly higher mean than waxy or white sorghum. Waxy sorghum gave the lowest mean glycerol level.

Because glycerol output was so strain-dependent, it could in principle serve as an indicator of which yeast is present in a fermentation [113], although this would require validation across a much wider range of strains and conditions. In principle, yeasts could be isolated from a reactor, grown in broth, and the supernatant assayed for glycerol. A characterized strain could then be identified by its glycerol output. Glycerol can be toxic to yeast and to humans at high enough doses [112, 114], and it is relevant to both the wine and baijiu industries [113, 115]. Across all yeasts and sorghums, glycerol ranged from about 0.9 to 1.7 g/L (0.07–0.13%, v/v). This is lower than the 7.5–10.6 g/L reported by Du et al. [116] across 10 wine yeast strains, which is expected given the lower sugar concentration and osmotic stress of a grain mash than of grape must. It lies within the 0–31.33 g/kg range that Wei et al. [117] reported for Chinese baijiu fermentations, where glycerol depended on

the yeasts and filamentous fungi involved.

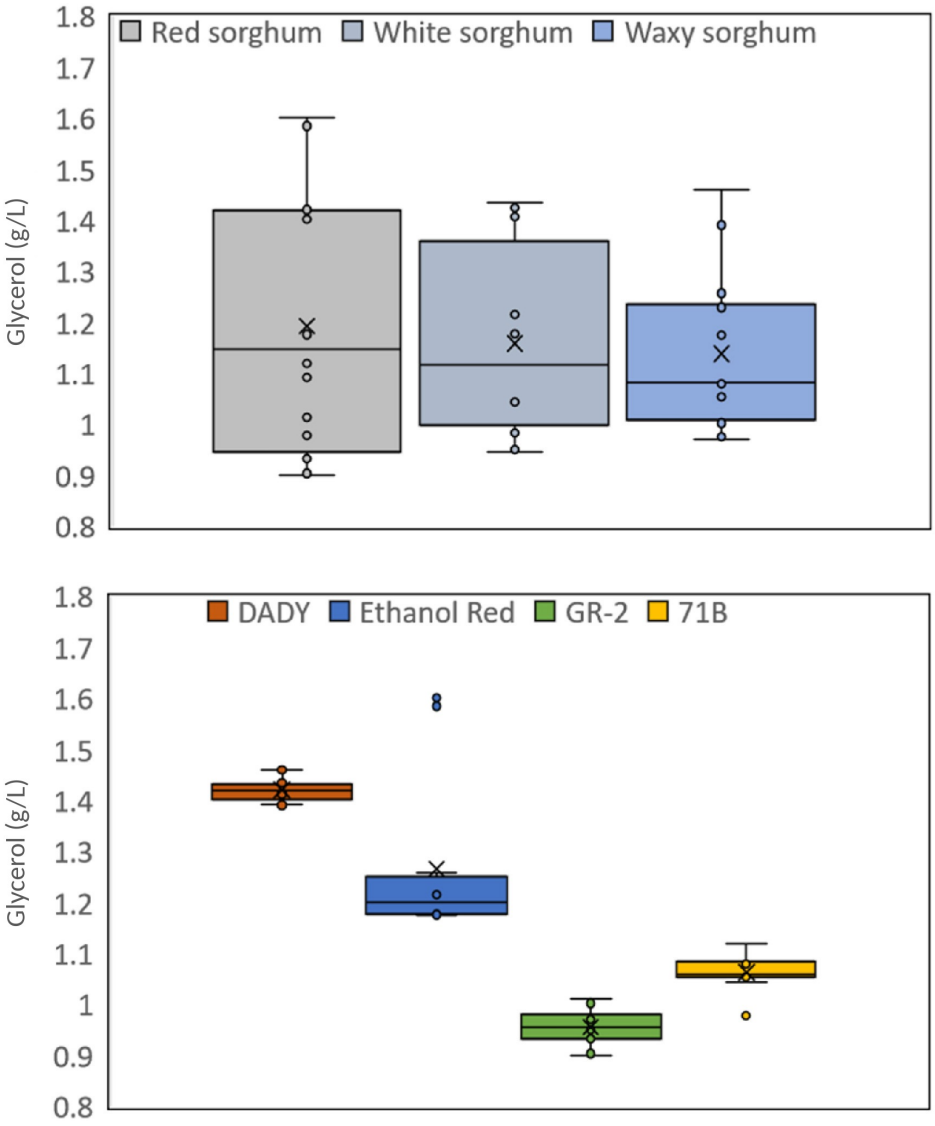


Figure 2.2: Effects of yeast strain and sorghum variety on glycerol formation during spirit fermentation (g/L; 1 g/L $\approx$ 0.079% v/v).

Lactic acid is a common metabolite in alcoholic fermentations. In Moutai-flavor baijiu, for example, lactic acid can reach 36.20 g/kg of fermented grain [118]. Most yeasts do not naturally produce lactic acid, so the lactic acid found here was most likely produced by other microorganisms [119]. Acid formation during fermentation is generally attributed to oxidation and to contamination by lactic acid bacteria [91, 103]. Lactic acid can also stress yeast and lower alcohol yield [120].

Figure 2.3 shows how sorghum variety and yeast strain affected lactic acid formation. Red

sorghum supported slightly more lactic acid than white or waxy sorghum, but the difference in mean levels was small. Yeast strain, by contrast, had a significant effect. Ethanol Red fermentations contained significantly more lactic acid than those with the other three strains, and DADY fermentations contained the least. Because yeasts do not normally produce lactic acid, this strain effect is probably indirect, and further work is needed to explain it. Lactic acid can inhibit fermentation and reduce yield, but the concentrations measured here (at most about 1 g/L, or 0.08% v/v) are well below the levels usually associated with appreciable yeast inhibition. Consistent with this, higher lactic acid levels were not associated with lower yield in this small set of four strains. Ethanol Red produced both the most lactic acid (up to about 1.0 g/L; 0.08%, v/v) and the highest alcohol yield (87.33%), while DADY produced the least lactic acid (below 0.5 g/L; 0.04%, v/v) and the lowest yield (83.94%). Other factors therefore likely govern the relationship between lactic acid and alcohol yield. This relationship has received little study, but it may matter in practice [120, 121]. It is also relevant to the staged process proposed in Chapter 1, where lactate is a potential electron donor for chain elongation (Chapter 5).

2.3.4 Volatile compounds

Alcoholic fermentation also produces many volatile compounds. The types and amounts of volatiles in a distilled spirit are closely tied to its flavor, aroma, and consumer acceptance [122]. More than 1730 compounds have been reported in Chinese baijiu [123]. The main classes are acetals, acids, alcohols, aldehydes, esters, ketones, lactones, and nitrogen- and sulfur-containing compounds [91]. Which volatiles form, and in what amounts, depends strongly on the fermenting organisms, the raw material, and the fermentation conditions. Szambelan et al. [97] identified 28 volatile compounds in Polish sorghum distillates made with two yeast strains (Ethanol Red and Fermiol) and two enzyme preparations for starch hydrolysis and saccharification. Aldehydes, esters, methanol, and higher alcohols were the four main groups.

In the present work, three sorghum varieties were fermented with four yeast strains

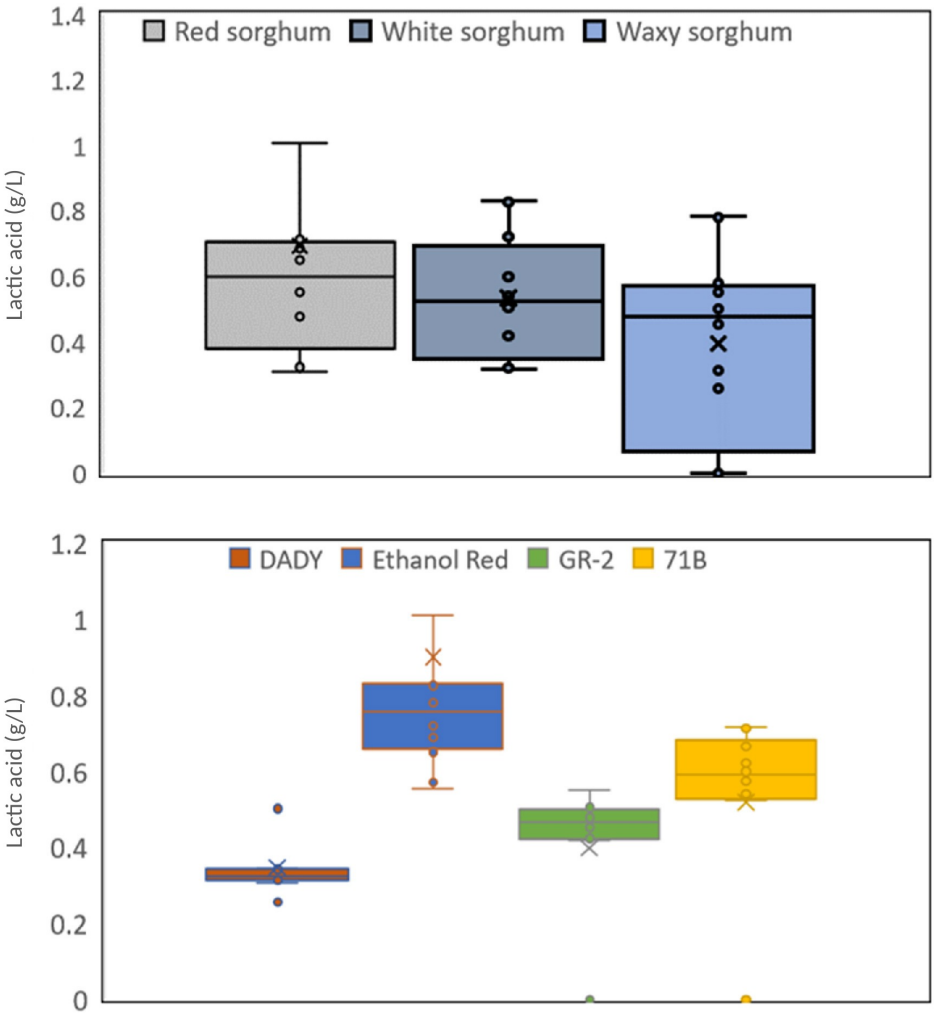


Figure 2.3: Effects of yeast strain and sorghum variety on lactic acid formation during spirit fermentation (g/L; 1 g/L $\approx$ 0.083% v/v).

(71B, GR-2, DADY, and Ethanol Red). Eight major volatile compounds were identified in the fermented broths against the NIST (National Institute of Standards and Technology) library with match scores above 90. TIC peak areas were integrated in ChemStation and normalized to the internal standard. The compounds identified are associated mainly with fruity, sour, sweet, floral, buttery, and creamy flavors. In most cases, sorghum variety, yeast strain, and their interaction all had significant effects on the volatile profile (Table 2.6). The exceptions were methyl isobutyrate, which none of the factors affected significantly, and 2-methyl-1-propanol, which sorghum variety did not affect significantly. Phenylethyl alcohol varied widely among the spirits (Figure 2.4). Spirits fermented with Ethanol Red contained significantly more phenylethyl alcohol than those made with the other strains (Table 2.7). Their phenylethyl alcohol peak area was more than six times that of DADY-fermented spirits (Figure 2.4). The strong dependence of higher alcohols such as phenylethyl alcohol on yeast strain is revisited in Chapter 3, where the same experimental design was applied to maize.

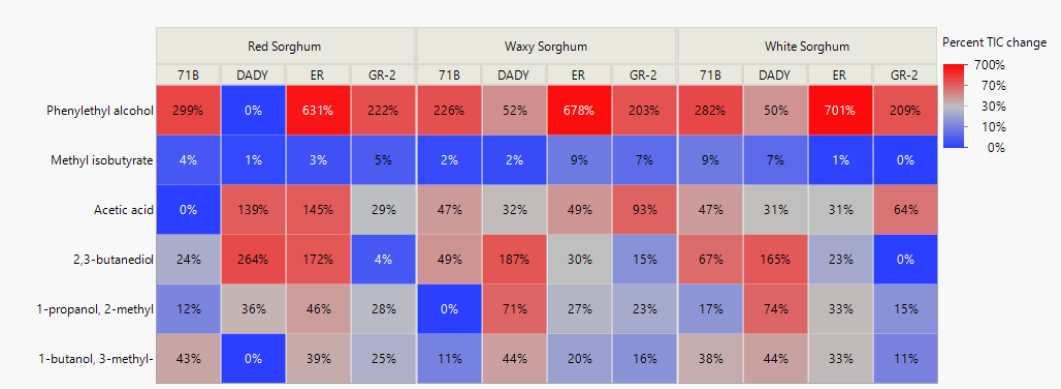


Figure 2.4: Total ion current (TIC) peak areas of the major volatile compounds identified in the fermented sorghum broths. Mean peak areas (triplicate measurements) are shown as the percent increase relative to the smallest peak area observed for that compound among the samples.

2.4 Conclusions

This chapter evaluated the fermentation performance of three US sorghum varieties with four yeast strains for distilled spirit production. It also examined how variety and strain affected alcohol and coproduct yields and the formation of volatile compounds. Alcohol concentration

Table 2.6: Analysis of variance for the effects of sorghum variety, yeast strain, and their interaction on the TIC peak area of selected volatile compounds. Significance was assessed with partial F-tests; p-values are shown.

	p-value		
Volatile compound[a]	Sorghum	Yeast	Sorghum × yeast
2-Methyl-1-propanol	0.2792	< 0.0001	< 0.0001
Methyl isobutyrate	0.8175	0.9638	0.4077
Acetic acid	< 0.0001	< 0.0001	< 0.0001
3-Methyl-1-butanol	0.0017	< 0.0001	< 0.0001
2,3-Butanediol	< 0.0001	< 0.0001	< 0.0001
Phenylethyl alcohol	< 0.0001	< 0.0001	< 0.0001

[a]3-(Methylthio)-1-propanol and 4-hydroxybenzeneethanol were also detected in all fermented broths, but their TIC peaks were too small to integrate reliably.

Table 2.7: Tukey's test for the effect of yeast strain on the TIC peak area of selected volatile compounds ($\alpha = 0.05$). Strains not sharing a letter differ significantly; A denotes the highest and D the lowest peak area.

Volatile compound	DADY	Ethanol Red	GR-2	71B
2-Methyl-1-propanol	A	B	C	D
Methyl isobutyrate	–	–	–	–
Acetic acid	AB	A	B	C
3-Methyl-1-butanol	A	A	B	A
2,3-Butanediol	A	B	C	D
Phenylethyl alcohol	D	A	C	B

–: the effect of yeast strain on this compound was not significant.

ranged from 10.26 to 11.34% (v/v) and yield from 80.93 to 90.77%. Sorghum variety had a significant effect on both. Ethanol Red gave the highest average concentration (11.10%, v/v) and yield (87.33%) on every substrate, although the overall effect of yeast strain was not statistically significant. Waxy sorghum outperformed white and red sorghum in both average concentration (11.20% vs. 10.74% and 10.28%, v/v) and yield (89.65% vs. 84.74% and 82.27%). Starch structure (amylopectin content and ease of swelling) and tannin content were the grain properties most closely associated with these differences. Glycerol and lactic acid were the main byproducts. Glycerol formation depended strongly on yeast strain, with DADY producing the most and GR-2 the least. Lactic acid remained below about 0.10% (v/v; 1.2 g/L) under all conditions. Eight major volatile compounds were identified in the fermented broths, and they are associated mainly with fruity, sour, sweet, floral, buttery, and creamy flavors.

These results show that US sorghums, particularly waxy varieties, are well suited to liquid-state spirit fermentation. They also show that the substrate and the yeast both shape the primary-fermentation stage of the process proposed in Chapter 1. Chapter 3 applies the same approach to maize, the grain most commonly used in liquid-state baijiu and American whiskey, and extends it to specialty blue, red, and white maize varieties.

Chapter 3

Blue, Red, and White Maize as Sustainable Resources for Distilled Spirit Production

This chapter is adapted from the following published article: Weiss, T., Barretto, R., Chen, G., Hong, S., Li, Y., Zheng, Y., Sun, X.S., and Wang, D. (2023). Blue, red and white maize as a sustainable resource for production of distilled spirit. Journal of Agriculture and Food Research, 14, 100770. https://doi.org/10.1016/j.jafr.2023.100770. *The article is published open access under a CC BY-NC-ND license, and it is included here under the author rights retained by the author for use in a thesis or dissertation. The text has been edited for consistency with the rest of this dissertation.*

Chapter Overview

Chapter 2 showed that the primary fermentation stage of a liquid-state spirit process depends strongly on grain starch properties and on the yeast strain. Liquid-state baijiu in China is most often made from maize rather than sorghum, and maize is also the dominant grain in American whiskey and vodka. This chapter applies the same experimental framework to four maize varieties: yellow dent, white, blue, and red. Each was fermented with four commercial *Saccharomyces cerevisiae* strains (GR-2, DADY, HG-1, and USW-6). Because the distillates

were analyzed by headspace SPME GC–MS, a much larger set of esters was detected than in Chapter 2. These include the medium- and long-chain ethyl esters that define many baijiu styles (Chapter 1).

Blue maize gave the highest average alcohol concentration (12.42%, v/v) and the numerically highest average yield (about 90%) of the four varieties, although its yield did not differ significantly from that of yellow or red maize. Red maize fermented about as efficiently as yellow dent maize (89.0% vs. 89.3%), while white maize was less efficient (85.9%). Average alcohol concentration was similar for white (11.9%) and yellow maize (12.0%) and lower for red maize (11.5%). Yeast strain also had a significant effect. GR-2 gave the highest average alcohol concentration (12.18%, v/v) and yield (90.16%) averaged across varieties and was the top strain on white, yellow, and blue maize (HG-1 performed slightly better on red maize); HG-1 and USW-6 performed similarly (about 11.94% and 88.35%), and DADY gave the lowest values. Glycerol and lactic acid remained low in the distillates, with lactic acid below 0.1% (v/v). 3-Methyl-1-butanol, ethyl octanoate, ethyl tridecanoate, and ethyl 9-oxononanoate were the most abundant volatile compounds and give maize spirits their characteristic alcoholic, fruity, sweet, and floral profile. Overall, blue, red, and white maize, and blue maize in particular, are viable and sustainable raw materials for spirit production.

3.1 Introduction

As outlined in Chapter 2, the distilled spirits market is large and growing. The global alcoholic beverage market was estimated at about $1.48 trillion in 2021 and is expected to reach about $2.8 trillion by 2028 [89]. The U.S. alcoholic beverage market was worth about $250 billion in 2021, and spirits made up more than 30% of U.S. alcohol sales [90]. By volume, vodka is the best-selling spirit in the United States, followed by whiskey and gin [124]. In 2021, about 78.1 million 9-liter cases of vodka, 76.5 million cases of whiskey, and nearly 10 million cases of gin were sold. Most of these spirits are produced from maize, wheat, and rye, although some vodkas are made from potatoes.

Maize is well suited to the production of baijiu, vodka, whisky, and gin [125, 126]. It is

the most widely used grain for distilled beverages in North America. Many vodkas are made entirely from maize, and bourbon must contain at least 51% maize in its mash bill (typically 70–80%). Some straight corn whiskeys use more than 90% maize, and Abasolo, the first Mexican whiskey, is made entirely from maize [99, 125, 126]. Maize also gives the highest alcohol yield of the common spirit grains. In one study, maize gave a significantly higher ethanol yield (86.94%) than sorghum (80.15%) [97]. Another comparison of maize, wheat, and sorghum likewise found the highest fermentation efficiency for maize (87.5–89.9%), compared with wheat (86.6–87.6%) and sorghum (85.6–88.9%) [127].

Genetics (variety) and environment (soil, climate, and agronomic management) can both affect spirit yield, quality, flavor, and coproduct formation [125]. Arnold et al. [125] studied four yellow dent maize hybrids grown at four locations in Texas and their effects on bourbon flavor and alcohol yield. Variety, location, and their interaction all significantly affected important sensory attributes. Variety accounted for 32% and location for 24% of the variation in alcohol yield. Starch composition also matters. Agu et al. [128] found a higher whiskey alcohol yield from yellow maize (475–477 L per dry ton) than from white maize (468 L per dry ton). Amylose content also strongly affects fermentation efficiency [127]. With cooking at 95°C, efficiency fell as amylose content rose: 89.6% for waxy maize (<5% amylose), 88.7% for normal maize (25%), 80.4% at 35% amylose, 61.8% at 55%, and 52.9% at 70%. These studies clarify how variety, growing environment, and starch composition influence maize spirit fermentation. However, they are almost entirely limited to yellow dent maize, and only one included white maize. Very little is known about the potential of blue, red, and white maize for distilled spirits.

Maize variety may also affect the flavor profile of the spirit, which is a key quality attribute. Maize spirits are generally sweeter than spirits from other grains [126]. Grain composition, including starch composition and amino acid content and profile, can influence spirit flavor [125]. Red and blue maize are thought to contain more polyphenols than yellow maize. Polyphenols contribute color as well as sour, bitter, and astringent notes [129], so these pigmented varieties may enrich the flavor of the resulting spirits.

Yeast strain also plays a major role in both alcohol yield and flavor formation. The yeast's

main role is to convert glucose to ethanol, but it also produces coproducts and secondary metabolites, including volatile compounds. For example, some yeasts can decarboxylate phenolic acids and polyphenols to form flavor-active volatile phenols, and some can reduce these compounds further, changing their sensory character entirely [130]. Substrate and yeast therefore interact, and this interaction may affect the quality of the spirit.

The objectives of the work described in this chapter were to (1) assess blue, red, and white maize as sustainable raw materials for distilled spirits, (2) determine how maize variety and yeast strain affect alcohol yield, alcohol concentration, coproducts, and volatile flavor compounds, and (3) identify interactions between yeast strain and maize variety in maize spirit production.

3.2 Materials and Methods

3.2.1 Maize samples

Four open-pollinated maize varieties were obtained from Hoss Tools (Norman Park, GA, USA): Reid's Yellow Dent, Hickory King (white), Ohio Blue, and Jimmy Red. Each sample was cleaned on a Gamet sieve shaker (Dean Gamet Mfg. Co., Minneapolis, MN) fitted with a 4.76-mm (12/64-in) triangular-hole sieve to remove broken kernels and fine foreign material, and larger broken kernels and debris were removed by hand. Clean grain was milled in an Udy cyclone mill (Udy, Fort Collins, CO) with a 1.0-mm screen. The flour was sealed in plastic bags and stored in a closed plastic container at 4°C until use.

3.2.2 Chemical, physical, and thermal properties of maize

Moisture was measured by AOAC method 930.15. Starch was measured with a Megazyme total starch assay kit (Bray, Ireland) following AACC method 76-13. Crude protein was measured by combustion nitrogen analysis (AOAC 990.03) with a conversion factor of 6.25. Crude fat and ash were measured by AOAC methods 920.39 and 942.05, respectively. Crude fiber was measured by the filter bag technique (AOCS Ba 6a-05) [131]. Breakage suscepti-

bility was measured with a Stein breakage tester (Fred Stein Laboratories, Inc., Atchison, KS, USA). Hundred-kernel weight was the mass of 100 kernels, measured in triplicate. Test weight (pounds per volumetric bushel) was measured by the standard ASABE method, and true kernel density was measured by toluene displacement [132]. Starch gelatinization temperatures and enthalpy were measured by differential scanning calorimetry (DSC; Q200, TA Instruments, Schaumburg, IL, USA). Pasting properties were measured with a Rapid Visco Analyser (RVA-3c, Newport Scientific Ltd., Warriewood, Australia) using the same 13-min profile described in Chapter 2. Maize flour (4.0 g at 14% moisture) was mixed with 25 mL of water at 50°C, held for 1 min, heated to 95°C, held for 2.5 min, cooled to 50°C, and held for 2 min.

3.2.3 Selection of yeast strains

Four commercial *S. cerevisiae* strains used for vodka and whiskey production were selected (Table 3.1): SafSpirit GR-2 (GR-2; Fermentis, Marcq-en-Barœul, France), Red Star Distillers Active Dry Yeast (DADY), SafSpirit HG-1 (HG-1), and SafSpirit USW-6 (USW-6) (Lesaffre, Milwaukee, WI, USA). They were chosen on the basis of preliminary trials, published results [130], and the sorghum work in Chapter 2 [133]. Relative to Chapter 2, Ethanol Red and 71B were replaced by HG-1 and USW-6, which are marketed specifically for grain spirits and American whiskey. GR-2 is intended for neutral alcohol, especially grain vodka. DADY was selected for distillers' grain-mash fermentations and is used for light whiskey and neutral spirits. USW-6 is widely used by bourbon and American whiskey distillers and performs well on a range of grains and grain blends. HG-1 tolerates up to 18% (v/v) ethanol, is suitable for very-high-gravity fermentation, gives a neutral alcohol profile, and works with all common grains.

Table 3.1: Commercial yeast strains used for maize spirit production.

Supplier	Strain	Fermentation temperature	Intended products
Fermentis (Lesaffre)	SafSpirit HG-1	20–32°C	Neutral alcohol for all types of spirits
Fermentis, France	SafSpirit GR-2	20–32°C	Very neutral alcohol, especially vodka
Fermentis, United States	Red Star Distillers Active Dry Yeast (DADY)	32°C	Ethanol, light spirits, and whiskeys
Lesaffre, United States	SafSpirit USW-6	25–35°C	American whiskeys

3.2.4 Liquefaction and simultaneous saccharification and fermentation

Liquefaction and fermentation followed the procedure in Section 2.2.4, with a few changes. Slurries of 30% maize flour (db) were liquefied with α-amylase (240 KNU/g starch; Novozymes, New York, NY) in a water-bath shaker. The bath was ramped from 70 to 90°C, held briefly at 90°C with shaking at 180 rpm, and then held at 85°C for 60 min. After the mash had cooled, it was adjusted to about pH 4.2 with 2 M HCl. Each dry yeast (1.0 g) was rehydrated in 19 mL of preculture medium (per liter: 20 g glucose, 5.0 g peptone, 3.0 g yeast extract, 1.0 g KH_2PO_4, and 0.5 g $MgSO_4 \cdot 7H_2O$) at 38°C and 200 rpm for about 30 min. Each flask received 1.0 mL of activated culture (approximately 2.8×10^8 cells/mL), 100 µL of Spirizyme glucoamylase (Novozymes, Franklinton, NC), and 0.30 g of yeast extract. The flasks were sealed with S-type airlocks filled with mineral oil and incubated at 32°C and 150 rpm for 72 h. The broth was sampled for chemical analysis at intervals and at the end of fermentation. The finished mash was then transferred, with four 25-mL rinses of distilled water, to a 500-mL distillation flask. It was distilled on a Kjeldahl-type distillation apparatus into a 100-mL volumetric flask held in ice water, and distillation was stopped when about 50 mL of distillate had been collected.

3.2.5 Analytical methods

Ethanol, glycerol, and lactic acid in the mash and distillates were quantified by HPLC under the conditions described in Section 2.2.5: Aminex HPX-87H column at 60°C, refractive index detector at 45°C, and 5 mM H_2SO_4 at 0.6 mL/min. Alcohol yield was calculated as the measured ethanol mass divided by the theoretical ethanol mass, starch (g) × 1.11 × 0.511 [101].

Volatile compounds in the distilled spirits were extracted by headspace solid-phase microextraction (HS-SPME), following Tábua et al. [115] with minor modifications. Each 10-mL SPME vial received 1 mL of sample, 2 mL of distilled water, and 0.5 g of anhydrous sodium chloride. 1-Hexanol was added as an internal standard to a final concentration of 5.89 µg mL^{-1}. Vials were equilibrated in a 60°C water bath for 10 min with agitation, extracted for 20 min, and desorbed in the GC injector. Analysis was performed on a Shimadzu QP2010-SE GC–MS (Shimadzu Corp., Kyoto, Japan) fitted with a ZB-WAXplus capillary column (30 m × 0.25 mm i.d. × 0.25 µm; Phenomenex, Torrance, CA, USA). The oven was held at 40°C for 2 min, ramped at 5°C min^{-1} to 100°C, then ramped at 10°C min^{-1} to 240°C and held for 20 min. Mass spectra were acquired in electron-impact mode at 70 eV with a source temperature of 200°C over 35–350 amu. Compounds were identified by comparison with the NIST 08 spectral library. They were semi-quantified from peak areas as relative concentrations, expressed as 1-hexanol equivalents.

3.2.6 Statistical analysis

All fermentations were performed in duplicate. Data were compiled in Microsoft Excel (Microsoft Corporation, Redmond, WA), and means were compared by LSD at $p < 0.05$. ANOVA of the volatile data, testing maize variety, yeast strain, and their interaction, was performed in OriginPro 9.0 (OriginLab Corporation, Northampton, MA). Cluster analysis and plotting were done with Matplotlib [134].

3.3 Results and Discussion

3.3.1 Physical and chemical properties of the maize varieties

The physical properties of the four maize varieties are given in Table 3.2. They differed significantly in hundred-kernel weight (24.34–44.38 g), breakage susceptibility (1.36–1.68%), and test weight (62.65–64.94 lb/bu). White maize had the heaviest kernels and yellow maize the lightest. Red maize had the highest test weight and kernel density, and white maize had the lowest test weight.

Table 3.2: Physical properties of the maize varieties.

Maize	100-kernel weight (g)	Breakage susceptibility (%)	Kernel density (g/cm^3)	Test weight (lb/bu)
White	44.38 ± 0.75	1.36 ± 0.18	1.27 ± 0.01	62.65 ± 0.55
Yellow	24.34 ± 0.16	1.41 ± 0.35	1.26 ± 0.01	63.13 ± 0.13
Red	32.37 ± 0.57	1.68 ± 0.15	1.28 ± 0.01	64.94 ± 0.09
Blue	28.10 ± 0.18	1.67 ± 0.12	1.25 ± 0.01	63.77 ± 0.22

Values are mean ± standard deviation.

The chemical composition of the maize varieties is given in Table 3.3. Starch ranged from 65.24 to 70.44% (db), which falls within the 63.60–74.0% (db) range reported previously [108, 125, 135–137]. Protein ranged from 9.06 to 11.15% (db), and varieties with more starch tended to have less protein. Blue maize had the highest starch (70.44%, db) and the lowest protein (9.06%, db), while red maize had the lowest starch (65.24%, db) and the highest protein (11.15%, db). Crude fat ranged from 3.93 to 5.45% (db). Crude fiber (1.49–1.92%, db) and ash (1.42–1.76%, db) were below 2% in all varieties. All four contained small amounts of tannin. Blue maize contained the most (0.585%), followed by red (0.113%), yellow (0.023%), and white maize (0.017%). All four were therefore far lower than the high-tannin red sorghum in Chapter 2 (3.61%).

Table 3.3: Chemical composition of the maize varieties.

Maize	Moisture (%, w/w)	Starch (%, db)	Crude protein (%, db)	Crude fat (%, db)	Crude fiber (%, db)	Ash (%, db)	Tannins (%, db)
White	7.77 ± 0.03	69.86 ± 0.81	10.75 ± 0.07	5.04 ± 0.04	1.56 ± 0.02	1.43 ± 0.07	0.017 ± 0.001
Yellow	10.37 ± 0.03	69.44 ± 2.33	10.61 ± 0.57	3.93 ± 0.01	1.92 ± 0.04	1.50 ± 0.08	0.023 ± 0.004
Red	8.59 ± 0.03	65.24 ± 0.73	11.15 ± 0.03	5.45 ± 0.02	1.75 ± 0.02	1.76 ± 0.14	0.113 ± 0.009
Blue	8.96 ± 0.07	70.44 ± 0.50	9.06 ± 0.11	4.71 ± 0.06	1.49 ± 0.09	1.42 ± 0.06	0.585 ± 0.039

Values are mean ± standard deviation.

3.3.2 Alcohol concentration and yield

Table 3.4 shows the effects of maize variety and yeast strain on alcohol concentration and yield. Alcohol concentration ranged from 11.30 to 12.64% (v/v), and yield ranged from 84.03 to 91.37%. Both maize variety ($p < 0.0001$) and yeast strain ($p \approx 0.02$) had significant effects, and their interaction did not ($p = 0.4346$; Table 3.5). GR-2 gave the highest average alcohol concentration (12.18%, v/v) and yield (90.16%) averaged across maize varieties, and it was the best strain on white, yellow, and blue maize, although HG-1 gave slightly higher values on red maize. HG-1 and USW-6 were nearly identical in average concentration (11.94% vs. 11.93%, v/v) and yield (88.37% vs. 88.33%). DADY had the lowest average concentration (11.84%, v/v) and yield (87.29%). High, consistent alcohol concentration is desirable for product consistency, so GR-2 is the recommended strain for maize spirit production. In Chapter 2, the fuel-ethanol strain Ethanol Red was the most efficient strain on sorghum. Together, the two chapters show that the most efficient yeast depends on the grain being fermented.

Yeast choice can be used to adjust spirit yield [99], but the substrate is just as critical. Maize variety significantly affected both alcohol concentration and yield ($p < 0.0001$; Table 3.5). Blue maize gave the highest average alcohol concentration (12.42%, v/v). White (11.9%) and yellow maize (12.0%) were similar, and red maize (11.5%) was lower. Fermentation efficiency was similar for red (89.0%) and yellow maize (89.3%) and lower for white maize (85.9%). Higher starch content has been associated with lower fermentation efficiency [138]. Blue maize, however, combined the highest starch content with a yield (about 90%) at least as high as any other variety. Two properties of its starch likely explain this.

Table 3.4: Effect of maize variety and yeast strain on alcohol concentration and alcohol yield.

Maize	GR-2	DADY	HG-1	USW-6	Average[b]
Alcohol concentration (%, v/v)					
White	12.28 ± 0.54	11.75 ± 0.31	11.69 ± 0.18	11.92 ± 0.12	11.91^{b}
Yellow	12.28 ± 0.03	11.75 ± 0.12	12.02 ± 0.38	11.96 ± 0.05	12.00^{b}
Red	11.55 ± 0.10	11.30 ± 0.40	11.69 ± 0.11	11.57 ± 0.11	11.53^{c}
Blue	12.64 ± 0.10	12.41 ± 0.31	12.34 ± 0.10	12.28 ± 0.30	12.42^{a}
Average[a]	12.18^{a}	11.84^{b}	11.94^{ab}	11.93^{ab}	11.97
Alcohol yield (%)					
White	88.30 ± 4.55	85.58 ± 2.23	84.03 ± 1.31	85.72 ± 0.85	85.91^{b}
Yellow	91.35 ± 0.22	87.48 ± 0.87	89.49 ± 2.82	89.05 ± 0.37	89.34^{a}
Red	89.69 ± 0.74	86.46 ± 3.08	90.81 ± 0.84	89.84 ± 0.89	89.00^{a}
Blue	91.37 ± 0.75	89.63 ± 2.26	89.15 ± 0.73	88.70 ± 2.20	89.71^{a}
Average[a]	90.16^{a}	87.29^{b}	88.37^{ab}	88.33^{ab}	88.54

Values are mean ± standard deviation of replicate fermentations. [a]Yeast-strain averages in the same row followed by different letters differ significantly ($p < 0.05$). [b]Maize-variety averages in the same column followed by different letters differ significantly ($p < 0.05$).

Table 3.5: Analysis of variance for the effects of maize variety, yeast strain, and their interaction on final ethanol concentration and ethanol yield.

	Ethanol concentration (%, v/v)			Ethanol yield (%)		
Source of variation	df	F	p	df	F	p
Maize variety	3	23.00	< 0.0001	3	10.59	< 0.0001
Yeast strain	3	3.76	0.0202	3	3.77	0.0200
Variety × strain	9	1.02	0.4468	9	1.04	0.4346

First, DSC showed that blue maize starch had the lowest onset (61.89°C), peak (72.80°C), and end (81.75°C) gelatinization temperatures of the four varieties. It also had a relatively low gelatinization enthalpy (6.40 J/g; Table 3.6). Blue maize starch therefore gelatinizes at lower temperature and with less energy, and this greater digestibility more than offsets its high starch content. Second, RVA showed that blue maize had the lowest pasting temperature (77.45°C), setback viscosity (1022 cP), and final viscosity (1847 cP) (Figure 3.1). Its starch therefore swells and disintegrates more easily than that of the other varieties. This is the same behavior that distinguished waxy sorghum in Chapter 2. White maize, which gave the lowest yield, had the highest peak viscosity and a relatively high pasting temperature (Table 3.6 and Figure 3.1). The contrast between blue and white maize highlights how strongly starch properties govern fermentation performance. The effect of polyphenols was not tested directly, but tannin content was below 1% in every variety, far lower than in the red sorghum of Chapter 2, so a substantial tannin effect on viscosity or gelatinization is unlikely. Chapter 4 builds on this link between starch swelling and conversion. It asks whether partial swelling below the gelatinization temperature can replace high-temperature cooking altogether.

Table 3.6: Starch gelatinization properties of the maize varieties measured by differential scanning calorimetry.

Maize	Onset (°C)	Peak (°C)	End (°C)	Enthalpy (J/g)
White	67.62 ± 0.18^{b}	76.40 ± 0.05^{a}	88.74 ± 0.18^{a}	6.07 ± 0.11^{b}
Yellow	68.38 ± 0.09^{c}	76.02 ± 0.01^{b}	83.43 ± 0.73^{b}	7.20 ± 0.23^{a}
Red	68.36 ± 0.03^{a}	76.32 ± 0.00^{a}	87.80 ± 0.22^{a}	7.17 ± 0.26^{a}
Blue	61.89 ± 0.27^{d}	72.80 ± 1.50^{b}	81.75 ± 0.20^{c}	6.40 ± 1.01^{b}

Values are mean ± standard deviation of three replicates. Within each column, means followed by different letters differ significantly ($p < 0.05$).

Fermentation progress is summarized in Table 3.7, where completion is the alcohol concentration at each sampling time as a percentage of the final concentration. HG-1 fermented fastest initially and was more than 60% complete after 12 h. DADY started slowest, at 38.81% completion after 12 h. All four strains exceeded 98% completion by 60 h, so a fermentation time of 48–60 h is recommended for maize spirit fermentation. Among the maize

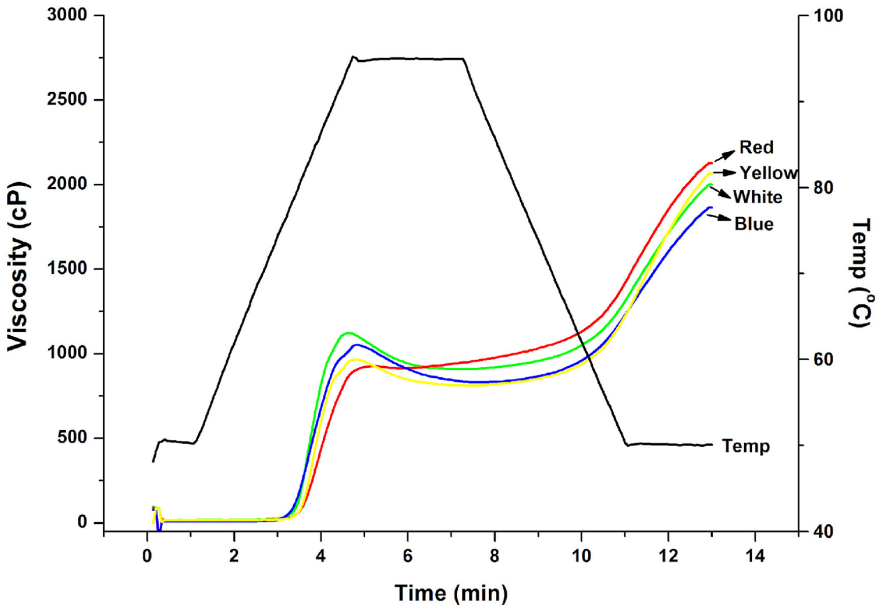


Figure 3.1: Rapid Visco Analyser pasting profiles of the four maize flours.

varieties, completion at 12 h ranged only from about 50 to 54%, and all varieties reached more than 99% by 60 h.

Table 3.7: Fermentation completion (%) over time as affected by yeast strain and maize variety.

	By yeast strain				By maize variety			
Time (h)	GR-2	DADY	HG-1	USW-6	White	Yellow	Red	Blue
0	0	0	0	0	0	0	0	0
12	54.49	38.81	60.28	55.06	52.31	51.27	50.14	53.81
24	84.43	82.04	89.04	80.54	81.66	86.82	83.92	84.47
48	97.50	97.86	98.52	98.96	97.76	98.51	97.93	98.57
60	98.56	99.46	99.61	99.67	98.88	99.51	99.41	99.53
72	100	100	100	100	100	100	100	100

3.3.3 Fermentation byproducts

Glycerol and lactic acid are the two main byproducts of alcoholic fermentation [111, 112]. Both have sensory consequences in spirits. Lactic acid tastes sour, while glycerol is sweet and gives a smoother mouthfeel. Glycerol is generally unwanted in clear spirits, but it is often added to liqueurs (about 0.15%) and whiskey (about 0.05%) [139]. In liqueurs it acts as a thickener and sweetener, and in whiskey it has been used to shorten the apparent aging

time [80]. Glycerol also has a high boiling point and is soluble in water and ethanol but not in hydrocarbons. These properties can help distillation by allowing higher-purity alcohol in a single pass [140].

Figure 3.2 shows glycerol and lactic acid levels by maize variety and yeast strain. Unlike Chapter 2, where byproducts were measured in the fermented broth, these samples came from the head fraction of the distillate, which is the fraction used industrially. Distillation reduced both glycerol and lactic acid in all samples. Glycerol (boiling point about 290°C) and lactic acid are essentially non-volatile under these conditions, so the small amounts detected in the head distillates most likely reflect mechanical carry-over (entrainment or foaming) during the small-scale distillation rather than true volatilization. The differences among treatments should therefore be interpreted with caution. Among the yeasts, HG-1 gave the highest average glycerol and GR-2 the lowest. Among the maize varieties, white maize gave the most glycerol and yellow dent maize the least. The highest single combination was blue maize with DADY, and the lowest was yellow dent maize with HG-1. For lactic acid, HG-1 gave the highest average level (about 0.05%, v/v) and USW-6 the lowest (about 0.01%, v/v). White maize gave the most lactic acid and yellow dent maize the least. The highest combination was blue maize with USW-6, and the lowest was red maize with DADY. Serafim et al. [80] found that lactic acid distills mainly into the tail fraction, which explains the low concentrations in these head distillates.

3.3.4 Volatile compounds

Fermentation also produces many volatile compounds that shape the flavor of the spirit. More than 1730 compounds have been identified in Chinese baijiu [3]. The types and amounts of volatiles strongly affect spirit quality and consumer acceptance [122]. The main classes in baijiu are acetals, acids, alcohols, aldehydes, esters, ketones, lactones, and nitrogen- and sulfur-containing compounds [91]. Which volatiles form depends on the organisms, raw material, additives, equipment, fermentation conditions, distillation, and aging [97]. Szambelan et al. [97] analyzed raw distillates from five maize varieties and found an average of

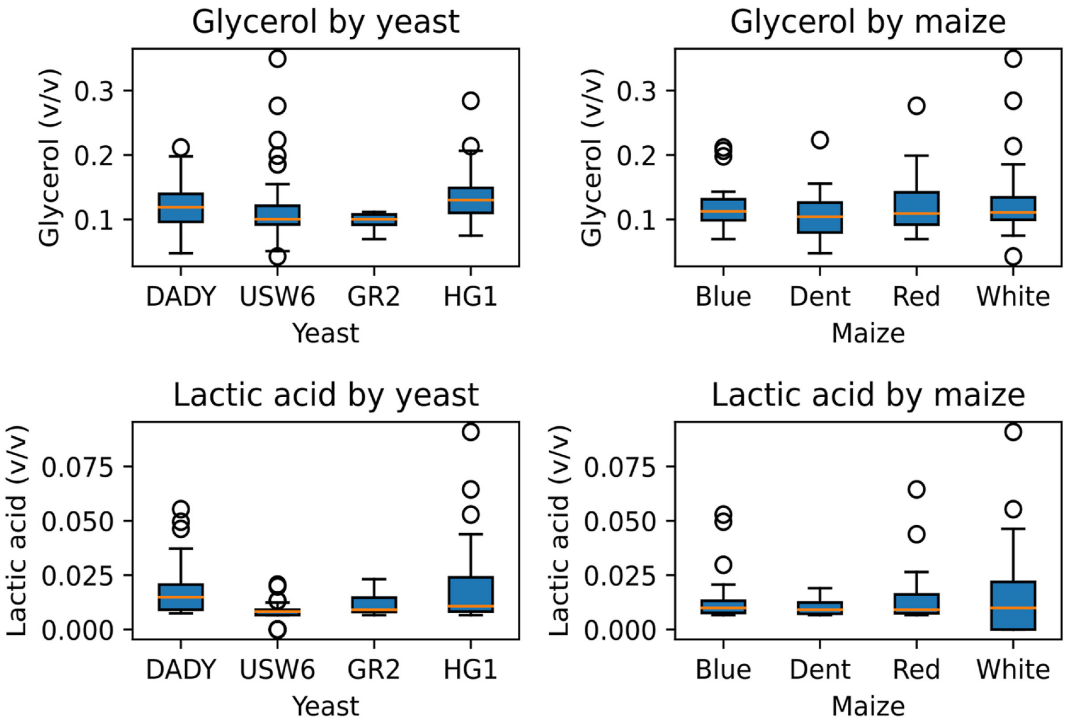


Figure 3.2: Effects of yeast strain and maize variety on glycerol and lactic acid in maize spirit distillates.

7104.22 mg/L of total volatiles. They identified 28 compounds, dominated by aldehydes, higher alcohols, esters, and ketones, using two yeasts (Ethanol Red and Fermiol) and two enzyme preparations.

In the present work, 15 volatile compounds were identified in the maize spirits at about 40% alcohol (Tables 3.8 and 3.9). They were 2-methyl-1-propanol, isoamyl acetate, 3-methyl-1-butanol, isoamyl octanoate, isoamyl decanoate, and the ethyl esters of hexanoic, heptanoic, octanoic, nonanoic, tridecanoic, tetradecanoic, hexadecanoic, oleic, and linoleic acids, plus ethyl 9-oxononanoate. They are associated mainly with fruity, sweet, alcoholic, and floral notes, which is consistent with earlier work [97]. 2-Methyl-1-propanol may contribute alcoholic and fruity aromas, while esters such as ethyl tetradecanoate may add creamy and nutty notes. 3-Methyl-1-butanol, ethyl octanoate, ethyl tridecanoate, and ethyl 9-oxononanoate were abundant in all samples. For example, white maize fermented with USW-6 contained 1464 µg mL^{-1} of ethyl octanoate, and yellow maize fermented with GR-2 contained 1988 µg mL^{-1} of ethyl tridecanoate. These compounds are associated mainly with

a baked-apple aroma. Because these values are semi-quantitative (1-hexanol equivalents, assuming equal detector response) and several lie far above the concentration of the internal standard, they should be read as relative rather than absolute concentrations. Ethyl 9-oxononanoate is also typically formed by oxidation of unsaturated grain lipids rather than by yeast metabolism, so its abundance may reflect lipid oxidation during mashing and distillation as much as fermentation. Compared with the sorghum spirits in Chapter 2, the maize spirits contained a much richer set of esters. This partly reflects the more sensitive HS-SPME method applied to the distillate. Ethyl hexanoate, the defining ester of strong-aroma baijiu (Chapter 1), was consistently one of the less abundant esters here (roughly 15–52 µg mL^{-1} as 1-hexanol equivalents), far below ethyl octanoate. With a single *S. cerevisiae* strain and no chain-elongating partner, hexanoate-derived esters therefore remained minor. This is consistent with the argument that a dedicated chain-elongation stage (Chapter 5) would be needed to approach strong-aroma profiles.

Table 3.8: Volatile compounds (µg mL^{-1})[a] in distilled spirits from white and yellow maize fermented with different yeast strains.

	White maize				Yellow maize				
Compound	USW-6	GR-2	DADY	HG-1	USW-6	GR-2	DADY	HG-1	Odor character[b]
2-Methyl-1-propanol	21.4 ± 0.1	17.1 ± 0.2	12.7 ± 0.9	26.7 ± 0.9	16.0 ± 0.3	20.5 ± 0.6	29.3 ± 0.7	13.3 ± 0.3	alcohol, apple, cocoa, malt
Isoamyl acetate	38.4 ± 0.5	73.8 ± 7.4	77.6 ± 4.9	42.3 ± 4.2	29.3 ± 4.1	81.9 ± 6.2	69.6 ± 5.5	25.9 ± 3.0	apple, banana, fruit, glue, pear
3-Methyl-1-butanol	156 ± 32	61.2 ± 9.9	191 ± 5.1	333 ± 37	229 ± 8.2	345.2 ± 8.9	287.3 ± 9.8	167 ± 26	banana, cheese, cocoa, floral
Ethyl hexanoate	51.6 ± 0.4	34.8 ± 3.5	23.7 ± 1.4	50.8 ± 0.1	32.1 ± 3.0	33.7 ± 1.5	26.6 ± 0.4	19.3 ± 2.8	anise, apple peel, brandy, cheese
Ethyl heptanoate	3.5 ± 0.1	2.9 ± 0.2	2.9 ± 0.1	7.7 ± 1.8	5.3 ± 1.5	2.1 ± 0.3	2.8 ± 0.2	3.4 ± 0.5	brandy, fruit, wine
Ethyl octanoate	1464 ± 27	873 ± 84	637 ± 23	689 ± 137	799 ± 133	805 ± 92	619 ± 46	236 ± 28	apricot, brandy, fresh, fruit
Ethyl nonanoate	35.0 ± 0.8	26.7 ± 2.7	14.0 ± 0.3	55.1 ± 13.3	24.0 ± 2.7	28.4 ± 3.1	10.1 ± 0.8	14.1 ± 1.7	banana, fruit, grape
Ethyl 9-oxononanoate	2581 ± 92	2221 ± 199	913 ± 32.4	1689 ± 342	1968 ± 186	2532 ± 247	841 ± 80	341 ± 44	baked apple
Isoamyl octanoate	190 ± 5.9	168 ± 16.8	36.7 ± 0.9	162 ± 20.4	95.0 ± 3.9	167.3 ± 15	21.3 ± 2.3	21.2 ± 2.5	baked apple
Ethyl tridecanoate	1051 ± 53	1703 ± 160	308 ± 8.8	963 ± 174	1171 ± 9.1	1988 ± 174	183 ± 27	75.2 ± 10.6	baked apple
Isoamyl decanoate	73.6 ± 4.1	155.9	10.7 ± 0.2	122 ± 21.8	61.3 ± 8.5	181 ± 15.5	4.5 ± 0.9	4.9 ± 0.6	wax, fatty
Ethyl tetradecanoate	43.0 ± 4.1	115.9	19.1 ± 1.4	83.2 ± 4.5	146 ± 5.3	172 ± 18	14.4 ± 2.0	54.6 ± 6.4	cream, ether, nut, oil, pleasant
Ethyl hexadecanoate	31.5 ± 3.7	195.0	13.7 ± 0.9	120 ± 10.4	306 ± 63	475 ± 62	16.8 ± 3.0	7.2 ± 1.2	fatty, fruit, sweet, wax
Ethyl oleate	1.7 ± 0.2	14.8	0.9 ± 0.1	11.6 ± 1.0	17.9 ± 4.8	44.5 ± 5.7	0.7 ± 0.1	0.6 ± 0.1	fatty, oily, dairy, milky
Ethyl linoleate	13.3 ± 1.6	73.2	8.5 ± 0.6	48.1 ± 4.1	157 ± 35	202 ± 25	10.2 ± 1.6	7.4 ± 1.3	fatty, fruity, oily

[a]Relative concentration expressed as equivalents of the internal standard 1-hexanol (5.89 µg mL^{-1}). [b]Odor characteristics from the spectral library.

Table 3.9: Volatile compounds (µg mL^{-1})[a] in distilled spirits from red and blue maize fermented with different yeast strains.

	Red maize				Blue maize				
Compound	USW-6	GR-2	DADY	HG-1	USW-6	GR-2	DADY	HG-1	Odor character[b]
2-Methyl-1-propanol	6.2 ± 0.9	7.1 ± 0.1	17.5 ± 2.4	10.1 ± 1.5	8.7 ± 1.7	24.2 ± 2.3	16.2 ± 0.6	25.2 ± 1.7	alcohol, apple, cocoa, malt
Isoamyl acetate	31.4 ± 2.9	30.1 ± 1.0	72.1 ± 4.9	46.3 ± 5.1	22.4 ± 1.2	93.0 ± 0.5	32.2 ± 0.6	31.2 ± 1.3	apple, banana, fruit, glue, pear
3-Methyl-1-butanol	129 ± 19	154 ± 10	216 ± 19	190 ± 17	161.3 ± 24	336 ± 3.7	181 ± 3.8	311.0 ± 60	banana, cheese, cocoa, floral
Ethyl hexanoate	41.4 ± 4.2	25.3 ± 0.1	22.1 ± 1.4	40.6 ± 1.6	24.3 ± 0.9	44.5 ± 1.3	15.1 ± 0.1	28.6 ± 2.1	anise, apple peel, brandy, cheese
Ethyl heptanoate	3.6 ± 0.3	3.1 ± 0.1	2.8 ± 0.3	4.3 ± 0.6	3.6 ± 0.2	4.6 ± 0.1	2.0 ± 0.1	4.8 ± 0.3	brandy, fruit, wine
Ethyl octanoate	959 ± 82	315 ± 5.0	586 ± 40.2	518 ± 24	594 ± 50	1063 ± 19	458 ± 29	463 ± 34	apricot, brandy, fresh, fruit
Ethyl nonanoate	19.2 ± 1.6	15.5 ± 1.3	20.9 ± 1.3	21.8 ± 0.9	32.3 ± 2.6	44.9 ± 0.6	18.1 ± 3.9	46.1 ± 3.7	banana, fruit, grape
Ethyl 9-oxononanoate	1855 ± 153	551 ± 12	1177 ± 88	1119 ± 43	1280 ± 114	2613 ± 6.6	1369 ± 64	1129 ± 91	baked apple
Isoamyl octanoate	83.7 ± 7.5	26.8 ± 0.4	51.9 ± 3.8	71.4 ± 2.7	35.9 ± 6.6	130 ± 2.0	78.9 ± 5.2	37.9 ± 3.6	baked apple
Ethyl tridecanoate	762.7 ± 69	114 ± 4.0	641 ± 52	482 ± 22	328 ± 21.5	1626 ± 21	947 ± 36	599 ± 50.7	baked apple
Isoamyl decanoate	32.0 ± 3.1	8.5 ± 0.3	23.0 ± 2.1	54.8 ± 2.6	8.4 ± 0.5	83.4 ± 2.3	63.1 ± 1.5	38.4 ± 2.9	wax, fatty
Ethyl tetradecanoate	24.2 ± 1.9	4.9 ± 0.2	34.5 ± 3.0	30.2 ± 1.9	15.3 ± 1.8	156 ± 5.0	84.3 ± 3.4	49.3 ± 2.9	cream, ether, nut, oil, pleasant
Ethyl hexadecanoate	47.5 ± 3.5	7.4 ± 0.3	31.6 ± 1.7	149 ± 14	21.1 ± 2.3	141 ± 3.9	105.2 ± 8.9	62.2 ± 2.1	fatty, fruit, sweet, wax
Ethyl oleate	3.4 ± 0.1	0.5 ± 0.0	2.1 ± 0.3	21.9 ± 2.5	1.6 ± 0.5	9.9 ± 0.1	7.8 ± 0.9	4.6 ± 0.7	fatty, oily, dairy, milky
Ethyl linoleate	21.4 ± 1.7	4.5 ± 0.1	17.1 ± 0.08	73.6 ± 7.9	20.9 ± 4.9	92.8 ± 0.6	46.2 ± 4.3	38.6 ± 1.6	fatty, fruity, oily

[a]Relative concentration expressed as equivalents of the internal standard 1-hexanol (5.89 µg mL^{-1}). [b]Odor characteristics from the spectral library.

In most cases, maize variety (Figure 3.3A), yeast strain (Figure 3.3B), and their interaction (Table 3.10 and Figure 3.4) all had significant effects on the volatile profile. Higher alcohols such as 2-methyl-1-propanol and 3-methyl-1-butanol were strongly affected by maize variety ($p < 0.0001$). Yeast strain had a significant effect on esters such as ethyl octanoate and ethyl tridecanoate ($p < 0.0001$). The cluster analysis in Figure 3.4 confirms that the yeast–maize interaction significantly affected flavor development ($p < 0.0001$). With GR-2, every variety except red maize produced large amounts of ethyl 9-oxononanoate (up to about 2500 µg mL^{-1}; baked apple), ethyl tridecanoate (baked apple), and ethyl octanoate (apricot, brandy, fresh fruit). White maize gave a good flavor yield with GR-2 and a much higher one with USW-6. The white maize–USW-6 combination produced more ethyl octanoate than any other. The yellow maize–GR-2 combination produced the widest range of flavor compounds. Yellow maize with GR-2 gave the most flavor overall, and red maize with GR-2 gave the least. The choice of yeast–substrate pairing is therefore a real design lever for flavor, in addition to yield.

Table 3.10: Significance of maize variety, yeast strain, and their interaction on the formation of each volatile compound (ANOVA p-values).

Volatile compound	Maize	Yeast	Maize × yeast
2-Methyl-1-propanol	< 0.0001	< 0.0001	< 0.0001
Isoamyl acetate	< 0.0001	< 0.0001	< 0.0001
3-Methyl-1-butanol	0.0001	0.0015	< 0.0001
Ethyl hexanoate	< 0.0001	< 0.0001	< 0.0001
Ethyl heptanoate	0.2790	0.0004	0.0095
Ethyl octanoate	< 0.0001	< 0.0001	< 0.0001
Ethyl nonanoate	< 0.0001	< 0.0001	0.0005
Ethyl 9-oxononanoate	< 0.0001	< 0.0001	< 0.0001
Isoamyl octanoate	< 0.0001	< 0.0001	< 0.0001
Ethyl tridecanoate	< 0.0001	< 0.0001	< 0.0001
Isoamyl decanoate	< 0.0001	< 0.0001	< 0.0001
Ethyl tetradecanoate	< 0.0001	< 0.0001	< 0.0001
Ethyl hexadecanoate	< 0.0001	< 0.0001	< 0.0001
Ethyl oleate	< 0.0001	< 0.0001	< 0.0001
Ethyl linoleate	< 0.0001	< 0.0001	< 0.0001

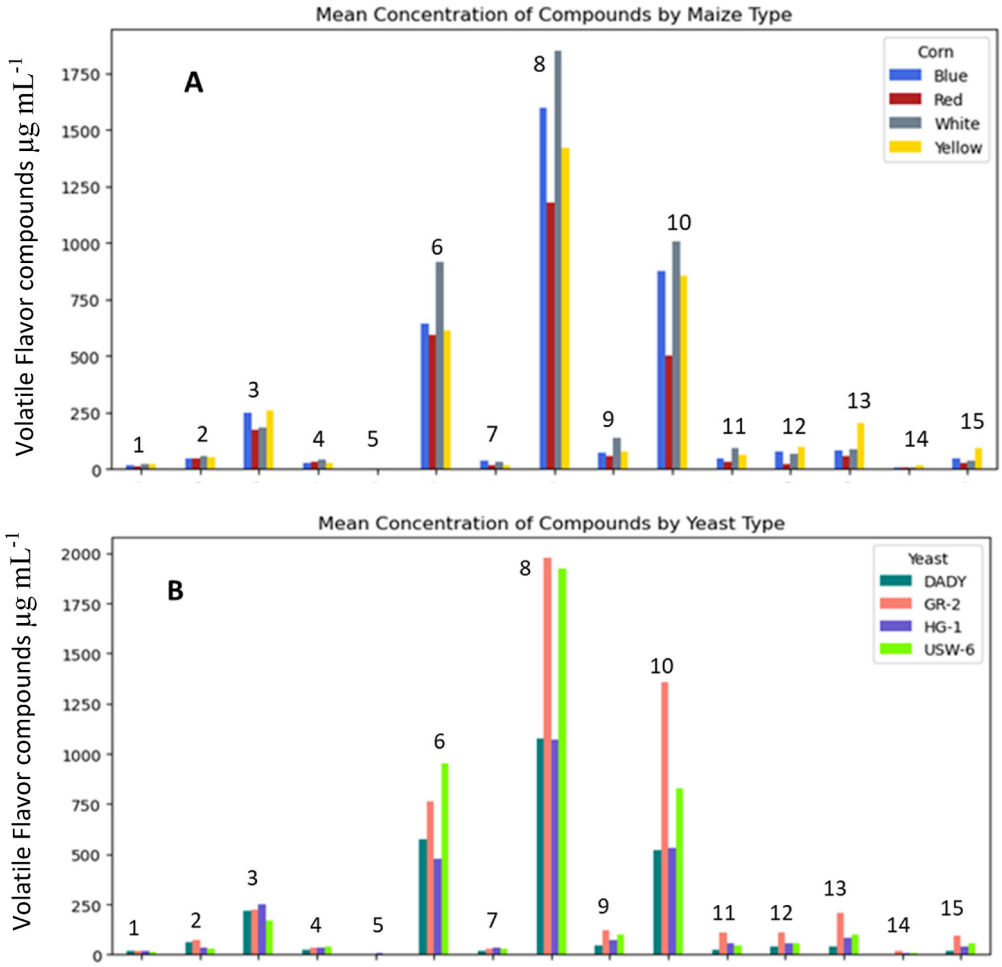


Figure 3.3: Mean concentration of volatile flavor compounds (µg mL^{-1}) produced (A) by each maize variety and (B) by each yeast strain. Compounds: 1, 2-methyl-1-propanol; 2, isoamyl acetate; 3, 3-methyl-1-butanol; 4, ethyl hexanoate; 5, ethyl heptanoate; 6, ethyl octanoate; 7, ethyl nonanoate; 8, ethyl 9-oxononanoate; 9, isoamyl octanoate; 10, ethyl tridecanoate; 11, isoamyl decanoate; 12, ethyl tetradecanoate; 13, ethyl hexadecanoate; 14, ethyl oleate; 15, ethyl linoleate. White maize gave the highest overall concentration of secondary flavor compounds, followed by blue and yellow maize; GR-2 gave the highest amounts among the yeasts, followed by USW-6.

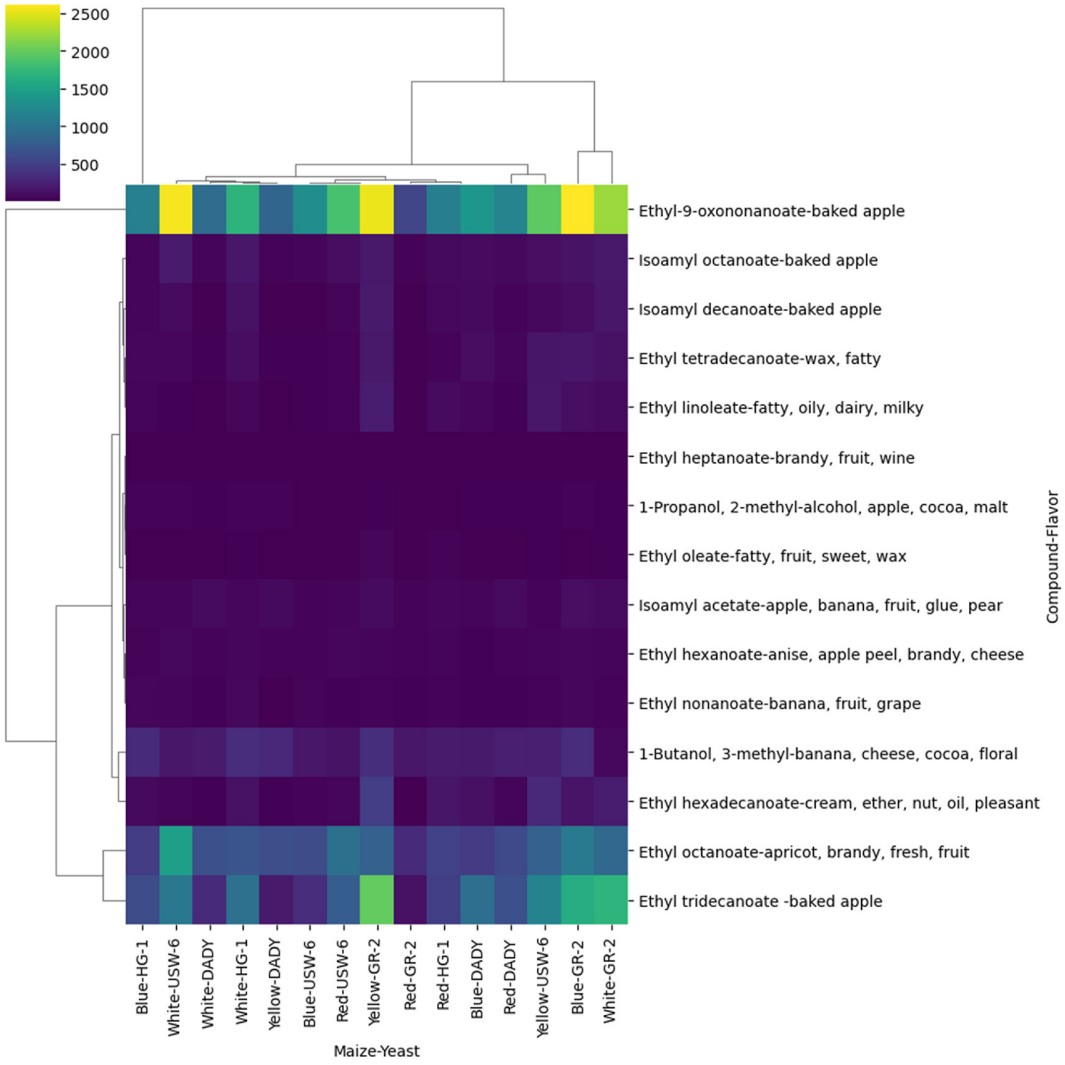


Figure 3.4: Cluster analysis of the interactions among yeast strain, maize variety, and flavor compounds. Yellow maize with GR-2 produced the most flavor, and red maize with GR-2 produced the least.

3.4 Conclusions

This chapter evaluated blue, red, and white maize as sustainable raw materials for distilled spirits. Blue maize gave the highest average alcohol concentration (12.42%, v/v) and a yield (about 90%) as high as any variety. Its easily gelatinized, readily swelling starch offset its high starch content. Red maize fermented about as efficiently as yellow dent maize (89.0% vs. 89.3%), and white maize was less efficient (85.9%). Average alcohol concentration was similar for white (11.9%) and yellow maize (12.0%) and lower for red maize (11.5%). Yeast strain also mattered. GR-2 gave the highest average alcohol concentration (12.18%, v/v) and yield (90.16%) averaged across maize varieties, HG-1 and USW-6 performed similarly, and DADY gave the lowest values. Glycerol and lactic acid were the main byproducts and remained low in the head distillates. The concentration of volatile compounds differed significantly among maize varieties and yeast strains and depended on their interaction. 3-Methyl-1-butanol, ethyl octanoate, ethyl tridecanoate, and ethyl 9-oxononanoate dominated the volatile profile.

Chapters 2 and 3 together establish how grain choice and yeast choice govern the hydrolysis and primary-fermentation stages of a liquid-state spirit process. In both grains, the ease with which starch swells and gelatinizes was the property most closely linked to conversion efficiency. Chapter 4 exploits this property directly. It uses partial starch swelling with granular starch hydrolyzing enzymes to lower the energy demand of liquefaction and to protect the protein value of the distillers' grains coproduct.

Chapter 4

Granular Starch Hydrolyzing Enzymes and Partial Starch Swelling: Ethanol Yield and Distillers' Grains Protein Quality

This chapter is adapted from the following published article: Weiss, T., Hong, S., Xiao, R., Wu, X., Li, Y., Tilley, M., and Wang, D. (2025). Assessment of granular starch hydrolysis enzyme on ethanol yield from partially swollen sorghum starch and analysis of extracted protein properties. Journal of Agriculture and Food Research, 19, 101621. https://doi.org/10.1016/j.jafr.2024.101621. Thomas Weiss and Shan Hong contributed equally to the original article. It is published open access under a CC BY-NC license and is included here under the author rights retained by the author for use in a thesis or dissertation. The text has been edited for consistency with the rest of this dissertation.

Chapter Overview

Chapters 2 and 3 showed that the ease with which grain starch swells and gelatinizes largely determines conversion efficiency in liquid-state fermentation. In those chapters, as in almost all grain distilleries and fuel ethanol plants, the starch was liquefied by cooking at 85–95°C.

Cooking is energy-intensive, and it also damages the proteins that end up in the distillers' grains (DG). DG is the main coproduct of grain fermentation and an important source of revenue for distillers and ethanol producers alike. In a staged liquid-state process like the one proposed in Chapter 1, this coproduct stream matters. The hydrolysis stage sets the energy cost of the whole process, and it also sets the value of the protein-rich solids that leave it.

This chapter tests an alternative hydrolysis stage. Granular starch hydrolyzing enzymes (GSHE) were combined with partial starch swelling below the gelatinization temperature (50, 60, or 70°C for 30 min), using waxy and normal sorghum as model substrates. Ethanol yield and the quality of the kafirin proteins extracted from the wet distillers' grains (WDG) were then compared with those from conventional 95°C liquefaction. Waxy sorghum again fermented more efficiently than normal sorghum. For waxy sorghum, partial swelling at 70°C significantly increased ethanol concentration and yield relative to unheated GSHE fermentation; for normal sorghum the gains were small and not statistically significant. Swelling did not reduce protein quality. GSHE fermentation after swelling at 70°C for 30 min gave the highest ethanol concentration (12.02%, v/v) and yield (92.74%), both from waxy sorghum. Protein digestibility remained high after swelling at 70°C for both waxy (85.39%) and normal sorghum (85.21%). Surface hydrophobicity of the DG proteins increased relative to raw flour under most treatments. Partial swelling also produced markedly lighter (higher L^*) protein isolates. Molecular characterization showed how each process changed protein structure. Together, the results show that low-temperature swelling combined with GSHE can raise ethanol efficiency while producing higher-value distillers' grains.

4.1 Introduction

Bioethanol, produced by microbial fermentation of sugars, is a sustainable alternative to gasoline for transportation [141, 142]. Most of these sugars come from starchy crops such as corn, sorghum, and wheat. Conventional ethanol production from grain involves grinding, gelatinization, liquefaction, saccharification, fermentation, and distillation. The same

sequence is used in the spirits processes described in Chapters 2 and 3. α-Amylase and glucoamylase convert starch to fermentable sugars during liquefaction and saccharification. Gelatinization, however, requires high-temperature cooking, usually jet cooking at 100–170°C with a thermostable α-amylase [143]. This cooking step has been estimated to account for roughly 30–40% of the process energy used in conventional ethanol production [144, 145]. It also degrades the functional properties of the proteins in the resulting distillers' grains.

Granular starch hydrolyzing enzymes (GSHE) offer a way to address both problems. GSHE hydrolyze starch below its gelatinization temperature, even at yeast fermentation temperatures, which greatly reduces energy use [146–151]. They are synergistic blends of α-amylase and glucoamylase that convert granular starch to glucose under mild conditions. Because the grain is never cooked, DG protein quality should be better preserved, while starch conversion remains effective.

Native, uncooked starch granules resist enzymatic attack, so conversion to fermentable sugar is usually lower than in conventional processing [149, 152]. Mild heating below the gelatinization temperature, however, can substantially improve hydrolysis. Shariffa et al. [153] treated tapioca and sweet potato starches at 35–60°C before hydrolysis with GSHE. After 24 h, the dextrose equivalent of the heat-treated starches was 36–50% higher for tapioca and 27–34% higher for sweet potato than for the native starches. Li et al. [147] studied how granule swelling affects saccharification of normal corn starch by GSHE between 40 and 90°C. Granules pretreated at 67.5°C for 30 min converted to glucose at 32°C about three times faster than native starch at 4 h, and 26% more starch had converted by 24 h. Partial swelling therefore appears able to increase hydrolysis efficiency and, potentially, ethanol yield. Low-temperature processing also prevents the formation of amylose–lipid complexes, which form during starch cooking above about 85°C and resist hydrolysis [154]. Partial swelling at about 60°C is therefore not expected to form these complexes.

Sorghum is a drought-tolerant tropical grass that produces relatively high yields in semi-arid and arid regions too dry for corn [110]. More than 30% of the U.S. corn crop is now converted to ethanol [155]. About 95% of U.S. ethanol comes from corn and only about 3% from grain sorghum [156]. Sorghum's composition is similar to that of corn, so it remains an

underused ethanol feedstock with room to grow, particularly in sorghum-producing regions of the United States. The distillers' grains left after fermentation are valuable nitrogen sources for livestock and poultry feed [106, 157]. Sorghum contains more protein than corn, and sorghum DG with 30–40% protein is a good source of extractable proteins, especially kafirins [106].

Protein extraction is widely used in the agricultural, feed, pharmaceutical, and food industries [158]. Conventional extraction with solvents or pH adjustment is well established but energy- and chemical-intensive. Newer techniques, including ultrasound-, microwave-, ohmic-heating-, supercritical-fluid-, and pulsed-electric-field-assisted extraction, have been used to recover proteins, lipids, and bioactive molecules from food waste, plant material, and microalgae [159, 160]. Enzymatic hydrolysis of kafirins has also attracted attention as a sustainable route to functional and bioactive peptides with antioxidant and other health-promoting properties [161–163]. These peptides suggest new value-added uses for sorghum DG [162].

High-temperature cooking, however, lowers protein solubility and digestibility, reducing nutritional value for both animal feed and human food. It also impairs the antioxidant and other bioactivities of peptides derived from sorghum DG. Reduced digestibility results mainly from protein denaturation during cooking and from cross-links between kafirin and other grain components, including polyphenols, lipids, and non-starch polysaccharides [164, 165]. From a processing standpoint, high-temperature cooking lowers kafirin solubility and digestibility [165]. Duodu et al. [166] showed that cooking significantly reduces the in vitro protein digestibility of sorghum.

The hypothesis tested in this chapter was that partial starch swelling combined with GSHE hydrolysis would save energy in sorghum fermentation and also yield higher-quality distillers' grains with functional proteins. The objective was to determine how partial swelling of starch granules affects sorghum ethanol yield and the quality of DG proteins. Proteins extracted from the distillers' grains were characterized for purity, digestibility, surface hydrophobicity, color, electrophoretic banding pattern, and molecular size distribution. The results clarify how the swelling step affects ethanol yield, energy use, and coproduct

quality, and therefore process economics.

4.2 Materials and Methods

4.2.1 Materials

Waxy sorghum (WS) and normal sorghum (NS) from the 2020 Kansas Performance Tests were used. Both were planted on June 13, 2020, in Colby, KS, and harvested on November 6, 2020. The grain was cleaned, milled through a 1.0-mm screen in an Udy cyclone mill (Udy Corp., Fort Collins, CO), and stored in sealed plastic bags until use.

Granular starch hydrolysis used STARGEN™ 002 (a gift from DuPont, Rochester, NY), which has a minimum activity of 570 GAU/g. One glucoamylase unit (GAU) is the amount of enzyme that releases 1 g of reducing sugar per hour from soluble starch. Conventional processing used Liquozyme α-amylase (240 KNU/g) and Spirizyme glucoamylase (750 AUG/g) from Novozymes (Franklinton, NC). Fermentations used Ethanol Red dry yeast (Lesaffre, Milwaukee, WI, USA), the strain that gave the highest yield on sorghum in Chapter 2. Unless stated otherwise, chemicals were obtained from Thermo Fisher Scientific (Ward Hill, MA, USA) or Sigma-Aldrich (St. Louis, MO, USA).

4.2.2 Chemical, physical, and thermal properties of grain sorghum

Starch was measured with a Megazyme total starch kit (K-TSTA-100A; Bray, Ireland) following AACC Approved Method 76-13.01 [167]. Protein in the sorghum and DG samples was measured with a LECO nitrogen analyzer (AACC Method 46-30.01) using a conversion factor of 6.25. Fat, crude fiber, and ash were measured by AOAC methods 920.39, 962.09, and 942.05, respectively [168–170]. Kernel hardness, weight, and diameter were measured with a Single Kernel Characterization System 4100 (Perten Instruments, Huddinge, Sweden) [171]. Test weight was measured by AACC International Method 55-10.01 and converted to kg/hL. Starch gelatinization temperatures and thermal properties were measured by DSC (Q200, TA Instruments, Schaumburg, IL, USA).

4.2.3 Conventional liquefaction and simultaneous saccharification and fermentation

Conventional liquefaction and SSF followed the procedure used in the preceding chapters and in Zhao et al. [106]. A liquefaction buffer was prepared by dissolving 1.0 g KH_2PO_4 and 200 µL of α-amylase in 1 L of distilled water and warming it to 70°C. Sorghum flour equivalent to 20 g of starch was mixed in a 250-mL flask with 100 mL of the preheated buffer containing 20 µL of Liquozyme α-amylase. Each flask was covered with aluminum foil and placed in a 70°C rotary water-bath shaker at 180 rpm. The bath was heated to 95°C over 40 min and then held at 86°C for 60 min. The flasks were then removed, cooled to room temperature, and adjusted to about pH 4.2 with 2 N HCl.

Yeast culture broth contained, per liter of distilled water, 20.0 g glucose, 5.0 g peptone, 3.0 g yeast extract, 1.0 g KH_2PO_4, and 0.5 g $MgSO_4 \cdot 7H_2O$, and was autoclaved at 121°C for 20 min. Dry yeast (1 g) was added to 19 mL of broth and incubated at 38°C for 20 min, giving about 10^9 cells/mL [172]. SSF was started by adding 100 µL of glucoamylase, 1.0 mL of activated yeast culture, and 0.3 g of yeast extract to each flask. The flasks were sealed with airlocks and incubated in a rotary shaker (Model I2400, New Brunswick Scientific Inc., Edison, NJ, USA) at 32°C and 150 rpm for 72 h.

4.2.4 Fermentation using GSHE with partial starch swelling

Ground sorghum (about 30 g, equivalent to 20 g of starch) and 0.1 g of KH_2PO_4 were added to 250-mL Erlenmeyer flasks containing 100 mL of deionized water. The mixtures were left for 10 min or until the flour was fully dispersed, and any clumps were broken up with a spatula. Each flask and its airlock stopper were weighed before loading so that final liquid volume could be determined accurately. Flasks were placed in an orbital shaker bath (Model 290400 Hot Tub, Boekel Scientific, Feasterville, PA) preheated to the swelling temperature (50, 60, or 70°C) and shaken at 25 rpm for 30 min. A control was not heated (GSHE at 35°C). After swelling, the flasks were cooled to room temperature (about 25°C) and adjusted to pH 4.5–5.0 with 2 N HCl. Each flask then received 0.3 g of yeast extract, about 50 µg/L

of chloramphenicol (from a stock of 1 g in 200 mL of sterile deionized water) to suppress bacterial growth, 0.65 mL of STARGEN™ 002 (20 GAU/g starch), and 1 mL of activated yeast culture. The flasks were resealed, weighed, and incubated at 35°C and 150 rpm for 72 h. At the end of fermentation, the flasks were reweighed to determine mass loss, and the contents were centrifuged at 3000 rpm for 15 min (Allegra 6R, Beckman Coulter Inc., Indianapolis, IN) to separate liquid and solids.

4.2.5 Ethanol concentration and yield

Ethanol in the fermentation broth was measured by HPLC (1260 system, Agilent, Santa Clara, CA) under the conditions used throughout this dissertation: HPX-87H column at 60°C, 0.005 M H_2SO_4 at 0.6 mL/min, and refractive index detection at 45°C. Ethanol yield was calculated as the measured ethanol divided by the theoretical ethanol from the 20 g of starch in each flask. The calculation assumed that 1 g of starch yields 1.11 g of glucose and that 1 g of glucose yields 0.511 g of ethanol.

4.2.6 Protein isolation from wet distillers' grains

Proteins were extracted directly from wet distillers' grains (WDG) rather than from dried distillers' grains (DDG). Kafirin was isolated by the method of Zhao et al. [106]. Ethanol, sodium hydroxide, and sodium metabisulfite were added to the WDG in a metal container to give a slurry containing 70% (v/v) ethanol, 0.35% (w/v) NaOH, and 0.50% (w/v) sodium metabisulfite. The slurry was stirred in a 70°C water bath for 1 h, cooled at room temperature for 1 h, and centrifuged at 4000 g for 10 min. The clarified supernatant was transferred to a beaker and adjusted to about pH 2.5 with 2 N HCl. Its ethanol concentration was then brought to 50% with distilled water. The beaker was held at −20°C overnight to precipitate kafirin. The precipitate was recovered by centrifugation at 4000 g for 10 min, frozen at −20°C, and lyophilized.

4.2.7 Protein digestibility

In vitro digestibility of proteins extracted from sorghum flour and WDG was measured by a modification of the multienzyme method of Hsu et al. [173]. The main change was a smaller volume of protein solution, which was equilibrated at pH 8 for 10 min before analysis. Protein was dissolved in water to 6.25 mg/mL (30 mL), adjusted to pH 8.00 with 1 M NaOH, and preheated to 37°C for 10 min in a shaking water bath, with the pH held at 8.0. A freshly prepared multienzyme solution (1.6 mg/mL trypsin, 3.1 mg/mL α-chymotrypsin, and 1.3 mg/mL protease) was also adjusted to pH 8.0. Three milliliters of the enzyme solution were added to the 30 mL of protein solution, and the mixture was incubated at 37°C and 200 rpm for 10 min while the pH drop was recorded. Digestibility was calculated after Tinus et al. [174]:

$$\text{Protein digestibility } (\%) = 65.66 + 18.10\,\Delta\text{pH}_{10\,\text{min}} \tag{4.1}$$

where $\Delta\text{pH}_{10\,\text{min}}$ is the pH change over 10 min from the initial pH of 8.0.

4.2.8 Surface hydrophobicity

Surface hydrophobicity was measured by the sodium dodecyl sulfate (SDS) binding method of Tang et al. [175]. Kafirin (10 mg) was dispersed in 40 mL of 0.1 mmol/L SDS and shaken at 280 rpm for 1 h at room temperature. The suspension was dialyzed (3.5 kDa cut-off) against deionized water for about 60 h. Ten milliliters of the dialyzed suspension were mixed with 25 mL of chloroform and 5 mL of methylene blue (24 mg/mL), vortexed for 30 s, and centrifuged at 2500 g for 15 min. Absorbance of the chloroform layer was read at 655 nm (UV-6300PC, VWR International, Radnor, PA, USA). Bound SDS was calculated from an SDS standard curve (0–0.025 mmol/L) and reported as µg SDS per mg protein.

4.2.9 SDS-PAGE

Each sample (100 mg) was suspended in 20 mL of phosphate-buffered saline (PBS, pH 6.8) containing 2% (w/v) SDS, shaken at 250 rpm for 1 h at room temperature, and centrifuged at 8000 g for 5 min. The supernatant was analyzed by SDS-PAGE under non-reducing and reducing conditions. For non-reducing gels, 60 µL of extract was mixed with 20 µL of 4× Laemmli buffer (Bio-Rad Laboratories, Inc., Hercules, CA, USA) and heated for 5 min in boiling water. Ten microliters were loaded onto a 4–20% Mini-PROTEAN TGX gel (Bio-Rad) and run at 200 V for about 38 min at room temperature, alongside 5 µL of Precision Plus Protein Dual Color Standards (Bio-Rad). Gels were stained with Brilliant Blue R (Sigma, St. Louis, MO, USA) for 10 min and destained with deionized water. Reducing gels were prepared the same way, except that the Laemmli buffer contained 10% (w/v) β-mercaptoethanol.

4.2.10 Size-exclusion chromatography

Molecular weight distribution of proteins from sorghum flour and WDG was analyzed by size-exclusion HPLC (SEC-HPLC) under reducing and non-reducing conditions. Samples were prepared at 5 mg/mL in PBS containing 2% (w/v) SDS (pH 6.8). For non-reducing analysis they were diluted with the same buffer. For reducing analysis, 60 µL of sample was mixed with 20 µL of 4× Laemmli buffer containing 10% (w/v) β-mercaptoethanol. Samples were boiled for 5 min, diluted to 1 mg/mL, filtered through 0.45-µm PVDF membranes (Fisher Scientific, Hampton, NH, USA), and injected (20 µL) onto an Agilent 1100 system (Agilent Technologies, Santa Clara, CA, USA) fitted with a Yarra 3 µm SEC-4000 column (7.8 × 300 mm; Phenomenex, Torrance, CA, USA). The mobile phase was water with 0.1% (v/v) trifluoroacetic acid (A) and acetonitrile (B), run at 0.7 mL/min and 30°C with the gradient 0 min, 80% A; 20 min, 70% A; 25 min, 65% A; and 40 min, 80% A. Proteins were detected at 214 nm with a diode array detector. Bovine thyroglobulin (670 kDa), bovine γ-globulin (150 kDa), and chicken egg albumin (44 kDa) (Sigma-Aldrich) were run under the same conditions as approximate molecular weight markers.

4.2.11 Color analysis

The color of kafirin extracted from raw flour, conventionally processed WDG, and GSHE-processed WDG was measured with a Minolta Chroma Meter CR-300 (Minolta Camera Co., Osaka, Japan). Results were recorded as L^* (lightness), a^* (red–green), and b^* (yellow–blue).

4.2.12 Statistical analysis

Data were compiled in Microsoft Excel (Microsoft Corporation, Redmond, WA) and analyzed by one-way ANOVA in IBM SPSS Statistics 25.0 (SPSS Inc., Chicago, IL, USA). Two-group comparisons used independent-sample t-tests in SciPy (version 1.11). Multiple comparisons used Tukey's test, and $P < 0.05$ was considered significant throughout.

4.3 Results and Discussion

4.3.1 Chemical composition, physical characteristics, and thermal properties of grain sorghum

The chemical, physical, and thermal properties of the waxy and normal sorghums are given in Table 4.1. These properties are central to both ethanol yield and distillers' grains quality. Starch, crude fat, and ash did not differ significantly between the two sorghums ($P > 0.05$). Normal sorghum contained significantly more crude protein than waxy sorghum, and waxy sorghum contained significantly more crude fiber ($P < 0.05$). Normal sorghum kernels were significantly harder than waxy kernels (hardness index 79.31 vs. 68.72; $P < 0.05$). Waxy sorghum kernels were significantly heavier. Kernel diameters were numerically similar, but the difference was still statistically significant ($P < 0.05$). Waxy sorghum also had the higher test weight, consistent with its larger kernels.

DSC showed that normal sorghum starch was more thermally stable than waxy sorghum starch. Normal sorghum had significantly higher onset (71.17 vs. 68.29°C) and peak gelatinization temperatures (76.50 vs. 74.22°C; $P < 0.05$), although end temperatures did not

Table 4.1: Chemical composition, physical characteristics, and thermal properties of the waxy and normal sorghums. Properties that differ significantly between the two sorghums ($P < 0.05$) are marked with an asterisk.

Property	Waxy sorghum	Normal sorghum
Chemical composition		
Starch (%, db)	67.91 ± 0.77	68.05 ± 0.06
Crude protein (%, db)*	11.49 ± 0.04	12.63 ± 0.25
Crude fat (%, db)	2.45 ± 0.29	2.71 ± 0.23
Crude fiber (%, db)*	1.72 ± 0.01	1.64 ± 0.02
Ash (%, db)	1.72 ± 0.01	1.72 ± 0.03
Physical characteristics		
Kernel hardness index*	68.72 ± 1.94	79.31 ± 2.63
Single kernel weight (mg)*	28.99 ± 1.20	25.24 ± 1.06
Kernel diameter (mm)*	2.53 ± 0.03	2.51 ± 0.01
Test weight (kg/hL)*	71.99 ± 0.36	70.32 ± 0.63
Thermal transitions measured by DSC		
Onset temperature (°C)*	68.29 ± 0.22	71.17 ± 0.28
Peak temperature (°C)*	74.22 ± 0.23	76.50 ± 0.08
End temperature (°C)	82.56 ± 1.77	83.47 ± 0.09
Peak height (mW)*	1.27 ± 0.11	2.04 ± 0.01
Area (mJ)*	69.96 ± 3.45	97.80 ± 4.29
ΔH (J/g)*	1.77 ± 0.09	2.45 ± 0.14

differ (83.47 vs. 82.56°C; $P > 0.05$). Normal sorghum also had a significantly larger peak height (2.04 vs. 1.27 mW). It required more energy per unit of starch gelatinized (2.45 vs. 1.77 J/g) and more total energy for gelatinization (97.80 vs. 69.96 mJ; $P < 0.05$). Waxy sorghum starch therefore needs less energy to gelatinize. This agrees with the RVA results for waxy sorghum in Chapter 2 and for blue maize in Chapter 3.

4.3.2 Effect of partial starch swelling on ethanol yield

Table 4.2 summarizes ethanol concentration and yield from conventional fermentation and from GSHE fermentation with or without partial swelling (50, 60, or 70°C for 30 min). Ethanol concentration ranged from 11.35 to 12.02% (v/v), and yield ranged from 86.35 to 92.74%, so both sorghum type and swelling treatment affected fermentation performance. Waxy sorghum generally gave higher ethanol concentrations and yields than normal sorghum, in line with previous reports that waxy sorghums yield more ethanol than non-waxy sorghums at the same starch content [107–109, 133]. The waxy sorghum here, like the one in Chapter 2, gave significantly higher ethanol concentration and yield than the normal sorghum. Waxy sorghum has lower peak and end gelatinization temperatures than normal sorghum, so its starch is more easily hydrolyzed [107–109]. Its mashes are also typically less viscous during liquefaction, which further aids hydrolysis [108].

Partial swelling is known to improve hydrolysis efficiency and can increase ethanol yield. Low-temperature processing also avoids the formation of amylose–lipid complexes, which occur during cooking above about 85°C and would not be expected to form during swelling at around 60°C [154]. In this study, the highest ethanol concentration (12.02%, v/v) came from GSHE fermentation of waxy sorghum after swelling at 70°C for 30 min. Higher swelling temperatures, still below the gelatinization range, therefore improved ethanol production, particularly for waxy sorghum. Ethanol yield followed the same pattern as concentration and was consistently higher for waxy sorghum. The highest yield (92.74%) also came from waxy sorghum swollen at 70°C for 30 min. This yield was numerically higher than, and statistically comparable to, that of conventional 95°C liquefaction of the same grain (90.16%), so partial

Table 4.2: Ethanol concentration and yield after 72 h under conventional and GSHE processing with partial starch swelling.

Treatment	Sorghum	Ethanol concentration (%, v/v)	Ethanol yield (%)
Conventional, 95°C	Waxy	11.68 ± 0.02^{b}	90.16 ± 0.11^{abc}
	Normal	11.35 ± 0.02^{c}	86.35 ± 0.06^{d}
GSHE, 35°C	Waxy	11.51 ± 0.11^{bc}	88.86 ± 0.86^{bcd}
	Normal	11.50 ± 0.07^{bc}	87.51 ± 0.68^{cd}
GSHE, 50°C, 30 min	Waxy	11.74 ± 0.07^{b}	90.63 ± 0.43^{ab}
	Normal	11.54 ± 0.06^{bc}	88.20 ± 0.42^{bcd}
GSHE, 60°C, 30 min	Waxy	11.63 ± 0.04^{bc}	89.80 ± 0.34^{bc}
	Normal	11.54 ± 0.06^{bc}	87.79 ± 0.49^{bcd}
GSHE, 70°C, 30 min	Waxy	12.02 ± 0.08^{a}	92.74 ± 0.62^{a}
	Normal	11.66 ± 0.04^{b}	88.72 ± 1.93^{bcd}

Values are mean ± SD ($n = 2$). Means in the same column followed by different letters differ significantly ($p < 0.05$). GSHE, granular starch hydrolyzing enzyme.

swelling with GSHE matched conventional cooking without the high-temperature step. Yield was therefore closely tied to how efficiently each treatment converted starch. For waxy sorghum, more severe swelling, at higher temperatures that remained below gelatinization, significantly increased ethanol concentration and yield; for normal sorghum the increases were not significant. Of all the processes tested, GSHE fermentation after swelling at 70°C for 30 min was the most effective. Swelling likely enlarges the accessible surface of the starch granules, giving GSHE more access and faster hydrolysis. It may also reduce starch crystallinity and hence resistance to enzymatic attack [151].

4.3.3 Protein purity, digestibility, and surface hydrophobicity

Distillers' dried grains (DDG) are the main coproduct of grain ethanol and spirit production. They contain a complex mixture of macromolecules [106]. Because of their high protein content, DDG are used mainly as livestock feed, and their composition is judged largely by its value for animal nutrition [176]. Fermentation concentrates protein almost fourfold relative to the raw grain, to 40.21–45.13 g/100 g [106]. Table 4.3 shows the purity, digestibility, and surface hydrophobicity of the proteins extracted from each WDG, with commercial soy and pea protein isolates included for comparison. The treatments were raw flour, WDG from

conventional fermentation at 95°C, and WDG from GSHE fermentation with or without partial swelling (50, 60, or 70°C for 30 min). Proteins from raw flour were 91.41% (waxy) and 89.69% (normal) pure. Partial swelling did not significantly affect purity, which exceeded 80% (81.97–85.39%) in all treatments except GSHE at 35°C (79.87% and 78.69% for waxy and normal sorghum). Unexpectedly, proteins from conventional 95°C WDG were about as pure as those from the swelling treatments.

Table 4.3: Properties of proteins extracted from sorghum flour and wet distillers' grains (WDG).

Source	Sorghum	Protein purity (%, db)	Protein digestibility (%)	Surface hydrophobicity (µg/mg protein)
Raw flour	Waxy	91.41 ± 0.22^{a}	81.53 ± 0.38^{fg}	56.99 ± 0.33^{f}
	Normal	89.69 ± 0.27^{a}	81.41 ± 0.48^{fg}	52.02 ± 0.11^{h}
WDG				
Conventional, 95°C	Waxy	84.67 ± 0.29^{bc}	85.39 ± 0.01^{c}	60.07 ± 0.89^{de}
	Normal	82.18 ± 0.07^{cd}	85.75 ± 0.26^{c}	62.06 ± 0.44^{c}
GSHE, 35°C	Waxy	79.87 ± 0.12^{de}	84.12 ± 0.77^{c}	62.61 ± 0.93^{c}
	Normal	78.69 ± 0.12^{e}	81.23 ± 0.26^{fg}	54.22 ± 0.11^{g}
GSHE, 50°C, 30 min	Waxy	84.77 ± 2.68^{bc}	85.57 ± 0.26^{c}	68.26 ± 0.26^{a}
	Normal	84.34 ± 0.40^{bc}	80.59 ± 0.13^{g}	54.08 ± 0.54^{g}
GSHE, 60°C, 30 min	Waxy	84.88 ± 0.80^{bc}	82.04 ± 0.38^{ef}	61.17 ± 0.45^{a}
	Normal	81.97 ± 0.40^{cd}	83.04 ± 0.26^{e}	54.08 ± 0.54^{g}
GSHE, 70°C, 30 min	Waxy	85.39 ± 0.19^{bc}	85.39 ± 0.26^{c}	62.26 ± 1.29^{c}
	Normal	82.90 ± 1.85^{cd}	85.21 ± 0.01^{c}	58.36 ± 0.31^{ef}
Commercial pea protein isolate		80.89 ± 0.16^{de}	90.91 ± 0.13^{a}	64.87 ± 0.36^{b}
Commercial soy protein isolate		86.52 ± 0.13^{b}	88.47 ± 0.26^{b}	68.00 ± 0.53^{a}

Values are mean ± SD ($n = 2$). Means in the same column followed by different letters differ significantly ($p < 0.05$). GSHE, granular starch hydrolyzing enzyme.

Protein digestibility

Proteins extracted from raw waxy and normal sorghum flours had similar digestibility, about 81.5%. This is well above the 23–68% previously reported for sorghum proteins across varieties [164, 177, 178]. The difference most likely reflects methodology. This study used a multienzyme digestion, which is more efficient than the single-enzyme systems used in some earlier work. Zhang et al. [179], for example, found higher digestibility of rice proteins with a four-enzyme system than with a three-enzyme system, which shows how much the enzyme

system matters in digestibility assays.

In general, proteins from WDG were more digestible than proteins from raw flour, whether the WDG came from conventional 95°C processing or from partial swelling. The one exception was normal sorghum swollen at 50°C. Microbial action on protein structure during fermentation is a likely cause. Correia et al. [180] compared several processing methods and found that fermentation significantly increased sorghum protein digestibility through the action of microbial enzymes. For conventional 95°C WDG, digestibility rose significantly to 85.39% (waxy) and 85.75% (normal). Wet cooking is widely reported to lower digestibility through the formation of disulfide cross-links [164, 181]. Here, however, high-temperature hydrolysis of the starch granules in the presence of α-amylase probably exposed more protein to microbial activity during fermentation. That exposure may have offset some of the negative effects of heat-induced polymerization.

GSHE fermentation at 35°C without any heat treatment raised the digestibility of waxy sorghum protein to above 84%. Partial swelling at 50, 60, or 70°C did not reduce digestibility, and swelling at 70°C for 30 min gave some of the highest values for both waxy (85.39%) and normal sorghum (85.21%). Digestibility is a key measure of protein quality. More digestible proteins are more accessible to digestive enzymes, which break them into small peptides that are readily absorbed [182]. The results therefore indicate that GSHE hydrolysis with low-temperature swelling can produce high-quality distillers' grains with minimal change to protein nutritional properties, without sacrificing ethanol yield. The highest ethanol yield was also obtained at 70°C, so swelling at 70°C for 30 min can be considered the optimum condition.

Sorghum proteins were less digestible than the commercial pea (90.91%) and soy (88.47%) protein isolates. Low-temperature GSHE fermentation nevertheless improved the digestibility of the extracted sorghum proteins. This makes them better suited as high-quality protein for feed and food and as a source of bioactive peptides. The approach is therefore an attractive alternative to conventional high-temperature fermentation because it improves protein quality and broadens the uses of the coproduct.

Protein surface hydrophobicity

Surface hydrophobicity describes how strongly a protein associates with hydrophobic environments. It governs how proteins interact with each other and with other components of foods and biological systems. It therefore influences key functional properties such as solubility, emulsification, foaming, and gelation. Table 4.3 compares the surface hydrophobicity of the sorghum protein isolates with that of commercial pea and soy isolates. Proteins from raw waxy (56.99 µg/mg) and normal sorghum flour (52.02 µg/mg) provide the baseline. Almost every processing treatment increased surface hydrophobicity for both sorghums. The treatments were conventional processing at 95°C, GSHE at 35°C, and GSHE with swelling at 50, 60, and 70°C. Protein structure is highly sensitive to its environment, and heating can denature proteins and aggregate their less stable fractions [183]. Heating generally increases surface hydrophobicity [184] because it exposes hydrophobic amino acids previously buried inside the molecule. Heat treatment has been reported to change kafirin structure and to promote complex formation between kafirin and other molecules [178]. Sulfhydryl–disulfide interchange between subunits and cross-linking among the more stable fractions may rearrange the subunits. Above the denaturation temperature, however, proteins tend to degrade, and surface hydrophobicity can fall. Semwal and Meera [185], for example, found that microwave and infrared heating significantly reduced the surface hydrophobicity of sorghum protein.

The commercial pea and soy isolates, which are known for their functional properties, had surface hydrophobicities of 64.87 and 68.00 µg/mg. These values are significantly higher than those of proteins from raw waxy or normal sorghum flour. Some sorghum treatments approached these values, in particular waxy sorghum swollen at 50°C before GSHE fermentation (68.26 µg/mg). Fermentation conditions can therefore strongly influence the surface hydrophobicity of sorghum proteins. Surface hydrophobicity reflects how hydrophobic residues are exposed and distributed on the protein surface, which governs interactions with water and lipids. Zhu et al. [186] found that surface hydrophobicity of rice bran protein correlated positively with water absorption capacity (WAC), emulsifying properties, and foaming, and

negatively with the least gelation concentration. These properties determine how proteins can be used. High WAC matters in viscous foods such as soups and gravies, and good emulsifying properties matter in dressings and mayonnaise. Surface hydrophobicity also affects protein solubility [187], which in turn influences digestibility and nutritional quality. Proteins from raw sorghum flour were less functional than pea or soy isolate by this measure. Fermentation, however, increased their surface hydrophobicity, which may improve their functional and nutritional value for food and industrial uses.

4.3.4 Color

Color, expressed as L^* (lightness), a^* (red–green), and b^* (yellow–blue), matters for food applications of proteins because it strongly affects consumer perception. Table 4.4 shows the color of the sorghum proteins from each WDG and of commercial soy and pea protein isolates.

Table 4.4: Color of proteins extracted from sorghum flour and wet distillers' grains (WDG).

Source	Sorghum	L^*	a^*	b^*
Raw flour	Waxy	79.73 ± 0.05^{i}	3.55 ± 0.02^{d}	9.84 ± 0.06^{i}
	Normal	80.55 ± 0.06^{h}	3.71 ± 0.04^{cd}	11.53 ± 0.07^{g}
WDG				
Conventional, 95°C	Waxy	78.61 ± 0.09^{j}	4.89 ± 0.02^{a}	12.84 ± 0.18^{f}
	Normal	79.93 ± 0.19^{hi}	4.50 ± 0.08^{ab}	11.69 ± 0.04^{g}
GSHE, 35°C	Waxy	90.51 ± 0.16^{f}	1.83 ± 0.02^{ef}	16.29 ± 0.09^{c}
	Normal	97.92 ± 0.23^{ab}	0.85 ± 0.03^{g}	10.58 ± 0.05^{h}
GSHE, 50°C, 30 min	Waxy	90.66 ± 0.16^{f}	2.24 ± 0.05^{e}	16.54 ± 0.06^{c}
	Normal	97.46 ± 0.10^{bc}	1.99 ± 0.07^{ef}	13.12 ± 0.17^{f}
GSHE, 60°C, 30 min	Waxy	94.10 ± 0.14^{e}	4.09 ± 0.10^{bc}	13.95 ± 0.36^{e}
	Normal	98.24 ± 0.38^{a}	1.84 ± 0.04^{ef}	10.14 ± 0.15^{i}
GSHE, 70°C, 30 min	Waxy	95.29 ± 0.40^{d}	4.22 ± 0.13^{b}	14.68 ± 0.26^{d}
	Normal	97.17 ± 0.40^{c}	0.27 ± 0.03^{h}	11.78 ± 0.10^{g}
Commercial pea protein isolate		77.65 ± 0.02^{k}	4.91 ± 0.01^{a}	20.89 ± 0.05^{a}
Commercial soy protein isolate		82.85 ± 0.03^{g}	1.97 ± 0.01^{f}	17.59 ± 0.11^{b}

Values are mean ± SD ($n = 3$). Means in the same column followed by different letters differ significantly ($p < 0.05$). GSHE, granular starch hydrolyzing enzyme.

Across all treatments, proteins from normal sorghum were consistently lighter (higher

L^*) than those from waxy sorghum. Conventional fermentation changed L^* very little relative to unprocessed flour. GSHE fermentation, by contrast, raised L^* markedly, especially for normal sorghum, which reached 98.24 after swelling at 60°C for 30 min. GSHE processing, particularly at the higher swelling temperatures, therefore substantially lightened the sorghum proteins. This may reflect more effective removal of pigmented components, or structural changes in the protein that increase light reflectance.

Proteins from conventional fermentation had higher a^* values than those from raw flour, indicating that hydrolysis at 95°C made them redder. For normal sorghum, partial swelling significantly reduced a^* relative to both raw flour and conventional processing. For waxy sorghum, a^* increased at the higher swelling temperatures (60 and 70°C). Waxy sorghum proteins also had higher b^* (more yellow) than raw flour, so waxy sorghum proteins tended to be yellower than normal sorghum proteins across treatments.

Sorghum proteins, especially those from partial swelling, were generally lighter than the commercial pea and soy isolates. The commercial isolates were redder (higher a^*) and yellower (higher b^*) than most sorghum proteins. These lighter, more neutral colors make sorghum protein a potentially attractive ingredient where a neutral color is needed. Compared with an earlier study [188], the a^* values here were higher and the b^* values lower. This may reflect the low processing temperature and the chloramphenicol used with GSHE fermentation to limit contamination, although these explanations were not tested directly.

4.3.5 Molecular weight distribution by SEC-HPLC

Figure 4.1 shows SEC-HPLC chromatograms of proteins extracted from WDG after GSHE fermentation at 35°C without swelling and after swelling at 50, 60, or 70°C for 30 min. Under non-reducing conditions, proteins from normal and waxy sorghum gave similar profiles. Each had a major peak at about 670 kDa, most likely from large polymeric proteins, and a minor peak at about 44 kDa, possibly from kafirin dimers [189]. The polymeric fraction (about 670 kDa) is far larger than individual kafirins (about 20–30 kDa). It may occur naturally in sorghum flour, but heating during processing probably also contributes to its

formation [188, 190]. Normal and waxy sorghum responded slightly differently to swelling. In normal sorghum (Figure 4.1A), the major peak decreased slightly as temperature increased. The minor peak rose up to 60°C and then fell sharply at 70°C. In waxy sorghum (Figure 4.1B), both peaks increased with temperature. This difference likely reflects the lower thermal stability of waxy sorghum noted above, which makes its proteins more prone to polymerization and cross-linking on heating.

With a reducing agent (β-mercaptoethanol), proteins from both sorghums gave peak patterns similar to those under non-reducing conditions (Figure 4.1C and D). Much of the polymeric fraction (about 670 kDa) remained, indicating that some of the polymers are not held together by disulfide bonds. The ratio of the major (about 670 kDa) to the minor (about 44 kDa) peak did, however, decrease relative to non-reducing conditions. This suggests that some of the high-molecular-weight fraction was broken down into smaller subunits.

4.3.6 SDS-PAGE

Kafirin polypeptide and monomer profiles were further examined by SDS-PAGE under non-reducing and reducing conditions (Figure 4.2). Under non-reducing conditions (Figure 4.2A), proteins from GSHE fermentation with and without swelling showed similar banding patterns, consistent with previous reports [188, 190]. Faint bands above 50 kDa appeared only in the swollen samples (N50, N60, N70, W60, and W70). These are likely kafirin trimers or oligomers formed during heating. They disappeared when β-mercaptoethanol was added (Figure 4.2B), indicating disulfide cross-linking of kafirin monomers under non-reducing conditions [188]. A darker band at about 47 kDa was attributed to γ-kafirin [189, 190]. A dominant band at about 20–23 kDa in all samples corresponded to the α_1- and α_2-kafirins [165, 190, 191]. Faint bands at about 15–20 kDa corresponded to β-kafirins [165]. A small fraction below 10 kDa was slightly darker after swelling at 50, 60, and 70°C, which may also be related to heating during swelling. Under reducing conditions, all samples gave similar profiles. The main differences were the loss of the polypeptides above 50 kDa and a slightly higher proportion of β-kafirins (15–20 kDa). This suggests that β-kafirin does not

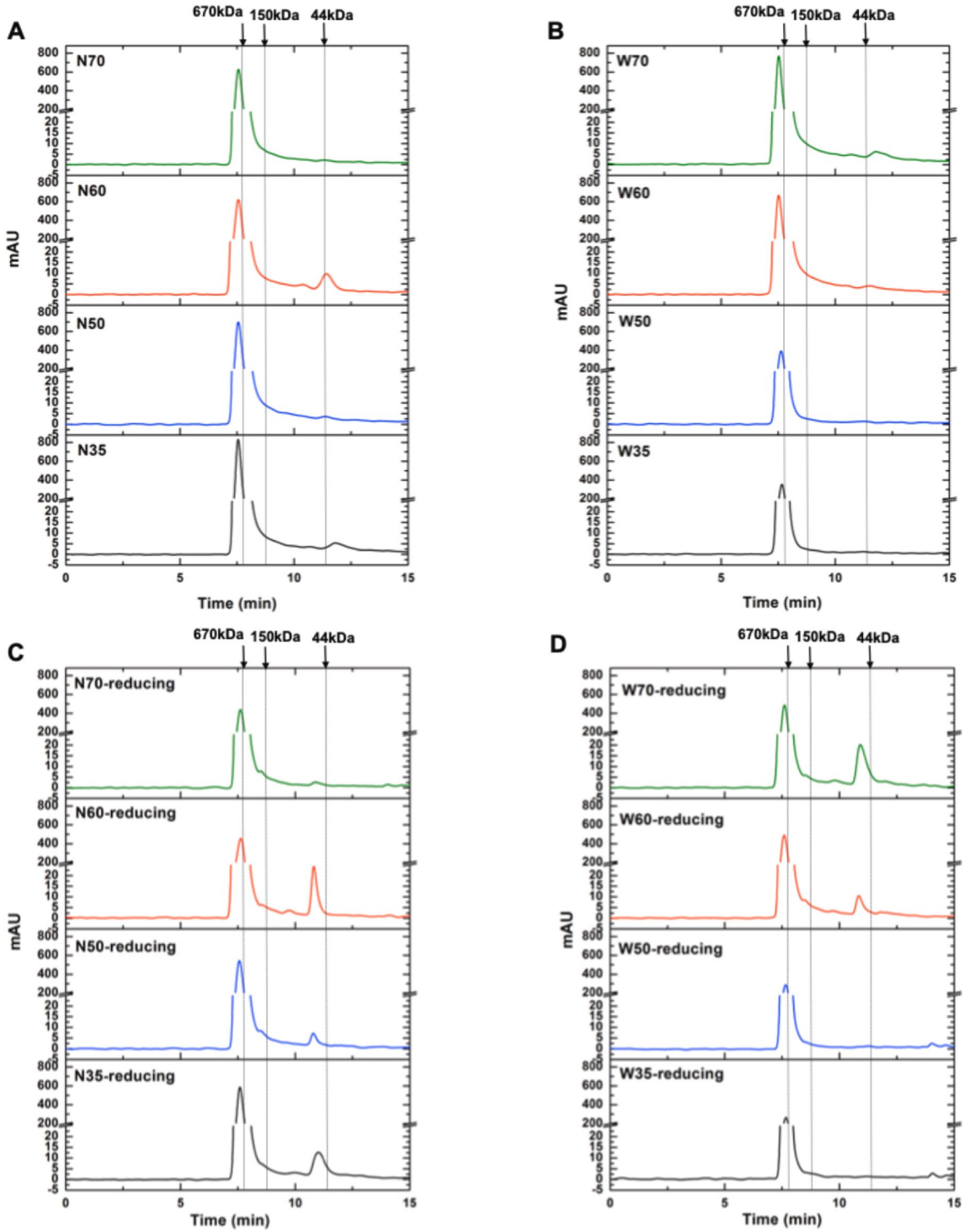


Figure 4.1: SEC-HPLC chromatograms of proteins extracted from wet distillers' grains after GSHE fermentation at 35°C (N35, W35) and after partial starch swelling at 50, 60, and 70°C (N50–N70, W50–W70). (A) Normal sorghum, non-reducing; (B) waxy sorghum, non-reducing; (C) normal sorghum, reducing; (D) waxy sorghum, reducing. N, normal sorghum; W, waxy sorghum.

occur as a free monomer but is associated with oligomers under non-reducing conditions, as reported by Espinosa-Ramírez and Serna-Saldívar [188].

4.4 Conclusions

This chapter examined how sorghum type and partial starch swelling affect ethanol yield, the digestibility and surface hydrophobicity of WDG proteins, and the molecular characteristics of the extracted kafirins. Optimizing GSHE hydrolysis can reduce energy use while improving the protein quality of the distillers' grains. This could benefit the animal feed industry and improve the sustainability of grain-based ethanol and spirits production. Waxy sorghum, with its high amylopectin content, lower gelatinization temperatures, and more efficient hydrolysis, again outperformed normal sorghum. Partial starch swelling improved ethanol yield, significantly so for waxy sorghum. The highest ethanol concentration (12.02%, v/v) and yield (92.74%) came from GSHE fermentation of waxy sorghum swollen at 70°C for 30 min, matching (and numerically exceeding) conventional 95°C liquefaction of the same grain.

Just as importantly, swelling improved ethanol yield without compromising protein quality in the WDG. Swelling did not significantly reduce protein digestibility, which remained high even at 70°C for both waxy (85.39%) and normal sorghum (85.21%). Surface hydrophobicity increased relative to raw flour under most treatments, with the highest value for waxy sorghum swollen at 50°C. Partial swelling significantly increased L^* for both sorghums. Its effect on a^* differed between them, and b^* increased notably for waxy sorghum. The SEC-HPLC and SDS-PAGE results showed how processing changes kafirin structure and interactions. Overall, optimizing the swelling step can substantially improve ethanol yield while maintaining protein quality in the WDG, which could make current biofuel and distilling operations more profitable. A techno-economic analysis would help quantify the benefits of the energy savings and higher-quality DDG.

In the context of this dissertation, this chapter shows that the hydrolysis stage of a liquid-state spirit process need not rely on high-temperature cooking. A low-temperature swelling

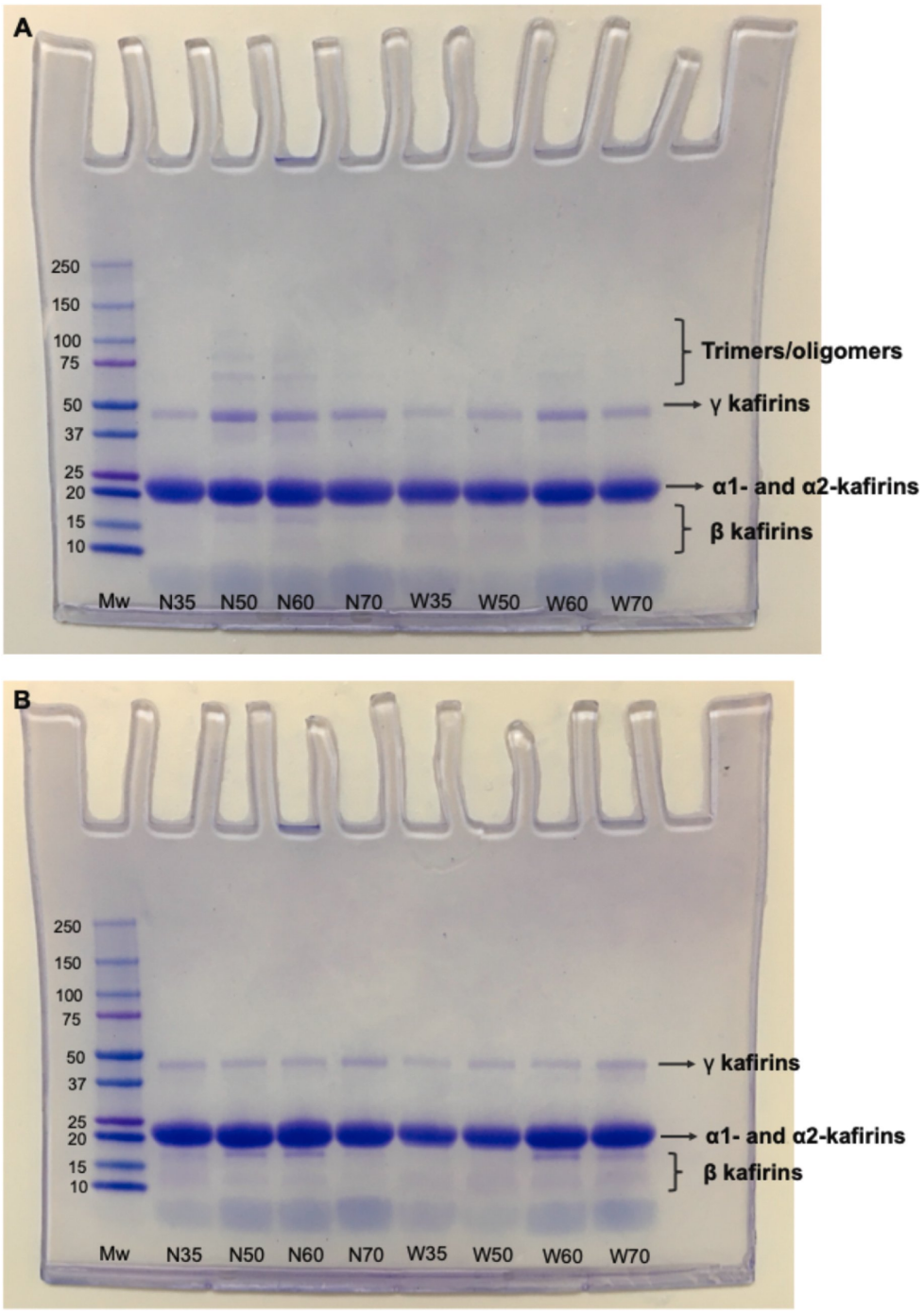


Figure 4.2: SDS-PAGE of kafirins extracted from wet distillers' grains under (A) non-reducing and (B) reducing conditions. Mw, molecular weight standards (kDa); N, normal sorghum; W, waxy sorghum; numbers give the GSHE processing or partial swelling temperature (°C).

step combined with GSHE delivered yields statistically comparable to conventional cooking and left a more valuable protein coproduct. Chapters 2 through 4 thus address the first two stages of the process proposed in Chapter 1, hydrolysis and primary fermentation, along with their coproducts. Chapter 5 turns to the next stage, the enrichment of a chain-elongating microbial community capable of converting the ethanol, lactate, and short-chain acids from primary fermentation into the medium-chain fatty acids behind baijiu's characteristic esters.

Chapter 5

Enrichment of Rumen Fluid toward Chain Elongation Activity via Ethanol, Lactate, or Glucose to Produce Medium-Chain Fatty Acids

This chapter is based on the manuscript "Enrichment of Rumen Fluid Towards Chain Elongation Activity Via the Inclusion of Ethanol, Lactate, or Glucose to Produce Medium-Chain Fatty Acids," co-authored by Thomas Weiss, Yonghui Li, Xiaorong Wu, Mark Wilkins, Lisa R. Wilken, Abby E. Xinyi, and Donghai Wang. It has been edited for consistency with the rest of this dissertation.

Chapter Overview

Chapters 2–4 addressed the hydrolysis and primary-fermentation stages of the liquid-state process proposed in Chapter 1. Those stages produce ethanol, lactic acid, and short-chain acids. The maize spirits of Chapter 3, however, showed that yeast fermentation alone produces only modest amounts of the medium-chain esters that define strong-aroma baijiu. In traditional production, the missing function is supplied by chain-elongating bacteria in the pit mud. This chapter asks whether that function can be recreated in liquid culture, without

pit mud, by adaptively enriching a readily available anaerobic community: bovine rumen fluid.

Medium-chain fatty acids (MCFAs), particularly hexanoic acid, are valuable platform chemicals and flavor precursors produced by microbial chain elongation. Here, rumen fluid was used as the inoculum for adaptive enrichment of MCFA-producing consortia under controlled liquid-state conditions. Sequential-transfer enrichments were fed ethanol, lactic acid, or glucose as the primary substrate. Reducing conditions, methanogen suppression, bicarbonate buffering, and acetate supplementation were progressively adjusted to favor reverse β-oxidation and hexanoate production. Although all cultures came from the same rumen inoculum, they diverged widely in metabolic activity and community structure. Hexanoate was detected in only a subset of lineages because chain-elongating organisms were unexpectedly scarce in the starting rumen fluid. Four cultures (Eth-1, Lac-1, Lac-6, and Glu-5) were selected for reactor-scale validation on the basis of hexanoate production. The three most productive lineages (Eth-1, Lac-1, and Lac-6) were dominated by *Clostridium kluyveri*, including the lactate-fed cultures Lac-1 and Lac-6, which received no external ethanol. Community composition and a sibling-referenced electron balance suggest that in these lineages lactate-fermenting *Clostridia* supplied *C. kluyveri* with butyrate as an electron acceptor and H_2 as an electron donor, with ethanol formed in situ as a possible secondary donor. Only Eth-1 sustained hexanoate production through reactor operation, consistent with continuous gas purging removing the H_2 on which the lactate-derived lineages depended. With enhanced ethanol feeding, it then reached 4.6 $g\,L^{-1}$ hexanoic acid, with hexanoate making up about 73% of combined butyrate and hexanoate production (Figure 5.1).

5.1 Introduction

As outlined in Chapter 1, the defining step in strong-aroma baijiu flavor development is the microbial production of medium-chain fatty acids in the pit mud. Medium-chain fatty acids (MCFAs) such as hexanoic and octanoic acid are increasingly recognized as valuable biogenic platform molecules with applications spanning renewable chemicals, food fermenta-

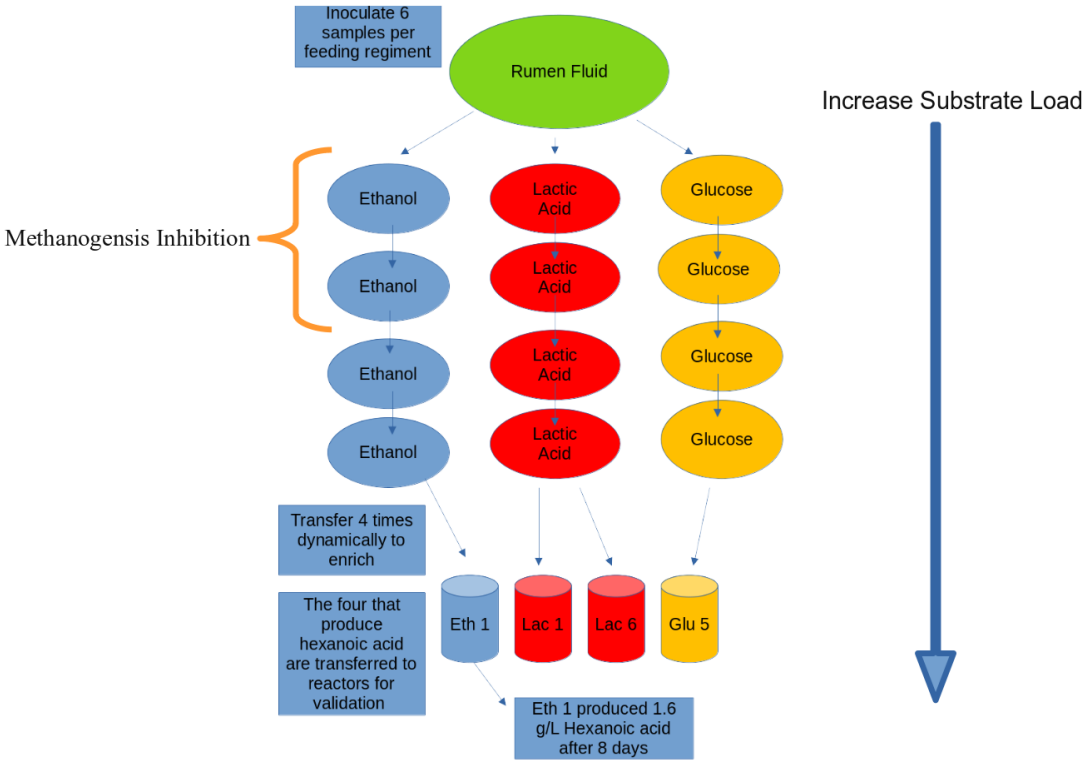


Figure 5.1: Overview of the enrichment scheme. Rumen fluid was used to inoculate six replicate serum bottles per feeding regimen (ethanol, lactic acid, glucose), with methanogenesis inhibition during the first two transfers and progressively increasing substrate load across four sequential transfers. The four lineages that produced hexanoic acid (Eth-1, Lac-1, Lac-6, Glu-5) were transferred to bioreactors for validation.

tion, and flavor production. In distilled spirits and fermented foods, MCFAs serve as critical precursors for ethyl esters that impart fruity, floral, and sweet aroma characteristics [48]. Strong-aroma baijiu in particular is distinguished by exceptionally high concentrations of ethyl hexanoate, a compound strongly associated with product quality and sensory complexity [8, 47, 50]. Unlike many Western distilled spirits, which rely primarily on barrel aging and thermal reactions for flavor development, strong-aroma baijiu derives much of its characteristic profile directly from microbial metabolism during fermentation [8, 49]. These metabolic activities occur within the fermentation vessel itself, which functions as a microbial reservoir supporting complex anaerobic consortia responsible for flavor compound production [51]. In strong-aroma baijiu production, fermentation takes place within large earthen mud pits lined with a dense red clay known as pit mud. During production, cooked grain is combined with a microbial starter culture and buried within these pits where fermentation and flavor development occur [17]. Over time, pit mud becomes enriched with highly specialized anaerobic microbial communities capable of efficient MCFA production; however, development of mature and productive pit mud ecosystems may require decades to centuries of continuous operation [20].

The organisms within pit mud that contribute substantially to the production of hexanoic acid and related flavor-active compounds are commonly referred to as chain elongators [8, 17, 20, 51, 52]. These organisms produce butyric, hexanoic, octanoic, and longer-chain fatty acids through the reverse β-oxidation (rBOX) pathway using substrates such as ethanol, lactate, glucose, acetate, and other fermentation intermediates [18, 52]. Reverse β-oxidation functions as an electron sink by consolidating short-chain fermentation products into longer-chain fatty acids through iterative carbon elongation reactions. In mixed anaerobic systems, this pathway can alter environmental toxicity, redistribute reducing equivalents, and influence broader microbial community structure. Depending on substrate availability and metabolic interactions within the consortium, chain elongation can selectively redirect carbon away from gaseous end products and toward the accumulation of value-added carboxylic acids [54]. Each cycle extends the acyl chain by two carbon atoms, allowing acetate (C2) to be converted to butyrate (C4), butyrate to hexanoate (C6), and hexanoate to octanoate

(C8). The identity of the electron donor and the mechanism by which reducing equivalents are generated distinguish different chain elongating organisms and can substantially influence pathway thermodynamics and product distributions [192, 193].

In the classical ethanol-based pathway of *Clostridium kluyveri*, ethanol serves as both a carbon source and electron donor, while acetate or a longer-chain carboxylate serves as the primer [54]. At the overall stoichiometric level, the initial elongation can be represented by the conversion of acetate and ethanol to butyrate, followed by further elongation of butyrate to hexanoate. A simplified representation of the first step is:

$$\text{Reaction 1:} \quad 6\,\text{Ethanol} + 4\,\text{Acetic acid} \rightarrow 5\,\text{Butyric acid} + 2\,\text{H}_2 + 4\,\text{H}_2\text{O}$$

and the subsequent elongation can similarly be represented as:

$$\text{Reaction 2:} \quad \text{Butyric acid} + \text{Ethanol} \rightarrow \text{Hexanoic acid} + \text{H}_2\text{O}$$

with the corresponding protonation and water terms depending on the chemical species and thermodynamic convention used. These reactions should be regarded as net representations of a more complex intracellular pathway rather than individual enzymatic reactions [19]. At the biochemical level, ethanol is oxidized to acetyl-CoA while generating reducing equivalents. The acetyl-CoA produced from ethanol provides the two-carbon extender required for reverse β-oxidation.

$$\text{Reaction 3:} \quad \text{Ethanol} + 2\,\text{NAD}^+ + \text{CoA} \rightarrow \text{Acetyl-CoA} + 2\,\text{NADH} + 2\,\text{H}^+$$

The primer is first activated to its CoA derivative, after which condensation with acetyl-CoA forms a β-ketoacyl-CoA intermediate. This intermediate undergoes sequential reduction, dehydration, and reduction to generate an elongated acyl-CoA, which is subsequently converted

to the corresponding carboxylate. For example, the C4-to-C6 step can be represented as:

$$\begin{aligned} &\text{Butyryl-CoA} + \text{Acetyl-CoA} \rightarrow \text{3-Ketohexanoyl-CoA} \\ \text{Reaction 4:} \qquad &\text{3-Ketohexanoyl-CoA} \rightarrow \text{3-Hydroxyhexanoyl-CoA} \\ &\rightarrow \text{Hexanoyl-CoA} \end{aligned}$$

followed by transfer of the CoA group from hexanoyl-CoA to acetate by a CoA transferase, which releases hexanoate and regenerates acetyl-CoA:

$$\text{Reaction 5:} \quad \text{Hexanoyl-CoA} + \text{Acetate} \rightarrow \text{Hexanoate} + \text{Acetyl-CoA}$$

If needed, acetate can be produced from acetyl-CoA, allowing the reactants to be balanced even when ethanol is the only external substrate (Reaction 3).

$$\text{Reaction 6:} \quad \text{Acetyl-CoA} + \text{ADP} + \text{P}_\text{i} \rightarrow \text{Acetate} + \text{ATP} + \text{CoA-SH}$$

The reduction steps require reducing equivalents, while oxidation of ethanol provides both the acetyl-CoA carbon unit and part of the reducing power required to drive the pathway (Reaction 3). Thus, ethanol-based chain elongation is intrinsically coupled to cellular redox balance and hydrogen metabolism. Hydrogen can also serve as the electron donor in place of ethanol. For the C4-to-C6 step, elongation of butyrate with acetate and H_2 can be represented as [194]:

$$\text{Reaction 7:} \quad \text{Butyrate} + \text{Acetate} + 2\,\text{H}_2 + \text{H}^+ \rightarrow \text{Hexanoate} + 2\,\text{H}_2\text{O}$$

Lactate-utilizing chain elongators employ a related rBOX pathway but generate the extender and reducing equivalents through a different upstream metabolism. Lactate is first converted to pyruvate and subsequently to acetyl-CoA, releasing carbon dioxide and generating reducing equivalents [195]. The acetyl-CoA can then enter the same type of reverse β-oxidation pathway used for ethanol-based chain elongation. In the presence of acetate, a

simplified overall reaction for lactate-driven hexanoate production can be represented as:

$$\text{Reaction 8:} \quad 2\,\text{Lactate} + \text{Acetate} \rightarrow \text{Hexanoate} + 2\,CO_2 + 2\,H_2O$$

depending on the protonation convention used. In organisms such as *Caproiciproducens*, lactate oxidation can generate both NADH and reduced ferredoxin, which must subsequently be integrated through the cellular electron-transfer network to provide the reducing equivalents required for the reductive steps of rBOX [192]. Consequently, lactate-based chain elongation differs from ethanol-based elongation not only in substrate conversion but also in the mechanisms governing intracellular electron distribution.

Other substrates can enter chain elongation at different points in this metabolic network. Hexoses such as glucose are generally metabolized through glycolysis to pyruvate and subsequently to acetyl-CoA, allowing carbon from primary fermentation products to enter the rBOX pathway through acetyl-CoA formation [18]. Thus, ethanol, lactate, and glucose can all ultimately contribute carbon to MCFA formation while imposing different requirements for carbon conservation, electron generation, and redox balancing. These differences provide a mechanistic basis for expecting substrate identity to influence both enrichment and final product distribution. The thermodynamic feasibility of each elongation step is also dependent on the surrounding fermentation environment. Under non-standard conditions, the Gibbs free energy of a reaction is determined by:

$$\text{Equation 1:} \quad \Delta G = \Delta G^{\circ\prime} + RT \ln Q$$

where $\Delta G^{\circ\prime}$ is the standard Gibbs free energy change at pH 7 and Q incorporates the activities of substrates and products and, for gaseous products, their partial pressures. This is particularly relevant for ethanol-based chain elongation because hydrogen is generated during substrate oxidation and chain elongation. Increasing hydrogen partial pressure can make hydrogen-producing reactions less favorable, whereas hydrogen removal can increase the thermodynamic driving force for ethanol oxidation and subsequent chain elongation [196].

Product accumulation can have the opposite effect: increasing hexanoate or other MCFA activity increases the thermodynamic constraint on further elongation and may additionally impose physiological inhibition.

Accordingly, chain elongation should be viewed as the interaction of substrate conversion, electron transfer, and product thermodynamics rather than as a single biochemical reaction. Substrate identity determines how carbon and reducing equivalents enter the pathway; the primer-to-extender ratio influences which chain-length intermediates can accumulate; and environmental conditions including hydrogen partial pressure, pH, substrate concentration, and product concentration determine the energetic feasibility of individual reactions [60]. These factors are particularly relevant during enrichment because selection of a microbial community may favor different chain elongating populations depending on the substrate and operating conditions imposed. Understanding these pathway-level differences is therefore important for interpreting how ethanol, lactate, and glucose influence the development and stability of MCFA-producing consortia.

Despite the effectiveness of pit mud ecosystems for MCFA production, reproducing these functions within controllable liquid-state fermentations remains difficult. Chain elongating organisms generally exhibit slow growth rates, depend heavily on syntrophic interactions, and are frequently outcompeted during early enrichment by faster-growing fermentative or methanogenic microorganisms [61]. Medium-chain fatty acids themselves may also become inhibitory at elevated concentrations while simultaneously being susceptible to volatilization and product loss during fermentation [197]. As a result, stable enrichment of reproducible chain elongation consortia remains a significant challenge for industrial fermentation engineering. These challenges are compounded by the ecological complexity of mixed anaerobic systems in which multiple microbial guilds compete for reducing equivalents, carbon intermediates, and electron sinks.

One of the primary competing metabolic pathways in anaerobic fermentation systems is methanogenesis [20]. Methanogenic archaea consume hydrogen, acetate, and other reduced intermediates, effectively removing reduced carbon from the environment through methane formation. In doing so, methanogens can stabilize broader syntrophic networks and increase

the thermodynamic favorability of upstream fermentative metabolism. Various fermentative organisms may therefore adapt their metabolic outputs to favor substrates preferred by associated methanogenic populations [198]. Consequently, methanogenesis can substantially reduce carbon flux toward MCFA accumulation by diverting reducing equivalents and fermentation intermediates away from reverse β-oxidation. Chain elongation communities also benefit from syntrophic interactions; however, these interactions are generally more specialized and selective than those supporting broader methanogenic ecosystems [52, 53]. Effective enrichment of MCFA-producing consortia therefore requires the establishment of selective conditions that favor chain elongation metabolism while suppressing competing methanogenic activity.

Several strategies have been proposed for suppressing methanogenesis in anaerobic fermentation systems. One commonly used approach is the addition of 2-bromoethanesulfonic acid (BESA) or related brominated compounds that inhibit methyl coenzyme M reductase activity in methanogens [62]. Alternative approaches include pH manipulation and selective electron acceptor supplementation. However, pH-based inhibition strategies present significant tradeoffs because many desirable chain elongators exhibit differing tolerance ranges. For example, *Megasphaera* species are generally less tolerant of acidic conditions than *Clostridium kluyveri* [63]. Consequently, pH conditions sufficient to inhibit acetoclastic methanogens may also partially suppress desired chain elongation activity [64]. Ferric iron (Fe III) supplementation represents another potential strategy for suppressing methanogenesis while simultaneously supporting chain elongation metabolism [65]. Iron cycling may facilitate electron transfer reactions and improve the thermodynamics of reverse β-oxidation under specific conditions [66]. An ideal enrichment strategy would therefore produce stable MCFA-generating consortia that require minimal continued methanogen inhibition while maintaining robust chain elongation activity under controlled reactor conditions.

Chain elongating microorganisms are metabolically diverse and capable of utilizing a broad range of substrates including lactate, ethanol, glucose, acetate, and short-chain carboxylic acids [52, 199]. Many chain elongators also benefit from acetate supplementation as a co-substrate during reverse β-oxidation [57]. Among currently characterized organisms,

Clostridium kluyveri is one of the best-known ethanol-utilizing chain elongators and has been identified in both pit mud and bovine rumen environments [19]. Additional rumen-associated organisms with chain elongation capability include *Caproiciproducens galactitolivorans*, *Megasphaera elsdenii*, and members of the *Ruminococcaceae* [200–202]. Collectively, these organisms occupy overlapping substrate niches and commonly thrive under neutral to mildly acidic anaerobic conditions between 30–40 °C. The presence of multiple potential chain elongators within bovine rumen fluid suggests that rumen-derived microbial communities may represent promising inoculum sources for directed enrichment of MCFA-producing consortia.

Rumen ecosystems are naturally adapted to fluctuating substrate availability, rapid fermentation dynamics, and dense anaerobic microbial interactions [60]. As with other functional microbial communities, chain elongation consortia may be adaptively enriched through selective manipulation of environmental conditions such as substrate composition, pH, temperature, and reactor operation [61]. Sequential transfer enrichment strategies can progressively alter microbial community structure by favoring organisms and syntrophic relationships best suited to the imposed operating conditions [203]. Such approaches may allow the development of stable and productive MCFA-producing communities without continuous reliance on strong chemical methanogen inhibitors. However, while sequential transfer enrichment strategies can progressively alter microbial community structure by favoring organisms and syntrophic relationships best suited to the imposed operating conditions, the predictability of enrichment outcomes depends critically on inoculum characteristics. Particularly, if the initial target organism is extremely low or poorly distributed in the system then there is a lower likelihood of those organisms sufficiently colonizing the selective environment to the degree required to be preferentially transferred to the next enrichment if they are present at all.

There is a broader opportunity for fermentation systems capable of selectively producing high-value flavor compounds and renewable chemicals directly from biomass-derived substrates. As modern fermentation industries favor liquid-state processing due to advantages in process control, scalability, and substrate utilization efficiency, there is growing interest in

developing steerable microbial consortia capable of producing value added compounds such as occurs in baijiu mud-pits. The objective of the work described in this chapter was therefore to adaptively enrich rumen-derived microbial consortia toward stable medium-chain fatty acid production under controlled liquid-state fermentation conditions. Ethanol, lactate, and glucose were evaluated as enrichment substrates during early enrichment stages in order to examine how substrate selection influenced chain elongation activity and community stability. Sequential transfer cultivation, selective methanogen suppression, and iterative process refinement were employed to progressively favor MCFA production and stable hexanoic acid accumulation. Particular emphasis was placed on identifying enrichment conditions capable of sustaining productive chain elongation activity under elevated ethanol loading conditions relevant to industrial fermentation systems. By combining adaptive enrichment strategies with controlled reactor operation, this chapter aims to establish a framework for generating stable MCFA-producing consortia suitable for flavor-focused fermentation systems and broader renewable biochemical applications.

5.2 Materials and Methods

5.2.1 Inoculum Collection and Preparation

Rumen fluid was used as an alternative inoculum source. Fresh rumen fluid was obtained from a healthy donor bovine at a USDA-inspected abattoir through the Kansas State University Meat Laboratory. The inoculum was prepared via manual expression of the rumen solids and filtered through four layers of cheesecloth to remove large particulate matter. To maintain anaerobic integrity and viability of the microbiota, the filtrate was collected in a pre-warmed (40 °C) vacuum-insulated flask and transported immediately to the laboratory [60].

5.2.2 Media and Reagent Preparation

A basal salt medium was prepared with the following components (per liter) based on that recommended by Reddy et al. [61]: 2.0 g $NH_4Fe(III)$ citrate, 1.0 g KH_2PO_4, 0.2 g $MgSO_4$, 0.05 g NaCl, 0.05 g $CaCl_2$, 8.3 mg $FeCl_2$, 1.4 mg $MgCl_2$, and 1.0 mg $ZnCl_2$. Serum bottles (150 mL) were filled with 90 mL of the basal salt media, loosely sealed with butyl rubber stoppers and aluminum crimp caps, and sterilized by autoclaving. Following sterilization, the bottles were transferred to a laminar flow hood. A concentrated anaerobic stock solution was then prepared and aseptically added to each bottle (2 mL per vial) to achieve final concentrations of 16 g/L $NaHCO_3$, 2.5 g/L cysteine (as a reducing agent), 0.44 g/L Na_2MoO_4 (to inhibit sulfur-reducing bacteria), 0.5 g/L yeast extract, and 3 g/L 2-bromoethanesulfonate (BESA) to inhibit methanogens for the first two transfers. BESA was omitted after the second transfer, once gas production and sulfur reduction had subsided. Each bottle was flushed for 30 minutes with a 80:20 mix of nitrogen and carbon dioxide prior to inoculation.

5.2.3 Initial Substrate Enrichment

Initial enrichment experiments were conducted in 150 mL serum bottles containing 100 mL working volume and inoculated with 20% (v/v) rumen fluid (20 mL). This larger initial inoculum was used to capture as many members of the rumen community as possible; subsequent transfers used 10% (v/v) to increase selective pressure. Three electron donor conditions were evaluated during early enrichment stages: ethanol, lactate, and glucose. Unamended controls lacking external electron donor were also maintained.

Initial substrate concentrations were normalized on a carbon-molar basis to ensure that each treatment received equivalent carbon loading despite differences in molecular weight and carbon content. Ethanol (2 carbons/mol), lactate (3 carbons/mol), and glucose (6 carbons/mol) concentrations were therefore adjusted such that equivalent quantities of carbon entered each enrichment culture. Ethanol was selected as the reference substrate because it is a well-characterized electron donor for reverse β-oxidation and possesses a higher degree of reduction than either lactate or glucose. This approach allowed substrate identity to be eval-

uated independently from gross differences in carbon availability. Substrate concentrations gradually increased over sequential transfer cycles to minimize stochastic culture collapse during early enrichment while progressively selecting for chain elongation activity. Initial donor concentrations were established at carbon-equivalent loading levels and increased during successive transfer stages.

Bottles were incubated statically at 38 °C under anaerobic conditions. Sequential transfers were performed weekly for the first three transfers to weed out fast growers then every three weeks for the last two to allow slow growers to enrich. All transfers consisted of 10% (v/v) culture into fresh anaerobic medium containing elevated substrate concentrations. T3 and T4 cultures were fed weekly to refresh their substrate supply. The substrate feedstock was created by preparing a 10X solution of primary substrate and 10% of that of acetic acid in a salt solution and adding 1 ml to each bottle upon feeding. Substrate amounts may be found in Table 5.1 and are molar equivalents of ethanol. Cultures were monitored throughout enrichment using pH measurements, gas production, turbidity, and periodic chemical analysis by HPLC. Cultures exhibiting sustained gas production, stable pH behavior, and detectable volatile fatty acid or ester formation were preferentially retained during subsequent transfer cycles. Sequential transfers were adaptively modified in response to observed metabolic performance.

Table 5.1: Transfer weekly feed as final added concentration of initial enrichments.

Transfer	Ethanol (g/L)	Lactic acid (g/L)	Glucose (g/L)
T0	0	0	0
T1	0.1	0.13	0.13
T2	0.5	0.65	0.65
T3	1 weekly	1.3 weekly	1.3 weekly
T4	2 weekly	2.6 weekly	2.6 weekly

Following repeated transfer enrichment, cultures were evaluated for sustained activity based on gas production behavior, pH stability, turbidity, and volatile product formation. Representative cultures from ethanol-, lactate-, and glucose-enriched lineages demonstrating consistent metabolic activity were selected for further stabilization and reactor-scale culti-

vation experiments.

5.2.4 Culture Validation

All four of the cultures which produced quantities of hexanoic acid detectable by HPLC were transferred to 800 ml of media and cultured in 1 L DASGIP parallel bioreactors (Eppendorf, Enfield, CT), one reactor per lineage, and run for 8 days using the same medium as the serum bottle enrichment, without the calcium carbonate. The pH was maintained at 6.5 using 0.25 M sulfuric acid and 0.25 M sodium hydroxide, and the reactors were flushed daily with a 20:80 mixture of carbon dioxide to nitrogen. Daily sampling took place, and 0.08 gmol of substrate and 0.008 gmol of acetate were fed (Table 5.2). These samples were analyzed using HPLC and optical density (OD_{600}) to measure cell growth.

Table 5.2: Cumulative theoretical concentrations in the validation reactors with feeding at 48-hour intervals.

Hours	gmol carbon	gmol acetate	Cumulative acetate (g/L)	Cumulative ethanol (g/L)	Cumulative lactate (g/L)	Cumulative glucose (g/L)
0	0.08	0.01	0.48	2	3.91	4.6
48	0.08	0.01	0.96	4	5.91	6.6
96	0.08	0.01	1.44	6	7.91	8.6
144	0.08	0.01	1.92	8	9.91	10.6
192	0.08	0.01	2.4	10	11.91	12.6
240	0.08	0.01	2.88	12	13.91	14.6

5.2.5 Substrate Optimization

After running the enrichment for 8 days the successful culture was used to inoculate the reactors again at 10% inoculum with 3 levels of substrate at 5, 10, and 20 g/L ethanol and 3 g/L acetic acid (one reactor per ethanol level) under the same conditions as the culture validation. These reactors were fed in a batch instead of a fed batch format to observe the effects of substrate levels. Sampling for sequencing was conducted successfully after 1 day and 8 days of running the reactors.

5.2.6 HPLC

Liquid metabolites were quantified using high-performance liquid chromatography (1260 Infinity System, Agilent Technologies, Santa Clara, CA, USA) equipped with an Aminex HPX-87H organic acid column (7.8 × 300 mm; Bio-Rad Laboratories, Hercules, CA, USA) and refractive index detector. Separation was performed at 60 °C using 5 mM sulfuric acid as the mobile phase at a flow rate of 0.6 $\mathrm{mL\,min^{-1}}$. Detector temperature was maintained at 45 °C. Concentrations of short- and medium-chain fatty acids were determined using external calibration curves generated from analytical standards. Propionate was quantified from the same chromatograms (retention time ∼17.0 min). A peak co-eluting with lactate (∼13.0 min) was present in ethanol- and glucose-fed bottles that received no lactate (∼2 $\mathrm{g\,L^{-1}}$ lactate equivalent at T4); lactate concentrations should therefore be read as upper bounds.

5.2.7 Sibling-Referenced Carbon and Electron Balances

Because absolute substrate inputs could not be reconciled with endpoint concentrations, carbon and electron balances for the lactate lineages were calculated relative to the non-producing sibling bottles (Lac-2 to Lac-5), which received identical medium and feed. For each producing bottle, the difference from the sibling mean was converted to carbon and electron equivalents using the degree of reduction of each compound (lactate and ethanol 12, acetate 8, propionate 14, butyrate 20, hexanoate 32 $\mathrm{e^{-}\,mol^{-1}}$). Electrons released by extra substrate consumption but not recovered in measured products were attributed to unmeasured sinks (H_2, biomass, or other products).

5.2.8 Sequencing and Bioinformatic Analysis

Genomic DNA was extracted from 2 ml samples after storage in a −80 °C freezer using the DNeasy PowerSoil Kit (Qiagen, Hilden, Germany) following the manufacturer's instructions. The V3–V4 hypervariable region of the bacterial 16S rRNA gene was amplified using the primer pair 341F (5′-CCTACGGGNGGCWGCAG-3′) and 805R (5′-GACTACHVGGGTA TCTAATCC-3′), following the Illumina 16S Metagenomic Sequencing Library Preparation

protocol. Qubit, Tapestation, and qPCR were used for quantification and concentration measurements with 2.5 μL at 5 ng/μL final concentration of DNA required before sequencing. Pooled libraries were sequenced on an Illumina MiSeq platform using a 2×300 bp paired-end MiSeq Reagent Kit v3, according to the manufacturer's protocol, at the Genome Sequencing Core at the University of Kansas.

Raw paired-end reads were processed using Cutadapt (v4.4) to remove primer sequences and discard reads lacking primer matches. Reads shorter than 100 bp after trimming were excluded. Trimmed reads were compressed and organized into a per-sample manifest file for downstream import. All downstream analyses were performed within the QIIME2 framework (v2026.4). Trimmed reads were imported as a paired-end demultiplexed artifact using the PairedEndFastqManifestPhred33V2 format. Amplicon sequence variants (ASVs) were inferred using the DADA2 plugin with forward reads truncated at position 234 and reverse reads truncated at position 232. Truncation lengths were selected based on per-base quality profiles to retain high-quality base calls across the read length while ensuring sufficient overlap for merging. No additional left-trimming was applied, as primer sequences had been removed during the Cutadapt step. Chimeric sequences were removed using DADA2's consensus chimera detection method. A phylogenetic tree was constructed using the SEPP (SATé-Enabled Phylogenetic Placement) fragment insertion method implemented in the q2-fragment-insertion plugin, using the SILVA 128 reference phylogeny as the backbone. Fragment insertion was preferred over de novo alignment approaches (e.g. MAFFT + FastTree) as it produces more accurate phylogenetic placement for short amplicon reads by inserting sequences into a pre-existing comprehensive reference tree rather than constructing a tree de novo from short, potentially gappy alignments. ASVs that could not be placed in the reference tree were removed from the feature table prior to diversity analyses using the fragment-insertion filter-features method. Taxonomic classification of ASVs was performed using the q2-feature-classifier plugin with a Naive Bayes classifier trained on the SILVA 138 NR99 reference database. The classifier was trained specifically on the V3–V4 amplicon region defined by the 341F/805R primers, with amplicons between 300 and 550 bp retained, to maximise classification accuracy for the target region. A confidence threshold of 0.7 was

applied. Following classification, sequences assigned to mitochondria, chloroplasts, or remaining unassigned reads were excluded from all analyses. Archaeal sequences, including putative methanogens, were retained.

5.3 Results and Discussion

5.3.1 Adaptive Enrichment

Despite identical starting conditions, enrichment cultures diverged sharply in metabolic behavior across serial transfers, exhibiting substantial replicate-specific variation in community structure and MCFA production. This divergence was not unexpected given the exceptionally low initial abundance of *C. kluyveri* (3 sequences) and other known chain elongating taxa in the rumen inoculum. Starting from near-undetectable levels of the target organism, stochastic differences in early community assembly would be expected to propagate through subsequent transfers. Indeed, this variation in early assembly outcomes directly predicted later productivity: lineages that established high *C. kluyveri* abundance early (Eth-1, Lac-1, Lac-6) became the productive cultures, while those that diverged toward alternative dominant taxa (Lac-2, Lac-3, -4, -5) did not accumulate hexanoate. During T0–T1, most cultures were active with gas production rising from ∼6–9 mL d^{-1} to ∼11–21 mL d^{-1}, indicating rapid establishment of anaerobic metabolism. From T2 onward, as carried-over rumen fluid diminished, cultures developed increasingly distinct phenotypes: glucose-fed cultures became dark and turbid; ethanol- and lactate-fed cultures varied widely in pigmentation, turbidity, and precipitate formation (some ethanol cultures turned purple with sulfurous odors; some lactate cultures stayed clear with dark precipitates). Gas production generally declined after T2, suggesting depletion or displacement of the populations driving initial activity. Divergence intensified by T3, with some lactate/ethanol lineages developing dark precipitates and pH drops while others became nearly inactive, indicating replicate-specific ecological trajectories rather than uniform enrichment.

HPLC measurements confirmed that visible activity did not predict MCFA production

(Figure 5.2). Butyrate accumulated broadly across lineages and substrates, but hexanoate formation was concentrated in a subset of replicates, especially among ethanol- and lactate-fed cultures by T4; glucose cultures favored shorter-chain products. This showed that productive chain elongation was lineage rather than substrate dependent. Early cultures showed gas production without sustaining MCFA accumulation. Initial samples showed probable sulfur reduction (deep purple colors and sulfurous smell) which cleared after the introduction of sodium molybdate. All samples maintained a pH of 6.5 due to sodium bicarbonate buffering. Under these restrictions and methanogenesis inhibition and substrate limitation the Shannon diversity decreased from 8.25 in the initial rumen fluid to less than five across all cases, with the lactate and ethanol fed lineages having more diversity than the glucose fed lineages (Table 5.3).

Table 5.3: Shannon diversity index after enrichment.

Sample	Shannon diversity
Eth 1	2.458
Eth 2	3.446
Eth 3	2.658
Eth 4	4.502
Eth 5	2.479
Eth 6	6.167
Glu 1	1.581
Glu 2	0.509
Glu 3	1.423
Glu 4	1.327
Glu 5	1.104
Glu 6	2.089
Lac 1	3.406
Lac 2	3.147
Lac 3	4.698
Lac 4	5.745
Lac 5	4.166
Lac 6	2.034
Rumen fluid	8.245

Based on combined HPLC and phenotypic data, four lineages (Eth-1, Lac-1, Lac-6, and Glu-5) were selected for reactor-scale validation based on quantifiable hexanoate output



Figure 5.2: HPLC results for the serum-bottle enrichments over transfers T1–T4, separated by feed substrate (ethanol, lactate, glucose). Bars show butyrate (C4) and hexanoate (C6) concentrations for each of the six lineages within a substrate group; lines show the concentration of residual primary substrate for each lineage (right-hand axis).

(Table 5.4, Figure 5.2). Eth-1 produced 0.28 $g\,L^{-1}\,wk^{-1}$ hexanoate and 0.680 $g\,L^{-1}\,wk^{-1}$ butyrate. Lac-1 was the top performer (0.31 $g\,L^{-1}\,wk^{-1}$ hexanoate, 1.132 $g\,L^{-1}\,wk^{-1}$ butyrate). Lac-6 and Glu-5 each produced 0.08 $g\,L^{-1}\,wk^{-1}$ hexanoate, with 0.660 and 0.555 $g\,L^{-1}\,wk^{-1}$ butyrate, respectively. Overall, adaptive enrichment drove strong ecological divergence rather than uniform chain elongation as demonstrated by PCoA (Figure 5.3). PCoA analysis of 16S sequencing data revealed that enrichment with lactic acid feeding diverged less from the original rumen fluid than the glucose fed lineages. Meanwhile, the ethanol fed lineages were split between both groups showing a greater level of stochastic variation than either of the other two substrates. Productive lineages emerged through progressive selection under shifting substrate and environmental conditions, with stochastic community succession and metabolic competition likely shaping early consortium establishment.

5.3.2 Lactic Acid Derived Cultures

Community sequencing of the lactate-fed lineages produced an unexpected result: both Lac-1 and Lac-6 were dominated by *C. kluyveri*, an organism whose canonical metabolism converts ethanol and acetate to hexanoic acid and which cannot use lactate [204]. (Species-level assignment from V3–V4 amplicons is tentative, and this identification should be confirmed by full-length 16S rRNA gene sequencing or isolation.) *C. kluyveri* occupied 74.197% of the Lac-1 community and 85.544% of Lac-6, but was present at only 5.157% in Lac-2, 5.127% in Lac-4, 0.997% in Lac-5, and was not detected at all in Lac-3, a pattern that tracks closely with hexanoate production (Figure 5.4).

Lac-1 and Lac-6, and no other lactate lineage, also contained substantial populations of *Clostridium tyrobutyricum* (1.979% in Lac-1, 9.503% in Lac-6), together with *Clostridium sensu stricto* 1 and *Clostridium butyricum*. These organisms ferment lactate (with acetate) to butyrate, CO_2, and H_2 [205] and readily participate in syntrophic relationships [206]. We propose that the lactate fermenters and *C. kluyveri* formed a division of labor in which the fermenters converted lactate into the three things *C. kluyveri* needs but cannot make from lactate itself: butyrate as an electron acceptor, H_2 as an electron donor, and CO_2, which

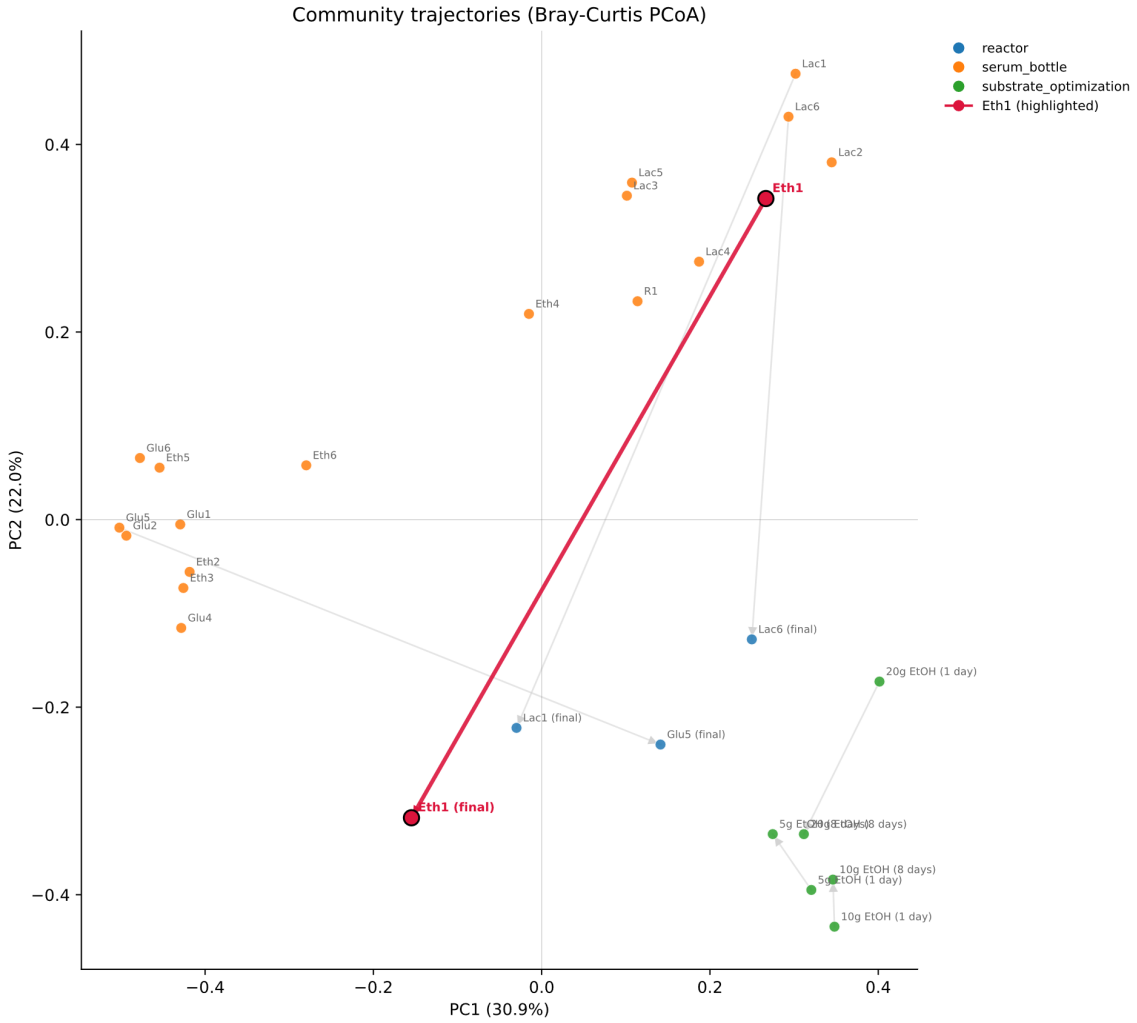


Figure 5.3: Bray-Curtis principal coordinates analysis (PCoA) of community trajectories across the serum-bottle enrichments, the validation reactors, and the substrate-optimization reactors. Arrows connect each serum-bottle lineage to its corresponding reactor endpoint; the Eth-1 trajectory is highlighted.

Table 5.4: Final product concentrations and characteristics of the initial enrichment cultures.

Lineage	Primary substrate	Feeding conditions	Butyrate production (g/L week)	Hexanoate production (g/L week)	Observed characteristics
Eth-1	Ethanol	2 g/L ethanol + 1 g/L acetate	0.680	0.28	Stable pH, persistent gas production, ester-associated aroma
Lac-1	Lactic acid	2 g/L lactate + 1 g/L acetate	1.132	0.31	Strong butyrate formation, sustained activity
Lac-6	Lactic acid	2 g/L lactate + 1 g/L acetate	0.660	0.08	Moderate gas production, persistent chain elongation activity
Glu-5	Glucose	2 g/L glucose + 1 g/L acetate	0.555	0.08	High turbidity, fruity volatile profile

C. kluyveri requires for biosynthesis. Elongating butyrate to hexanoate requires only one round of reverse β-oxidation, so a supply of fermentation-derived butyrate lowers the reducing equivalents *C. kluyveri* must obtain per mole of hexanoate compared with building hexanoate from acetate alone. Although H_2 is usually considered a product of, and an inhibitor to, ethanol-based chain elongation [196], it has been shown to serve as a supplemental electron source for *C. kluyveri* in co-culture [207]. In the lactate lineages, the relevant step is the elongation of butyrate with acetate, in which H_2 replaces ethanol as the electron donor (Reaction 7; 194). In pure culture, Yin et al. [194] observed that *C. kluyveri* consumed little added H_2 when ethanol was available, preferring ethanol as the electron donor, and attributed this to gas–liquid mass transfer resistance. Gas–liquid transfer was not measured in the present work, but two features of the lactate lineages would be expected to reduce this limitation: first, ethanol was scarce, and second, H_2 would be generated within the liquid phase by co-occurring lactate fermenters rather than supplied to the headspace. Whether this proximity was sufficient to sustain H_2 uptake by *C. kluyveri* remains to be tested directly. This route does not require an additional, unidentified ethanol-producing organism, which is consistent with no such organism being identified in the community data; however, that possibility cannot be ruled out.

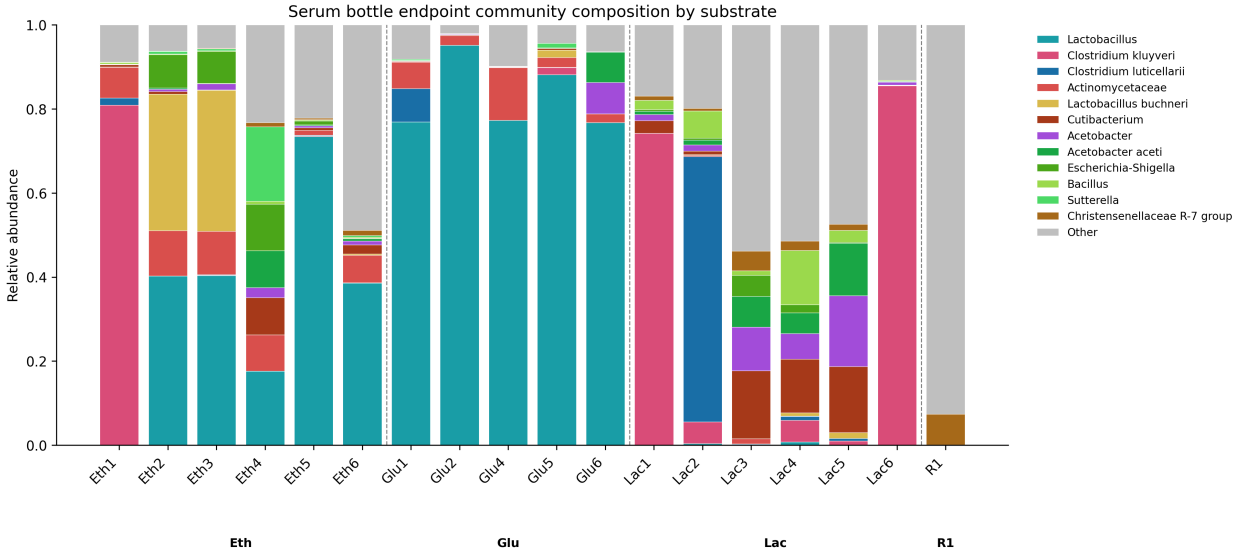


Figure 5.4: Community composition of serum bottle enrichments.

The HPLC data are consistent with the H_2 utilization hypothesis. In the transfer preceding hexanoate production (T3), Lac-1 and Lac-6 each consumed approximately 3.7 $g\,L^{-1}$ more lactate than the mean of their non-producing siblings (Lac-2 to Lac-5; Section 5.2.7). Lac-1 recovered roughly half of the electrons from this additional lactate as butyrate (+1.3 $g\,L^{-1}$) and ethanol (+0.58 $g\,L^{-1}$), while Lac-6, which also consumed an additional 1.0 $g\,L^{-1}$ acetate, recovered almost none of them in measured liquid products. The unrecovered electrons are consistent with H_2 evolution into the headspace and with biomass formation. In the non-producing lineages, electrons were instead diverted to propionate, which reached 2.3 $g\,L^{-1}$ in Lac-2 and 1.2 $g\,L^{-1}$ in Lac-5 at T3 compared with $\leq$ 0.56 $g\,L^{-1}$ in Lac-1 and Lac-6. During T4, when hexanoate appeared, the additional substrate consumed by Lac-6 relative to its sibling lineages accounted for all of the electrons recovered in its butyrate and hexanoate, with a surplus of approximately 85 mM electron equivalents that is consistent with H_2 and CO_2 production. The Lac-1 balance did not close during T4 because its products contained more carbon and electrons than could be attributed to measured substrate consumption, indicating either an overestimate of residual lactate (Section 5.2.6) or an unmeasured substrate such as yeast extract or cysteine.

If the butyrate and hexanoate formed in a single transfer were built from acetate with H_2 as the only electron donor, Lac-1 would have required approximately 50 mM H_2 ($\sim$130 mL per bottle at 38 °C) and Lac-6 approximately 19 mM ($\sim$50 mL), compared with a headspace of 50 mL. Hydrogen would therefore have had to be produced and consumed concurrently rather than accumulated, which is characteristic of tightly coupled interspecies hydrogen transfer. The bottles were vented only through septum needle punctures, which would allow H_2 partial pressure to build whenever production outpaced leakage. Ethanol is unlikely to have been entirely absent as a donor; it was detected in all lactate-fed cultures at a relatively stable $\sim$0.23 $g\,L^{-1}$, and Lac-1 reached the highest ethanol concentration of any lactate bottle at T3 (0.97 $g\,L^{-1}$), concurrent with its butyrate peak. The endpoint data cannot distinguish between H_2 and low-level in situ ethanol as the electron donor, since both are electron-equivalent; however, the hydrogen route requires fewer assumptions and is directly supported by the known metabolism of the co-occurring lactate fermenters.

The hypothesis is further supported by what happened upon transfer to the bioreactor. The *C. kluyveri* population in both lineages collapsed, and hexanoate production ceased in all but the ethanol-fed lineage (Eth-1). The serum bottles were vented only through needle punctures, whereas the bioreactors had an open offgas port and were flushed daily with N_2/CO_2. Under the hydrogen hypothesis, this difference alone removes the electron donor that *C. kluyveri* depended on in the lactate lineages, while Eth-1, supplied ethanol directly, was unaffected. Following transfer, the Lac-1 reactor community was dominated by *Lactobacillus* (30.11%, combining *Lactobacillus* and *Lactobacillus buchneri*), *Bacillus* (23.96%), and *Clostridium sensu stricto* 1 (34.85%), while the Lac-6 reactor community was dominated by *Clostridium sensu stricto* 1 (73.33%) and *Bacillus* (15.38%) (Figure 5.5). *C. tyrobutyricum* was also lost from both reactor communities.

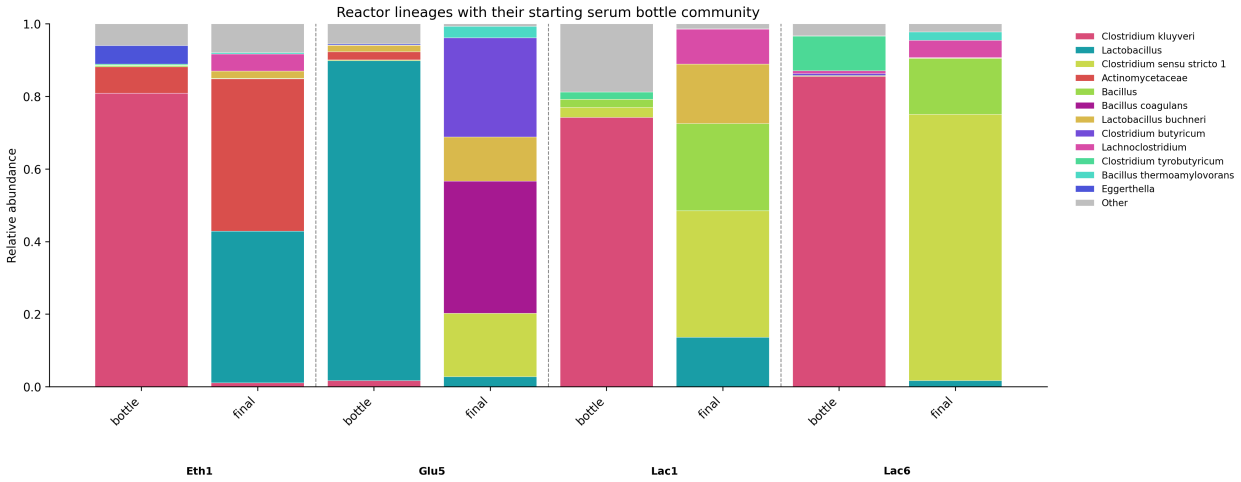


Figure 5.5: Comparison of community composition between the T4 serum bottles and endpoint of the validation reactors.

Caproiciproducens, a genus capable of producing caproate directly from lactic acid, was also detected at low abundance across several lineages (0.5% in Lac-1, 0.2% in Lac-6, 3% in Glu-1). Given these low abundances compared to *C. kluyveri* in producing serum bottles, it is unlikely that this organism contributed meaningfully to hexanoic acid production; it may, however, be positioned to take up production in a reactor environment more favorable to it, and its presence in Glu-1 in particular warrants further investigation.

Among the lactate lineages that failed to sustain chain elongation activity, Lac-2 was

notable for being dominated (63.07%) by *Clostridium luticellarii*, an organism capable of chain elongation from hydrogen, CO_2, and acetate or methanol, and one that was itself originally isolated from baijiu pit mud [208]. Despite this, no hexanoate accumulation was detected in Lac-2, paralleling the behavior of the glucose lineage Glu-1. Under the hydrogen hypothesis, *C. luticellarii* would compete directly with *C. kluyveri* for H_2, and Lac-2 also diverted a large share of lactate to propionate (2.3 gL^{-1} at T3), leaving little lactate-derived butyrate or H_2 for chain elongation. Lac-3, -4, and -5 lacked a single dominant organism and were instead occupied by comparable abundances of *Cutibacterium* (*Propionibacteriaceae*), *Acetobacter* (including *Acetobacter aceti*), and smaller fractions of *Escherichia–Shigella* and *Bacillus* (Figure 5.4). The presence of *Acetobacter*, an obligate aerobe and ethanol consumer, in these lineages may indicate localized oxygen contamination during handling or transfer.

5.3.3 Glucose Derived Culture

All glucose-fed enrichments were dominated by *Lactobacillus*, consistent with the rapid acidification and elevated turbidity observed for this substrate group during serum-bottle enrichment. Glu-5, the only glucose lineage to produce detectable hexanoic acid, additionally carried a small population of *C. kluyveri* (Figure 5.4). Glu-5 was successfully sequenced at two points during the reactor run, whereas biomass limitations prevented sequencing of the other enrichments prior to the end of the run. At the first sampling, *C. kluyveri* was present within the Glu-5 community alongside *Lactobacillus*, *Lactobacillus buchneri*, *Actinomycetaceae*, *Clostridium luticellarii*, *Clostridium sensu stricto* 1, *Clostridium butyricum*, *Bacillus coagulans*, and *Bacillus thermoamylovorans*. By the second and third samplings, *C. kluyveri* was no longer detectable, and the community had shifted toward a mix of butyrate-producing organisms, predominantly *Bacillus* species and *Clostridium butyricum* rather than *Lactobacillus*. However, perhaps the most surprising characteristic of these cultures is they all have an extremely low Shannon diversity, ranging from 0.5 (Glu-2) to 2.089 (Glu-6) (Table 5.3).

As with Lac-2, *C. luticellarii* was also detected in Glu-1, but no hexanoate production

was observed in that lineage, reinforcing the pattern that the presence of a known chain elongating organism was not, by itself, sufficient to guarantee productive chain elongation within these communities. Several organisms are capable of performing chain elongation directly from glucose or lactate, including *Caproiciproducens* [19], *Megasphaera elsdenii* [200], and *Caproicibacterium lactatifermentans* [193]. But the strong early dominance of *Lactobacillus* across the glucose lineages appears to have limited the opportunity for these organisms to establish, and the two- or three-step syntrophic process implicated in the lactate lineages does not appear to have taken hold in the glucose-fed cultures either (Figure 5.4). The loss of *C. kluyveri* and the shift toward *Bacillus* and *C. butyricum* dominated butyrate production upon transfer to the reactor again illustrates the substantial reshaping of community structure that accompanied the change from static, sealed serum-bottle culture to reactor operation (Figure 5.5). OD_{600} for Glu-5 spiked sharply within the first 24 hours before oscillating around 0.9–1.2 for the remainder of the run (Figure 5.6), a pattern broadly consistent with the shift from *Lactobacillus* to *Bacillus*/*Clostridium butyricum* dominance described above as the fast-growing *Lactobacillus* initially dominate but eventually give way to the slower growing *Bacillus* which can process the waste products of the former.

5.3.4 Ethanol Derived Culture

The ethanol fed cultures had the greatest Bray-Curtis distance between cultures (Figure 5.3), with Eth-1 and Eth-4 residing near the lactic acid cultures and the initial rumen fluid, while Eth-2, Eth-3, Eth-5, and Eth-6 all resided near the glucose fed cultures. About 80% of the Eth-1 culture was occupied by *C. kluyveri* with a Shannon diversity of 2.458, while Eth-4 had no single dominant taxon (*Lactobacillus*, *Sutterella*, *Escherichia–Shigella*, and *Cutibacterium* each at roughly 10–18%) and a higher Shannon diversity of 4.502 (Figure 5.4, Table 5.3). The ethanol fed cultures Eth-2 and Eth-3 were similar to the glucose cultures, with *Lactobacillus* split between *Lactobacillus* sp. and *Lactobacillus buchneri* (roughly 40% and 33% in each), while Eth-5 was dominated by *Lactobacillus* sp. (72.32%). The outlier was Eth-6 which contained 37.2% *Lactobacillus* sp. but also had the highest Shannon diversity of any of the

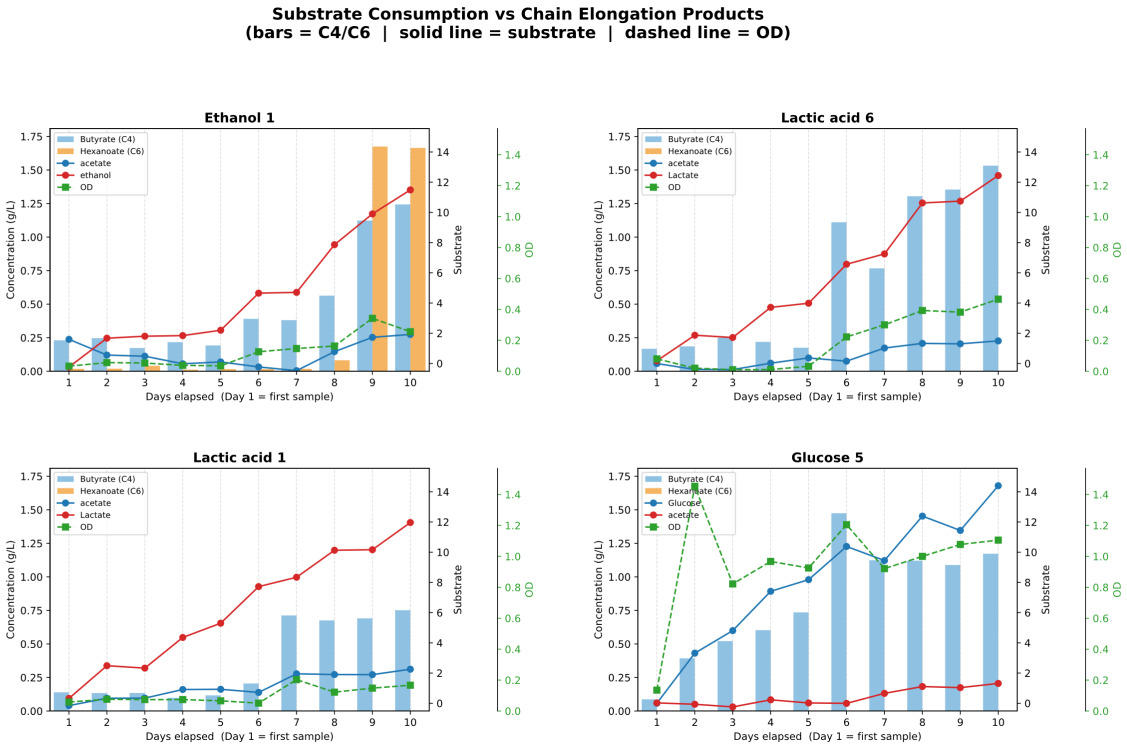


Figure 5.6: Substrate consumption and chain elongation products for the four validated lineages (Eth-1, Lac-1, Lac-6, Glu-5) over the 10-day bioreactor run. Bars show butyrate (C4) and hexanoate (C6); solid lines show substrate and acetate concentrations; dashed lines show OD_{600}.

cultures at 6.167.

Eth-1 was the only one of the six ethanol-fed serum-bottle lineages found to contain *C. kluyveri* at detectable levels, despite ethanol being the substrate directly supplied to all six. This is a striking contrast to the lactate lineages, in which roughly a third of the replicates (Lac-1 and Lac-6, out of six) developed high *C. kluyveri* ($> 70\%$) abundance and produced quantifiable levels of hexanoic acid and 5/6 lactic acid fed cultures had *C. kluyveri* in detectable levels despite being enriched in environments containing no native ethanol supply. Taken together with the community and operational evidence discussed in Section 5.3.2, this asymmetry is part of why we favor the hypothesis that lactate fermenters supplied *C. kluyveri* with butyrate and H_2 in the lactate lineages, rather than assuming that ethanol availability alone predicts *C. kluyveri* dominance. Upon transfer to the bioreactor, Eth-1 was also the only lineage among the four validated cultures to continue producing hexanoic acid; production was characterized by an extended lag phase, followed by an exponential release of hexanoic acid, followed by a stationary phase. This is reflected in the OD_{600} trajectory, which shows a comparatively flat lag phase through day 5 followed by sustained growth through the remainder of the run (Figure 5.6).

5.3.5 Bottle to Reactor Results and Implications

Across all four validated lineages, transfer from static, loosely sealed serum bottles to continuously stirred, gas-purged 1 L bioreactors produced a sharp discontinuity in chain elongation activity. Only Eth-1 continued to accumulate hexanoic acid in the reactor, reaching $\sim$1.7 g/L by day 9–10, while Lac-1, Lac-6, and Glu-5 produced no detectable hexanoate across the full 10-day run (Figure 5.6). The most direct explanation for this asymmetry follows from the mechanism proposed in Section 5.3.2: Eth-1 was supplied ethanol directly, whereas the hexanoate production observed in Lac-1 and Lac-6 during the serum-bottle stage most plausibly depended on butyrate and H_2 supplied by co-occurring lactate fermenters, and the small amount produced by Glu-5 likewise lacked a direct ethanol feed. If that in-situ supply depended on a specific consortium structure or on headspace conditions particular to the

sealed bottles, then losing either the responsible organisms or those conditions during transfer would be sufficient on its own to collapse *C. kluyveri* and halt chain elongation in the three indirect lineages.

The direct-versus-indirect distinction does not, however, account for everything the reactor data show. Eth-1's own hexanoate production was not immediate: OD_{600} remained flat through day 5 (0.03–0.06) before rising sharply from day 6 onward (0.13–0.34), and hexanoate accumulation was similarly delayed, appearing only after day 8 (Figure 5.6). This lag-then-growth pattern, together with the near-total turnover of the Lac-1 and Lac-6 reactor communities toward *Lactobacillus*/*Bacillus* and *Clostridium sensu stricto* 1, respectively (Figure 5.5), points to reactor gas handling as a factor operating alongside substrate mode. The open offgas port and daily gas flushing used in the bioreactors would be expected to strip headspace hydrogen far more effectively than the sealed serum bottles, removing the H_2 that served as an electron donor for *C. kluyveri* in the lactate-derived lineages. Even for Eth-1, the change in environment imposed a period of re-adaptation before chain elongation resumed.

These results indicate that the serum-bottle and bioreactor stages of this enrichment pipeline selected for meaningfully different communities, and that the indirect supply of electron donor that supported *C. kluyveri* during the bottle stage was not carried through to reactor-scale operation. Of the four lineages tested, only Eth-1 which was insulated from this dependency by receiving ethanol as a direct feedstock demonstrated stable, reproducible hexanoate production under reactor conditions. This made it the only lineage suitable as a starting culture for the substrate-ratio experiments that follow in Section 5.3.6.

5.3.6 Substrate Optimization

Once chain elongating communities had been established under the enrichment conditions, the next objective was to determine how substrate availability influenced product formation. Thus the reactors were run again and were inoculated with the Eth-1 culture from the previous reactor run, this time in a batch mode. Reported maximum hexanoate concentrations

from *Clostridium*-based systems vary considerably with reactor configuration and cultivation time. Reddy et al. [61] demonstrated the accumulation of 8.6 g/L hexanoic acid over the course of 40 days. Gomes et al. [209] achieved 10 g/L hexanoic acid in a 12-day batch process. Liu et al. [66] reached 10 g/L hexanoic acid over the course of 50 days with high variation in their reactors. That these systems plateau at similar concentrations is consistent with product inhibition: about 10 g/L is close to the aqueous solubility of undissociated hexanoic acid, and the undissociated acid becomes increasingly toxic to chain-elongating bacteria as it accumulates, which is why in-line product extraction is often used to exceed this level. The specificity for open cultures to produce hexanoic acid is primarily influenced by the ratio of ethanol to acetate with 10:1 being ideal [194]. There is currently no consensus on ideal concentrations of ethanol to use in *C. kluyveri* based consortiums other than that concentrations over 14 g/L ethanol can become progressively more inhibitory to chain elongation [209]. Thus, we tested 3 different concentrations of ethanol (5, 10, 20 g/L) and 3 g/L acetic acid for ethanol to acetic acid mass ratios of 1.7, 3.3, and 6.7, respectively (molar ratios of about 2.2, 4.3, and 8.7).

The 5 g/L reactor consumed 3.59 g/L ethanol and produced 3.42 g/L acetic acid, indicating ethanol oxidation and produced no hexanoic acid or butyric acid within the 8-day run (Figure 5.8). This reactor was increasingly dominated by *Actinobacteria* (73%–90%), a slow-growing group not generally associated with chain elongation (Figure 5.7). The 10 g/L reactor consumed 4.88 g/L ethanol and 1.9 g/L acetic acid and produced no significant butyric or hexanoic acid. The majority of the 10 g/L reactor was occupied by *Bacillus* (8.81%) and *Bacillus thermoamylovorans* (44.42%) as well as *Actinobacteria* (46.74%). After 7 days both *Clostridium luticellarii* (4.34%) and *Clostridium jeddahense* (12.39%) appeared. *Clostridium luticellarii*, as noted before, can perform chain elongation from syngas via the Wood-Ljungdahl pathway but, as before, did not produce hexanoic acid or butyric acid [208]. The 20 g/L reactor consumed 10.6 g/L ethanol, 2.9 g/L acetate (depleting the supply) and producing 4.6 g/L hexanoic acid and 1.3 g/L butyric acid. OD_{600} confirmed this dynamic: the 20 g/L reactor showed minimal growth through day 4 before a sharp increase beginning day 5 (Figure 5.8), coinciding with the period of active ethanol consumption and hexanoic

acid accumulation reported above, while the 5 and 10 g/L reactors grew steadily from the outset without a comparable lag. It is possible that the 10 g/L reactor could have developed chain elongating activity given time. At 20 g/L, which is above the 14 g/L documented inhibitory levels, enriched rumen cultures established and began producing hexanoic acid after a week of reactor operation and, once production began, accumulated hexanoic acid at a rate comparable to those reported in previous studies, although this comparison rests on a single reactor per treatment. However, there remain questions about community stability and succession dynamics that have yet to be established. In the 20 $\mathrm{g\,L^{-1}}$ reactor, *C. kluyveri* made up roughly a third of the community after 1 day but only a few percent after 8 days, when *Bacillus thermoamylovorans* and *Lachnoclostridium* dominated (Figure 5.7); its relative abundance was similarly low at the endpoint of the Eth-1 validation reactor (Figure 5.5). Because relative abundance at a single endpoint does not reflect activity or absolute cell numbers, absolute quantification (e.g., *C. kluyveri*-specific qPCR) at intermediate time points will be needed to confirm which organisms carried out chain elongation in the reactors.

Evaluating hexanoic acid production alone against the limiting-substrate stoichiometry (Reaction 1 and Reaction 2) gives an apparent yield of 82% (39.6 mM hexanoic acid produced per 48.3 mM acetic acid consumed). However, because chain elongation proceeds through sequential two-carbon additions in which acetate serves as the initial carbon skeleton for both butyrate and hexanoate, a complete accounting of elongation efficiency requires considering both products jointly relative to acetate consumption:

$$\text{Equation 2:} \quad Y_{\mathrm{HAc}} = \frac{\Delta[\text{butyrate}] + \Delta[\text{hexanoate}]}{\Delta[\text{acetate}]_{\text{consumed}}}$$

Applied to the 20 g/L reactor, this gives $Y_{\mathrm{HAc}} = (14.8\ \mathrm{mM} + 39.6\ \mathrm{mM})/48.3\ \mathrm{mM} = 112\%$. Because a yield exceeding 100% is not possible on a strictly consumptive basis, this result indicates that net acetate depletion underestimates the true (gross) quantity of acetate cycled through the elongation pathway, consistent with concurrent acetate regeneration via oxidative ethanol conversion (Reaction 3 and Reaction 6) [210]. Which was observed in the

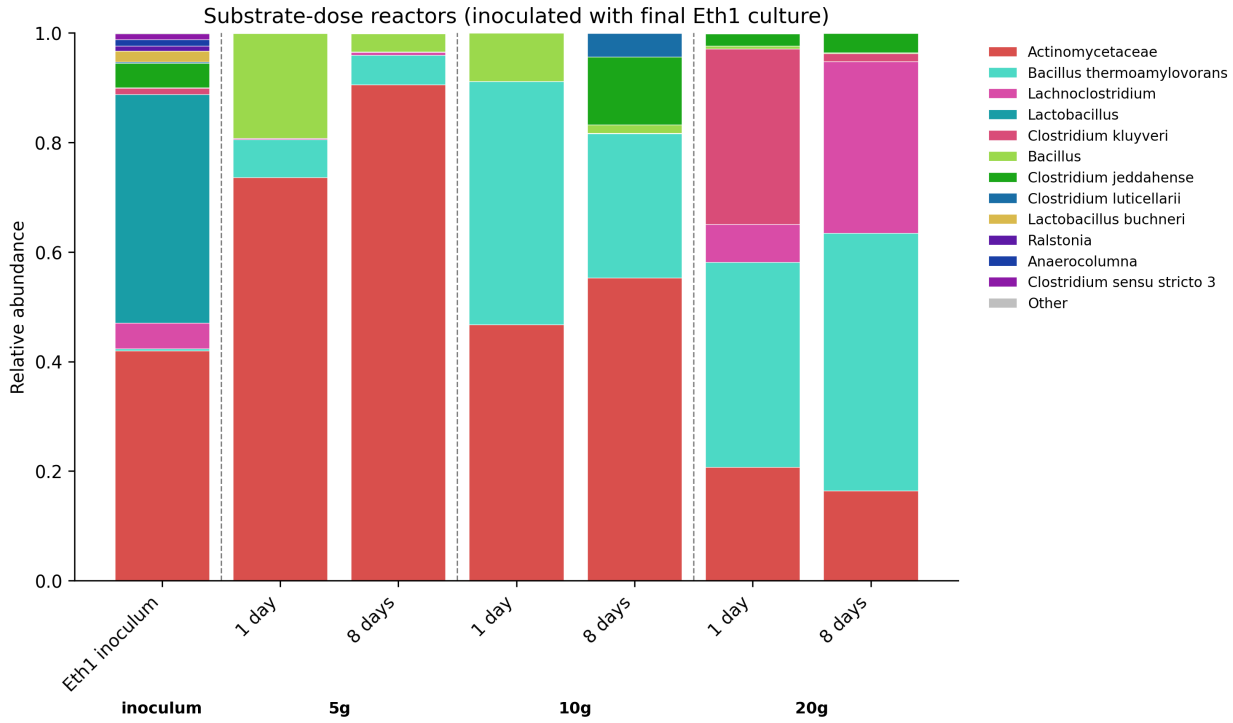


Figure 5.7: Relative community composition of the substrate-dose reactors inoculated with the final Eth-1 culture, shown for the inoculum and at 1 day and 8 days for each of the 5, 10, and 20 g/L ethanol treatments.

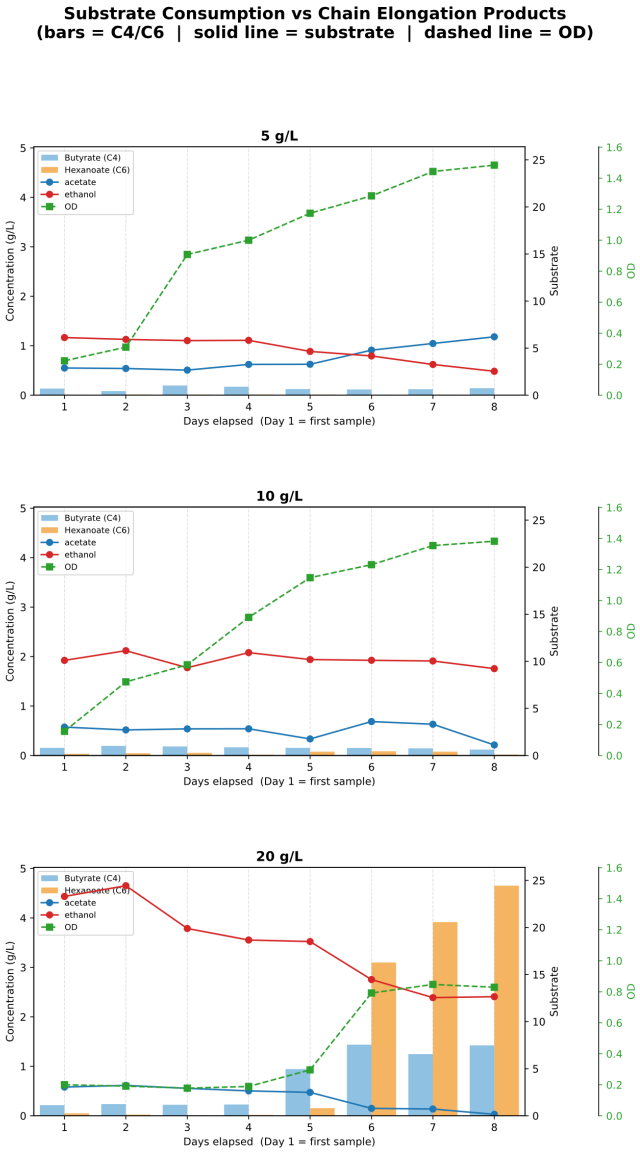


Figure 5.8: Substrate consumption and chain elongation products in the substrate-optimization reactors at 5, 10, and 20 g/L initial ethanol with 3 g/L acetic acid, over the 8-day batch run. Bars show butyrate (C4) and hexanoate (C6); solid lines show ethanol and acetate; dashed lines show OD_{600}.

5 g/L reactor which produced acetate. Acetogenic organisms in these reactors are likely responsible since they generate energy by oxidizing ethanol into acetic acid and are known to establish syntrophic relationships with *C. kluyveri* [211].

The combined stoichiometric requirement for the observed butyrate and hexanoate (1 mol ethanol per mol butyrate; 2 mol per mol hexanoate) was 94.0 mM, only 41% of the 230 mM ethanol actually consumed. The remaining ethanol was likely directed toward biomass production, hydrogen evolution, or the acetate-regenerating oxidation rather than directly toward chain elongation. On a product-distribution basis, hexanoate accounted for 73% of combined butyrate + hexanoate production (39.6 mM / 54.4 mM), indicating strong specificity toward complete elongation to C6 rather than accumulation of the C4 intermediate.

These results describe a consortium with genuine promise for MCFA production exhibiting rapid establishment and promising yields from a single reactor run, but built on an enrichment and transfer process that is not yet reliable. Replicate cultures diverged unpredictably from identical starting material; the lactate-derived lineages depended on an indirect, most likely H_2-based, supply of electron donor that did not survive scale-up; and only one of four validated lineages carried production through to the reactor at all. Thus, considerable work remains: directly measuring hydrogen exchange between lactate fermenters and *C. kluyveri*, determining whether reliability can be engineered into the enrichment protocol rather than left to stochastic community succession, and testing whether the speed advantage seen here holds under real optimization. Once a productive community is established, however, it may be possible to maintain it from batch to batch rather than re-enriching it each time [203]. Each serum bottle was established with only 20 ml of rumen fluid and productive cultures were expressed in ethanol and lactate fed enrichments at a rate of 1/6 for ethanol and 1/3 for lactate. This shows that even from extremely low-abundance inocula, selective enrichment conditions can identify and amplify productive chain-elongating consortia, although not yet reliably. When *C. kluyveri* was successfully enriched (Eth-1, Lac-1, Lac-6), it rapidly became dominant (74–86% of the community), indicating strong selective pressure for the target phenotype. The single lineage (Eth-1) that continued producing hexanoate under reactor conditions achieved production rates and yields in the range reported by stud-

ies starting from 10–100-fold larger inocula, although replicate reactors will be needed to confirm this. Future enrichments beginning with larger inoculum volumes or pre-enriched *C. kluyveri* starter cultures could plausibly improve reproducibility while retaining the productivity advantages demonstrated here.

5.4 Conclusion

This chapter demonstrates that rumen fluid can serve as a viable inoculum for the adaptive enrichment of microbial consortia capable of medium-chain fatty acid production, particularly hexanoic acid. However, enrichment outcomes were highly dependent on community succession and operating conditions rather than substrate identity alone. Although ethanol-, lactate-, and glucose-fed cultures all produced butyrate, sustained hexanoate production was restricted to a subset of lineages, indicating that successful chain elongation requires the establishment of specific microbial interactions and metabolic conditions.

The lactate-enriched cultures provided evidence for a syntrophic mechanism in which lactate-fermenting *Clostridia* supplied *Clostridium kluyveri* with butyrate and H_2. Both Lac-1 and Lac-6 contained high abundances of *C. kluyveri* together with *C. tyrobutyricum* and produced hexanoate despite receiving no external ethanol, and a sibling-referenced electron balance showed that their additional lactate consumption released more electrons than were recovered in liquid products. These communities lost chain elongation activity following transfer to gas-purged bioreactors, consistent with removal of the H_2 on which this partnership depended. Direct headspace and dissolved H_2 measurements, together with time-resolved sampling within a transfer cycle, will be needed to confirm this mechanism.

Among the cultures evaluated at reactor scale, Eth-1 was the only lineage that consistently maintained hexanoic acid production, reflecting both the challenge of scaling cultures derived from near-undetectable inoculum abundance and the importance of direct ethanol availability. Subsequent substrate optimization showed that 20 g/L ethanol and 3 g/L acetic acid produced 4.6 g/L hexanoic acid in approximately 8 days. Because each reactor condition was run once, these reactor results should be treated as a proof of concept; replicate

reactors are needed to estimate run-to-run variability. Replicate cultures originating from the same inoculum did develop markedly different microbial communities, though this variation was expected given that the target organism (*C. kluyveri*) comprised only 3 sequences in the starting rumen sample. This outcome suggests that path-dependent assembly during early transfers is a primary driver of divergence, rather than an inherent limitation of the enrichment approach itself.

Overall, these findings support rumen-derived microbial communities as a promising platform for the biological production of hexanoic acid, while demonstrating that successful scale-up requires greater control over microbial community structure and syntrophic interactions. The Eth-1 consortium provides a useful starting culture for further process optimization, and the observed production of 4.6 g/L hexanoic acid suggests that rumen-derived communities may offer a practical route toward liquid-state MCFA fermentation when enrichment and reactor conditions are appropriately controlled.

In the context of this dissertation, the Eth-1 consortium is a working example of the chain-elongation stage proposed in Chapter 1. It is a liquid-state enrichment that converts ethanol and acetate, the main products of the primary fermentations in Chapters 2–4, into hexanoic acid, the precursor of ethyl hexanoate. The lactate-fed lineages also point to a use for the lactic acid that accompanies grain fermentation (Chapters 2 and 3), provided that the lactate-fermenting partners and the hydrogen they produce are retained, for example by limiting gas purging. The last stage of the proposed process, maturation of the distilled spirit, is examined in Chapter 6.

Chapter 6

Exploring a Novel Chinese-Style Whiskey Using Baijiu as the Base Spirit: Effects of Small-Barrel Aging and Environmental Conditions

This chapter is based on the manuscript "Exploring the Production of a Novel Chinese-Style Whiskey Using Baijiu as the Base Spirit: Effects of Small-Barrel Aging and Environmental Conditions," co-authored by Thomas Weiss, Shan Hong, Yonghui Li, Xiaorong Wu, Mark Wilkins, Mike Tilley, and Donghai Wang. It has been edited for consistency with the rest of this dissertation.

Chapter Overview

Chapter 1 identified aging as the final selective environment in baijiu production. In that framing, aging is the stage that decides which fermentation-derived compounds survive into the finished spirit and how they are transformed. Traditional baijiu is aged in clay or porcelain vessels that contribute relatively little flavor of their own. Western whiskeys, by contrast, derive much of their character from oak. This chapter examines what happens when the two traditions are combined, using oak barrels to mature finished baijiu. The work

also tests how strongly the fermentation chemistry set upstream constrains what aging can achieve.

Chinese baijiu is one of the most chemically complex distilled spirits in the world. Its open solid-state fermentation produces a much broader volatile profile than conventionally aged bourbon whiskey. The hypothesis tested here was that aging baijiu in oak barrels would produce a spirit with greater flavor complexity than traditionally aged whiskey. Five baijiu varieties representing four major aroma categories were evaluated: strong aroma (Luzhou Laojiao), sauce aroma (HongHua Lang), light aroma (Red Star Erguotou), feng aroma (Xifeng), and miscellaneous aroma (Ming River). The spirits were aged for up to two months in 1-L oak barrels under two controlled regimes. The first was a varying temperature and humidity regime (15–26°C and 50–70% RH, each cycling on 12-h intervals). The second was a steady-state regime (23°C and 60% RH). Volatile compounds were characterized by headspace solid-phase microextraction GC–MS, and color development was followed by UV–Vis spectrophotometry. Before aging, all five baijiu varieties contained more distinct compounds than the reference bourbons. Oak aging increased compound richness in every baijiu type. It also reduced total volatile concentration in four of the five varieties, mainly through evaporation and ester hydrolysis. Feng-aroma Xifeng was the exception. Its total volatile concentration rose under both conditions, and it uniquely synthesized key bourbon esters, including ethyl octanoate and ethyl hexanoate, during maturation. All aged samples developed an amber color comparable to bourbon, but their volatile compositions did not converge toward bourbon. Oak-aged baijiu therefore appears to be a chemically distinct spirit category governed by baijiu's fermentation biology.

6.1 Introduction

Whiskey production consists of several distinct stages: malting, mashing, fermentation, distillation, aging, and bottling. Freshly distilled whiskey lacks complexity and smoothness. It is colorless, with a sharp and pungent aroma, an intense flavor, and a harsh, fiery texture. Aging is therefore among the most important production stages, because it largely

determines the final flavor profile and color of the whiskey. Over time, interactions between the spirit and the oak barrel drive complex chemical transformations that give each whiskey its character. Oak contributes lignin-derived compounds, lactones, and tannins, which impart vanilla, coconut, and woody notes, respectively [212]. Slow oxidation during aging also develops richer and smoother flavors, reduces harshness, and increases aromatic complexity [213, 214]. These compounds then interact with the ethanol and other components of the spirit, and these interactions depend on the composition of the wood and on the aging environment [215].

Chinese baijiu, in contrast, is a traditional distilled spirit produced mainly by solid-state fermentation of sorghum, barley, corn, rice, or wheat, alone or in combination [1]. As described in Chapter 1, baijiu is intensely aromatic, with scent profiles ranging from floral and fruity to earthy and nutty depending on the style. Its flavor can be sweet, savory, spicy, or even umami, reflecting the fermentation process and raw materials, and its texture is smooth and often oily. Baijiu is commonly classified into strong-aroma, light-aroma, sauce-aroma, and rice-aroma types, among others, each with distinct characteristics and regional associations [216].

Comparing the flavor profiles of new-make whiskey and baijiu led to the hypothesis that using baijiu as the base spirit for whiskey-style barrel aging would produce a "Chinese whiskey" with richer and more complex flavor than conventionally produced whiskey. An accelerated small-barrel aging approach was used to test this concept.

Whiskey aging depends on many factors, but environmental conditions and barrel size are the most important [49]. Whiskeys aged in cooler climates generally need longer aging because evaporation and wood extraction proceed more slowly, giving subtler maturation. Whiskeys aged in warmer regions mature faster, with more intense wood extraction, but they are at greater risk of over-aging if not monitored [214]. Recent innovations have tried to manipulate these processes to reach target flavor profiles more efficiently [217]. Controlled temperature cycling and ultrasound, for example, are being explored to accelerate aging without sacrificing quality. Ultrasonic treatment can accelerate aging by inducing rapid micro-vibrations in the spirit [218]. Elevated aging temperatures have also been reported to

improve color and increase phenolic compound concentrations [219].

Barrel size strongly affects aging time because it sets the surface-area-to-volume ratio. Smaller barrels expose more wood surface per unit volume of spirit, so extraction and maturation proceed faster [220]. Phenolic compounds are extracted more quickly in small barrels than in traditional 52–60-gallon barrels [221]. Small barrels also increase wood extraction and oxidation because of greater wood contact and greater oxygen exposure through the larger relative headspace. Spirits aged in them contain more wood-derived phenolic compounds, which strongly influence flavor [222]. Depending on barrel size, small barrels can accelerate aging by roughly two- to six-fold. Small barrels and other accelerated methods are therefore useful for studying spirit aging over shorter periods.

Environmental conditions also strongly influence aging. Distillers report that day–night and seasonal temperature swings improve whiskey quality. Because of its high alcohol content, whiskey expands and contracts with temperature, which drives exchange with the wood and with oxygen [223]. Humidity has a similar effect by causing the barrel wood to swell and shrink [224]. Temperature and humidity changes therefore act together to improve whiskey quality. This may partly explain why Kentucky bourbon is often considered superior to bourbon made elsewhere, since Kentucky experiences wide daily and seasonal swings in both temperature and humidity [215]. In general, higher temperature and lower humidity increase flavor intensity through greater evaporation and wood interaction, though oxygen penetration into the barrel is lower [219]. To capture this variability, two regimes were used here, one with large temperature and humidity fluctuations and one without.

The objective of the work described in this chapter was to use Chinese baijiu as the base spirit for small-barrel whiskey-style aging, producing a Chinese whiskey with richer and more complex flavor than conventionally produced whiskey. Such a product could introduce a new whiskey style to the American market and create economic opportunities for the whiskey industry. Within this dissertation, the study also serves as a test of how far aging can reshape a spirit whose chemistry was set during fermentation.

6.2 Materials and Methods

6.2.1 Selection of Chinese baijiu

Five commercial baijiu brands, representing four major aroma types and one miscellaneous type, were selected. Table 6.1 lists the brands, their aroma types, their distinctive aroma and flavor characteristics, and the sample codes used throughout this chapter. Two Kentucky straight bourbons served as reference spirits. Woodford Reserve (45.2%, v/v; Woodford Reserve Distillery, Versailles, KY) represented a mid-range bourbon, and Jim Beam (40%, v/v; Jim Beam Distillery, Clermont, KY) an entry-level bourbon. Bourbon is a well-characterized, standardized whiskey style. Its production in Kentucky makes it a reproducible and regionally relevant comparator.

Table 6.1: Baijiu brands used in this chapter, their aroma types, their distinctive aroma and flavor characteristics, and the sample codes used for unaged, varying-condition (chamber) aged, and steady-state aged samples.

Spirit	Aroma type	Aroma	Flavor	Codes (unaged / varying / steady)
Luzhou Laojiao	Strong aroma	Strong and fragrant; fruity and floral, with notable hints of apple and pear.	Rich and layered; spicy yet sweet, with nuances of herbs and fruit and a warm, lingering finish.	LL / LL_C / LL_S
HongHua Lang	Sauce aroma	Complex and aromatic; notes of fruit and nuts with a distinctive yeastiness reflecting its fermentation.	Deep and layered; sweet, savory, and umami, with hints of spice, herbs, and subtle smoke.	HL / HL_C / HL_S
Red Star Erguotou	Light aroma	Clean and light, with subtle grainy notes from its sorghum base; lacks the intense fruit or floral notes of other styles.	Mild, clear, and sharp, with slight sweetness and warmth; crisp finish with a somewhat earthy aftertaste.	RS / RS_C / RS_S
Xifeng	Feng aroma	Robust and complex; a potent, spicy scent with pepper and anise, supported by subtle fruit and a slight floral note.	Intense and spicy, mirroring the aroma, with layers of anise, licorice, and herbs; warm and smooth on the palate.	XI / XI_C / XI_S
Ming River	Miscellaneous aroma	Fruity and floral, with strong tropical-fruit (pineapple) and citrus notes over a subtle herbal and spicy base.	Bright and zesty; sweet and slightly sour, with pepper and spice; clean, somewhat spicy finish.	MR / MR_C / MR_S
Woodford Reserve	Bourbon (reference)	Kentucky straight bourbon whiskey, 45.2% (v/v)		WF
Jim Beam	Bourbon (reference)	Kentucky straight bourbon whiskey, 40% (v/v)		JB

6.2.2 Alcohol content

Alcohol concentration was measured by HPLC (1260 system, Agilent Technologies Inc., Santa Clara, CA) using the Aminex HPX-87H method described in Chapter 2: 60°C column temperature, 5 mM H_2SO_4 at 0.6 mL/min, and refractive index detection at 45°C.

6.2.3 Barrel aging conditions and sampling

Small barrels can accelerate aging by two- to six-fold, depending on their size [221], and can mature 750 mL of spirit or wine in under two months on average. One-liter oak aging barrels (Red Head Barrels, Wylie, TX), designed for aging rum, whiskey, bourbon, tequila, brandy, and wine, were used here. Each barrel was filled with 750 mL of baijiu and placed in a Conviron Gen2000 SH plant growth chamber (Conviron USA, Pembina, ND). Two aging regimes were applied. In the varying (chamber) regime, temperature cycled between 15 and 26°C every 12 h. Relative humidity cycled between 50 and 70% on a 12-h interval, offset from the temperature cycle by 6 h. In the steady-state regime, temperature was held at 23°C and humidity at 60% RH.

6.2.4 Volatile compounds and flavor analysis

Samples were taken at one-month intervals by gently rotating each cask and withdrawing 1 mL through the stopper. Volatile compounds were extracted by HS-SPME and analyzed by GC–MS using the method applied to the maize spirits in Chapter 3 [115]. Each 10-mL SPME vial received 1 mL of sample, 2 mL of distilled water, 0.5 g of anhydrous sodium chloride, and 1-hexanol internal standard (final concentration 5.89 µg mL^{-1}). Vials were equilibrated in a 60°C water bath for 10 min with agitation, extracted for 20 min, and desorbed in the GC injector. Analysis used a Shimadzu QP2010-SE GC–MS (Shimadzu Corp., Kyoto, Japan) with a ZB-WAXplus column (30 m × 0.25 mm i.d. × 0.25 µm; Phenomenex, Torrance, CA, USA). The oven was held at 40°C for 2 min, ramped at 5°C/min to 100°C, then ramped at 10°C/min to 240°C and held for 20 min. Spectra were acquired in electron-impact mode

(70 eV, source 200°C) from 35 to 350 amu. Compounds were identified against the NIST 08 library and semi-quantified as 1-hexanol equivalents.

6.2.5 Color analysis

Color development was assessed by UV–Vis spectrophotometry. Absorption spectra (320–668 nm) of the unaged and aged baijiu, the reference bourbons, and an oak-aged vodka control were compared by Pearson correlation.

6.2.6 Statistical analysis

The GC–MS output consisted of compound identities, retention times, and integrated peak areas for each sample. All output files were parsed with a custom Python pipeline that aggregated and cleaned peak areas by compound. To reduce sparsity, only compounds present (nonzero peak area) in at least 20% of samples were retained. Data were centered log-ratio (CLR) transformed to allow compositional multivariate analysis. Pairwise dissimilarities were computed as Aitchison distances, which are equivalent to Euclidean distances on CLR-transformed data. Permutational multivariate analysis of variance (PERMANOVA; 999 permutations) was used to test differences in composition across experimental factors. Permutational analysis of multivariate dispersions (PERMDISP) was used to check that PERMANOVA results were not driven by differences in dispersion. Compounds that responded significantly to the experimental factors were identified by linear mixed-effects (LME) modeling, with likelihood ratio tests comparing full and reduced models. Per-compound p-values were corrected with the Benjamini–Hochberg false discovery rate (FDR) procedure.

6.3 Results and Discussion

6.3.1 Comparison with traditional bourbon

Before the effects of aging are considered, the baseline volatile profiles of the five baijiu varieties need to be compared with those of the two reference bourbons. Woodford Reserve and Jim Beam contained 29 and 30 distinct volatile compounds, with Shannon diversity indices of 1.58 and 1.70, respectively (Table 6.2).

All five unaged baijiu samples were substantially richer chemically than the bourbons. Luzhou Laojiao (strong aroma, LL) was the most complex unaged spirit, with 86 distinct compounds and a Shannon index of 2.37. HongHua Lang (sauce aroma, HL) contained 64 compounds ($H' = 2.41$), and Red Star (light aroma, RS) contained 42 ($H' = 2.20$). Xifeng (feng aroma, XI) contained 37 ($H' = 2.51$), and Ming River (miscellaneous aroma, MR) contained 27 ($H' = 2.11$) (Table 6.2).

Table 6.2: Richness and Shannon diversity of volatile compounds in the unaged and aged samples.

Sample	Richness	Shannon (H')	Sample	Richness	Shannon (H')
WF	29	1.58	MR	27	2.11
JB	30	1.70	MR_C	56	2.31
LL	86	2.37	MR_S	51	2.33
LL_C	87	2.52	RS	42	2.20
LL_S	91	2.51	RS_C	61	1.95
HL	64	2.41	RS_S	52	1.91
HL_C	95	2.17	XI	37	2.51
HL_S	86	2.02	XI_C	74	1.72
			XI_S	56	1.33

Richness is the number of distinct compounds detected. Sample codes are defined in Table 6.1; _C, varying (chamber) conditions; _S, steady-state conditions.

The HS-SPME/GC–MS protocol used here was optimized for esters, alcohols, acids, and alkenes [225]. The compound counts therefore represent a targeted subset of each spirit's chemical profile rather than a complete inventory (Figure 6.1). Some baijiu types are reported to contain more than 1,700 flavor-active compounds [5, 226], so the richness values reported here almost certainly underestimate their true complexity. The observed richness difference between baijiu and bourbon is therefore a conservative estimate.

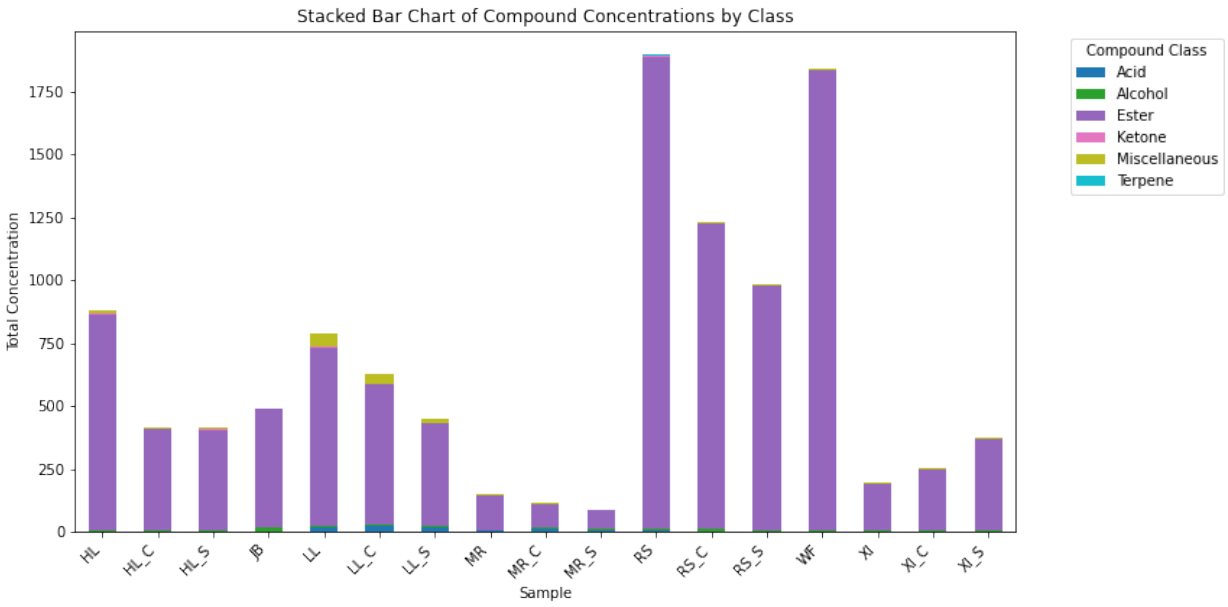


Figure 6.1: Total concentration (mg/L, 1-hexanol equivalents) of the major volatile compound classes in each unaged and aged sample. Sample codes are defined in Table 6.1.

These baseline differences reflect the fundamentally different production biology of the two spirit categories. Bourbon fermentation is driven by a defined yeast inoculum acting on a grain mash. Baijiu undergoes open solid-state fermentation by complex communities of bacteria, molds, and yeasts, whose combined metabolism produces a far broader range of volatiles [1, 26, 227, 228]. This is the same contrast between defined and community fermentations that runs through Chapters 1–5. The compound counts detected here are therefore consistent with the known biology of these fermentation systems, even though they capture only part of the complexity reported in the baijiu literature.

Total baseline flavor concentration also varied widely among baijiu types. Concentrations are reported in mg/L, semi-quantified against the 1-hexanol internal standard. Red Star had the highest initial concentration (1895.4 mg/L), about equal to Woodford Reserve (1841.0 mg/L). The other baijiu varieties ranged from 786.2 mg/L (LL) down to 152.6 mg/L (MR), all below both reference bourbons (Table 6.3). These differences are important for interpreting aging outcomes. They show that the baijiu varieties are far from a uniform starting material for aging.

Table 6.3: Total concentration (mg/L) and richness of flavor compounds in the reference bourbons and in unaged and aged baijiu.

	WF	JB	LL	LL_C	LL_S	HL	HL_C	HL_S	MR	MR_C	MR_S	XI	XI_C	XI_S	RS	RS_C	RS_S[a]
Total concentration	1841.01	490.4	786.2	624.3	451.74	880.4	415.99	414.62	152.64	116.88	89.52	194.76	252.16	371.85	1895.4	1231.8	983.9
Abs. diff. vs. WF	0	−1350.6	−1054.8	−1216.7	−1389.2	−960.6	−1425.0	−1426.4	−1688.4	−1724.1	−1751.5	−1646.3	−1588.9	−1469.2	54.4	−609.3	−857.1
Rel. diff. vs. WF (%)	0	−73.4	−57.3	−66.1	−75.5	−52.2	−77.4	−77.5	−91.7	−93.7	−95.1	−89.4	−86.3	−79.8	3.0	−33.1	−46.6
Abs. diff. vs. JB	1350.59	0	295.8	133.9	−38.68	389.98	−74.43	−75.8	−337.78	−373.54	−400.9	−295.66	−238.26	−118.57	1405.0	741.3	493.5
Rel. diff. vs. JB (%)	275.39	0	60.3	27.3	−7.9	79.5	−15.2	−15.5	−68.9	−76.2	−81.8	−60.3	−48.6	−24.2	286.5	151.2	100.6
Richness	29	30	86	87	91	64	95	86	27	56	51	37	74	56	42	61	52
Compounds added				35	39		42	32		37	31		50	32		35	n.r.
Compounds lost				34	34		11	11		8	7		13	12		16	n.r.
Concentration change				−161.9	−334.4		−464.4	−465.8		−35.8	−63.1		57.4	177.1		−663.7	−911.5

Concentrations are semi-quantified as 1-hexanol equivalents. Sample codes are defined in Table 6.1. [a]RS_S total concentration and richness are taken from the text and Table 6.2; differences are calculated from these values. n.r., not reported.

Global differences in volatile composition were evaluated by PERMANOVA of Aitchison distances on the CLR-transformed data (Table 6.4). Liquor type was the dominant source of compositional variation ($F = 5.97$, $p = 0.001$), confirming that fermentation-derived chemistry is the main determinant of volatile profile. Aging time was the second strongest factor ($F = 3.37$, $p = 0.001$), followed by aging condition ($F = 2.73$, $p = 0.002$). Both the duration and the environmental regime of oak contact therefore had independent, significant effects on composition. PERMDISP showed that the aging-condition effect reflected a real shift in group centroids rather than a difference in dispersion (PERMDISP $p = 0.32$). For aging time, however, dispersion also differed significantly (PERMDISP $p = 0.001$). Samples therefore became more variable as aging proceeded, probably because individual baijiu types followed divergent trajectories rather than a uniform directional shift. The PERMDISP result for liquor type was not significant ($p = 0.08$). The strong PERMANOVA effect for liquor type therefore reflects real differences in volatile centroids between baijiu classes and the reference bourbons.

Table 6.4: PERMANOVA and PERMDISP results for volatile composition (Aitchison distance).

	PERMANOVA		PERMDISP	
Factor	F	p	F	p
Aging time	3.37	0.001	19.04	0.001
Aging condition	2.73	0.002	0.89	0.32
Liquor type	5.97	0.001	5.21	0.08

Together, these results show that baseline fermentation chemistry (liquor type) is the main determinant of volatile composition. Aging time and aging condition act as secondary but significant modifiers, and their effects are best understood in light of each variety's chemical starting point.

6.3.2 Flavor compound diversity and concentration

Although flavor concentration responded in different directions, all five baijiu varieties gained compound richness after one month of oak aging under both conditions. Oak aging there-

fore consistently broadens the chemical richness of baijiu, even when it lowers total volatile concentration through evaporation. Two caveats apply. First, part of the gain may reflect wood-derived compounds and trace compounds concentrated above the detection threshold as the spirit evaporated, rather than new reaction products. Second, richness is a chemical measure; without sensory evaluation it cannot be equated with perceived flavor complexity, which was the property named in the original hypothesis.

HongHua Lang showed the largest gain in richness, rising from 64 compounds to 95 under varying conditions and 86 under steady-state conditions. Xifeng rose from 37 to 74 (varying) and 56 (steady). Ming River started with the fewest compounds (27) but more than doubled under both conditions (56 varying, 51 steady). Luzhou Laojiao, which had the highest baseline richness, showed the smallest relative gain, reaching 87 (varying) and 91 (steady) compounds. This small gain reflects nearly equal numbers of compounds gained and lost: 35 added and 34 lost under varying conditions, and 39 added and 34 lost under steady-state conditions (Table 6.3).

Compound exchange occurred in every baijiu type and condition. The comparatively high turnover in Luzhou Laojiao suggests that its dense initial chemical matrix may compete with or interfere with certain aging reactions, limiting its net gain in richness despite its high starting compound count. In contrast to the universal increase in richness, total flavor concentration fell in four of the five varieties. Red Star lost the most in absolute terms. Its total concentration fell from 1895.4 to 1231.8 mg/L (−35%) under varying conditions and to 983.9 mg/L (−48%) under steady-state conditions. HongHua Lang fell from 880.4 to about 415 mg/L under both conditions (−53%). Luzhou Laojiao fell from 786.2 to 624.3 mg/L under varying conditions (−21%) and to 451.7 mg/L under steady-state conditions (−43%). Ming River showed the smallest absolute losses (35.8 mg/L varying, 63.1 mg/L steady), but it also started from a low concentration.

Xifeng (feng aroma) was the only exception. Its concentration rose under both conditions, by 57.4 mg/L under varying conditions and by 177.1 mg/L under steady-state conditions. This threefold advantage for steady-state aging stands in contrast to the other varieties (Table 6.3). Xifeng's distinctive precursor chemistry helps explain this behavior. Sauce-

aroma baijiu is reported to contain considerably more free alcohols and phenolic compounds than strong-aroma baijiu [7], and Xifeng's behavior suggests a similarly alcohol- and phenol-rich precursor pool. These compound classes have a higher affinity for wood extractives than esters do [229]. Xifeng therefore appears to have entered aging with a larger pool of reactive, non-esterified substrates available for oak-mediated transformation. Consistent with this, Figure 6.2 shows that the main compounds gained during Xifeng aging were ethyl octanoate and ethyl hexanoate. Esterification, rather than hydrolysis, was therefore the dominant reaction in this variety. These are the same medium-chain ethyl esters whose acid precursors were the target of the chain-elongation enrichment in Chapter 5.

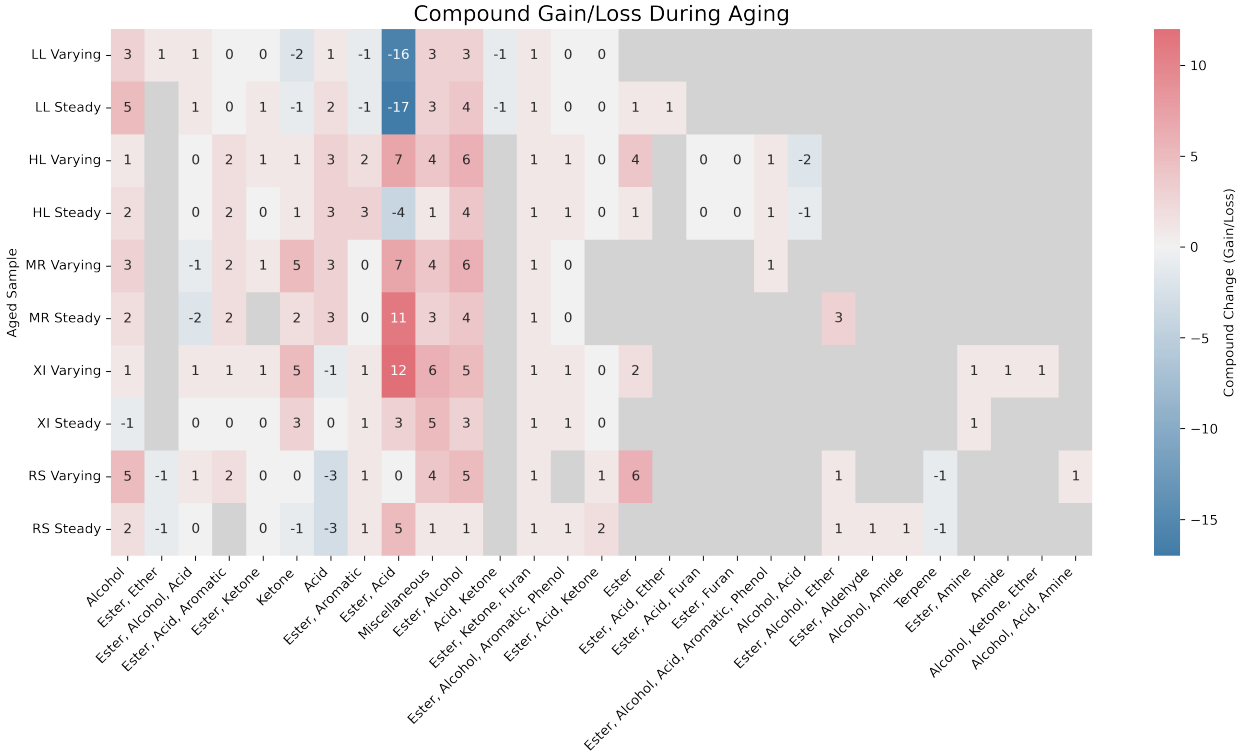


Figure 6.2: Net gain (positive) and loss (negative) in the number of compounds in each compound class during oak aging, for each baijiu type and aging condition.

This outcome agrees with the esterification kinetics described by Xu et al. [88] and Deng et al. [84]. They showed that esterification during baijiu aging has a high equilibrium constant (K), which favors ester formation while free acid concentrations are high. K falls as the acid pool is depleted, and the system eventually shifts toward hydrolysis. The concentration-rich,

ester-heavy profiles of Luzhou Laojiao and HongHua Lang likely represent systems already past this tipping point. In these spirits the acid pool is largely consumed, and hydrolysis is thermodynamically favored. Xifeng's higher alcohol and phenol content, combined with its relatively low initial ester load, places it on the productive side of this equilibrium, so net ester synthesis continued during the aging period studied.

The threefold advantage of steady-state over varying conditions for Xifeng can also be explained. In the varying regime, humidity oscillated between 50 and 70% RH, and the higher-humidity phases created a relatively moist microenvironment in and around the barrel. When humidity is high, ethanol and other low-molecular-weight volatiles evaporate preferentially relative to water. This dilutes the spirit and lowers the concentration of reactive substrates available for esterification [230]. The steady-state regime (23°C, 60% RH) provided a drier and more stable environment that limited preferential ethanol loss and allowed esterification to proceed without interruption. For feng-aroma baijiu in particular, controlled, lower-humidity aging may therefore be optimal for flavor development.

The concentration losses in the other four varieties are partly due to evaporation through the barrel staves. This is a known feature of small-barrel aging, amplified by the high surface-area-to-volume ratio of the 1-L barrels used here [221]. By month two of the planned four-month aging protocol, most samples had almost completely evaporated, and only Luzhou Laojiao retained enough volume for continued analysis. This limits the conclusions that can be drawn about longer-term aging, but its practical significance is probably small. The barrel manufacturer lists two months as the optimal aging time for these barrels, and phenolic extraction in small barrels has been observed to occur over days rather than months [231].

6.3.3 Compound volatility and aging

The compound-level data reveal a pattern that helps explain which volatiles are most vulnerable to loss during aging and which persist or accumulate. Compounds of lower volatility, meaning higher molecular weight, longer carbon chains, and lower vapor pressure, had a disproportionately large and lasting influence on the compositional trajectory of aged baijiu.

The LME results show this most clearly (Table 6.5). Of the nine compounds that remained significant after FDR correction, eight are medium- to long-chain fatty acid esters (C11–C16 acyl chains) or a long-chain primary alcohol (1-dodecanol, C12). These are among the least volatile compounds routinely detected by HS-SPME/GC–MS in distilled spirits (Figure 6.3). Because of their low vapor pressure, they are not preferentially lost through the barrel staves during aging. They stay in solution and remain available for continued esterification, hydrolysis, and oxidation throughout aging. By contrast, the short-chain esters and light alcohols that dominate the initial profiles of varieties such as Red Star and HongHua Lang have much higher vapor pressures. They are selectively depleted by evaporation, leaving the lower-volatility fraction increasingly prominent in the remaining matrix.

Table 6.5: Compounds responding significantly to the experimental factors, identified by linear mixed-effects modeling of CLR-transformed data (Benjamini–Hochberg adjusted $p < 0.05$).

Compound	LR statistic	df	p	p_{adj}
Ethyl undecanoate	24.73	3	< 0.001	< 0.001
Propyl hexanoate	20.59	3	< 0.001	0.003
Ethyl nonanoate	19.68	3	< 0.001	0.003
Ethyl tetradecanoate	18.60	3	< 0.001	0.004
Ethyl hexadecanoate	14.31	3	0.0025	0.025
3-Methylbutyl octanoate	13.55	3	0.0039	0.026
2-Tridecanone	12.99	3	0.0046	0.029
Ethyl dodecanoate	12.31	3	0.0064	0.036
1-Dodecanol	11.56	3	0.0090	0.045

This selectivity directly shapes the observed concentration changes. The net concentration losses in four of the five baijiu varieties (Table 6.3) are driven mainly by evaporative depletion of high-volatility compounds. Many of these are the signature esters of their aroma types, such as the ester–acid compounds characteristic of strong-aroma Luzhou Laojiao. What remains is not a random subset of the original profile. It is a volatility-filtered residue enriched in persistent, lower-vapor-pressure species. The PERMDISP result for aging time, which showed increasing compositional dispersion over time ($p = 0.001$), agrees with this interpretation. The high-volatility fraction evaporates at rates that depend on each type's initial ester–acid load, so the samples diverge rather than converge (Table 6.4).

Considered together, the PERMANOVA and PERMDISP results show how this process differs by factor. Aging condition (chamber vs. steady state) was significant by PERMANOVA ($F = 2.73$, $p = 0.002$) with non-significant PERMDISP ($p = 0.32$). The two regimes therefore produced distinct compositional outcomes, and samples within each regime clustered consistently around stable centroids. This consistency makes mechanistic sense. Each regime imposed a defined, repeatable physical environment on the barrel. The direction of chemical change, toward more esterification under steady-state conditions or faster volatile loss under fluctuating humidity, was applied uniformly across all baijiu types within that regime. The result is a clean, low-dispersion separation between conditions in multivariate space.

Aging time was also highly significant by PERMANOVA ($F = 3.37$, $p = 0.001$), but its PERMDISP result was also highly significant ($p = 0.001$). The spread of samples around their centroids therefore grew substantially over time. This dispersion effect is chemically meaningful: as aging proceeded, the five baijiu varieties diverged from one another rather than converging toward a common aged profile. Each variety's high-volatility pool was depleted at a rate governed by its own initial composition. The ester–acid-heavy strong-aroma types lost mass rapidly through hydrolysis and evaporation, while Xifeng's lower-volatility precursor pool supported continued esterification. By month two, samples that had been relatively similar in total concentration at baseline occupied increasingly separate positions in compositional space. Aging time therefore drives real compositional change, but the direction and magnitude of that change are specific to each variety.

These contrasting dispersion patterns have practical implications for experimental design. Aging condition produces consistent, low-variance separation between groups, so it is a tractable variable for controlled aging studies whose effects can be estimated cleanly. Aging time acts more as an amplifier of preexisting differences between baijiu types than as a uniform driver of maturation. Future studies of aging duration should therefore either control for baijiu type at each time point or model time as an interaction with liquor type rather than as an independent main effect. Xifeng's unusual behavior also fits this framework. Its precursor pool is relatively rich in free alcohols and phenolic compounds, which are less

volatile than the short-chain esters that dominate other varieties. These compounds are therefore retained in the barrel rather than lost to evaporation, and they remain available for esterification. This retention explains the net concentration gains and new ester synthesis seen only in this variety. In effect, Xifeng's aging advantage is partly a volatility advantage: its reactive compounds are less likely to leave the barrel before they can react.

The volatile profile of an unaged baijiu is therefore not only the raw material for aging chemistry but also a selectivity filter. Varieties whose baseline richness is concentrated in high-volatility compounds lose most of that chemical mass to evaporation. Varieties with a lower-volatility precursor pool, such as Xifeng, retain enough reactive substrate for productive oak-mediated transformation. For future aging studies, pre-aging characterization of vapor pressure distributions may therefore predict aging outcomes better than total compound count alone.

6.3.4 Flavor chemistry and aging

Changes in compound functional-group classes give further mechanistic insight into the transformations occurring in each baijiu type. In most samples the dominant change was a shift in ester composition: gains in simple esters and ester–alcohols, together with losses or rearrangements of ester–acid compounds (Figure 6.2).

Luzhou Laojiao lost more ester–acid compounds than any other sample, 16 under varying conditions and 17 under steady-state conditions. At the same time it gained alcohols (3–5 compounds) and ester–alcohols (3–4 compounds). This pattern is consistent with hydrolysis of complex ester–acid species followed by partial re-esterification. The net balance shifted away from Luzhou Laojiao's characteristic high-ester–acid profile toward simpler, alcohol-dominated chemistry. This is a fundamental change in strong-aroma character and may explain the large concentration losses observed.

Under both conditions, HongHua Lang (sauce aroma) gained aromatic esters (2–3 compounds), ester–alcohols (4–6 compounds), and phenol-containing esters (1 compound each). Under varying conditions it also gained 7 ester–acid compounds, whereas steady-state aging

produced a net loss of 4. The gain in aromatic and phenolic esters is consistent with contributions from the wood. Lignin degradation products from oak include phenolic aldehydes and acids that can react with spirit alcohols to form phenolic esters [231]. This is one of the few cases in which the data suggest oak-derived flavor contributions resembling bourbon chemistry.

Ming River (miscellaneous aroma) consistently gained ester–acid compounds under both conditions (7 varying, 11 steady), along with ketones (5 and 2) and ester–alcohols (6 and 4), suggesting net esterification. Xifeng (feng aroma) showed a similar pattern under varying conditions. It gained 12 ester–acid compounds, 5 ketones, 12 miscellaneous compounds, and 5 ester–alcohols, and lost only 1 acid. This broad addition of esters and ketones agrees with Xifeng's net concentration increase and supports active esterification rather than predominantly evaporative loss. Under steady-state conditions, Xifeng gained fewer compounds but showed a larger concentration increase. Stable thermal conditions may therefore favor more complete esterification than the cyclic stress of the varying regime.

Red Star (light aroma) gained 6 simple esters under varying conditions and lost 3 acids under both conditions, consistent with acids being consumed by esterification. Under steady-state conditions, Red Star instead gained 5 ester–acid compounds while still losing 3 acids, suggesting condition-dependent reaction pathways. Despite this esterification activity, Red Star lost a large share of its total concentration, which indicates that evaporation dominated the net outcome.

The LME modeling (Table 6.5) identified the individual compounds driving compositional differences across experimental factors. Nine compounds remained significant after FDR correction ($p_{\text{adj}} < 0.05$). Ethyl undecanoate was the most strongly significant (LR = 24.73, $p_{\text{adj}} < 0.001$). It is a medium-chain fatty acid ester with waxy, fruity notes that has been reported in aged baijiu but is rare in bourbon [9, 21]. Propyl hexanoate (LR = 20.59, $p_{\text{adj}} = 0.003$) and ethyl nonanoate (LR = 19.68, $p_{\text{adj}} = 0.003$) were also highly significant. The concentrations of such fatty acid esters are known to be sensitive to the esterification–hydrolysis equilibrium during aging [232]. Ethyl tetradecanoate (LR = 18.6, $p_{\text{adj}} = 0.004$) and ethyl hexadecanoate (LR = 14.31, $p_{\text{adj}} = 0.025$) are long-chain ethyl esters. Their

variation likely reflects differences in hydrolytic loss among baijiu types with different ester–acid precursor pools. 3-Methylbutyl octanoate (LR = 13.55, $p_{\text{adj}} = 0.026$) is notable because Red Star and the reference bourbons shared it at baseline. Its significant response to the experimental factors suggests condition-dependent stability rather than uniform retention. The ketone 2-tridecanone (LR = 12.99, $p_{\text{adj}} = 0.029$) was the only significant compound that was not an ester or alcohol, consistent with the ketone gains seen in Ming River and Xifeng. Ethyl dodecanoate (LR = 12.31, $p_{\text{adj}} = 0.036$) and 1-dodecanol (LR = 11.56, $p_{\text{adj}} = 0.045$) complete the list. The latter, a long-chain primary alcohol, probably reflects wood extraction or reductive transformation during barrel contact. The significant compounds are therefore mainly medium- to long-chain fatty acid esters, which gives compound-level statistical support to the mechanisms proposed above.

6.3.5 Comparison of barrel-aged baijiu with bourbon

To test whether aging increased the chemical overlap between baijiu and the reference bourbons at the level of individual compounds, the identity and concentration of compounds shared with Woodford Reserve and Jim Beam were tracked before and after aging. The results are shown as a $\log_2(x+1)$-transformed concentration heatmap in Figure 6.3. Even at baseline, both bourbons shared a core set of volatiles with every baijiu type, reflecting fermentation-derived esters and alcohols common to all spirit categories.

Ethyl octanoate stands out in Figure 6.3. It is widely recognized as one of the most important flavor-active esters in whiskey, contributing fruity, waxy, and floral notes [233]. Ethyl octanoate was present at meaningful concentrations in every unaged baijiu except Xifeng and was generally well represented in the reference bourbons. In most baijiu types it decreased with aging, in line with the overall trend of volatile loss. Xifeng was the clear exception. It contained negligible ethyl octanoate before aging but accumulated substantial amounts during oak maturation. This supports the conclusion that Xifeng undergoes productive esterification that the other varieties do not.

Red Star had the most distinctive shared-compound profile relative to the reference bour-

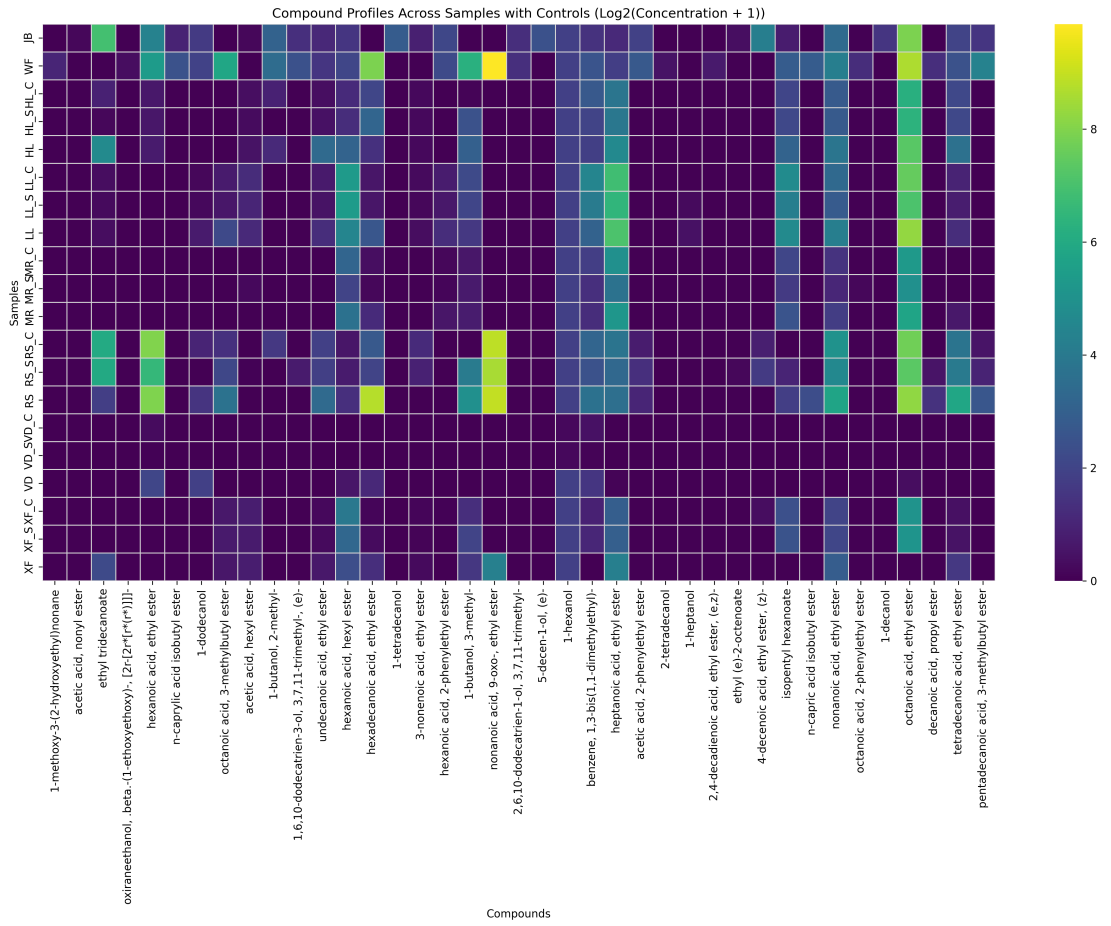


Figure 6.3: $\log_2(x+1)$-normalized concentrations of volatile compounds across the reference bourbons, the unaged and aged baijiu, and the vodka control. XF, Xifeng (XI in the text); VD, vodka; other sample codes are defined in Table 6.1.

bons. At baseline it shared seven compounds with Woodford Reserve but not with Jim Beam: ethyl octanoate, 3-methylbutyl octanoate, isobutyl octanoate, ethyl hexanoate, 3-methyl-1-butanol, ethyl 9-oxononanoate, and 3-methylbutyl pentadecanoate. This overlap persisted after aging. These compounds are therefore chemically stable under the aging conditions used and escaped the hydrolytic losses that affected other compound classes.

HongHua Lang shared 9 compounds with both bourbons at baseline, and 7 of these were retained after aging under both conditions. Aging added 2 new compounds shared with both bourbons regardless of condition. The varying regime also generated 1 compound shared only with Jim Beam, while steady-state aging removed 2 compounds that had been shared only with Jim Beam. Luzhou Laojiao shared 9 compounds with Woodford Reserve and 8 with Jim Beam at baseline. Under varying conditions it lost 4 shared compounds and gained 4 different ones, a net-neutral change. Steady-state aging preserved all compounds shared with Woodford Reserve and added 1 shared with Jim Beam. Ming River retained 5 of its 8 compounds shared with Woodford Reserve and 6 of its 9 shared with Jim Beam, and steady-state aging added 2 new compounds shared with Woodford Reserve.

Taken together, the shared-compound analysis shows that aging did not systematically make baijiu chemically more similar to bourbon at the level of compound identity. Most baseline overlaps were retained, and a few new shared compounds were formed, but in most varieties these gains were offset by equivalent losses. The net effect was neutral or slightly positive, depending on baijiu type and aging condition. The notable exceptions were Red Star, which retained its overlap with Woodford Reserve, and Xifeng, which uniquely gained key bourbon esters through active esterification. By comparison, an oak-aged vodka gained no new compounds. The chemical complexity of the distillate before aging is therefore essential.

6.3.6 Mass loss

Gravimetric mass loss was not reliably recorded during the main aging trial. To recover this measurement, a validation trial was run under matched barrel and environmental con-

ditions. It included two of the original five brands (Red Star, light aroma; HongHua Lang, sauce aroma), an additional sauce-aroma brand (Wuliang Chun, not otherwise characterized chemically), and a neutral vodka control. Barrels were weighed at filling and approximately weekly for seven weeks, and mass loss was calculated relative to each barrel's dry (empty) tare weight.

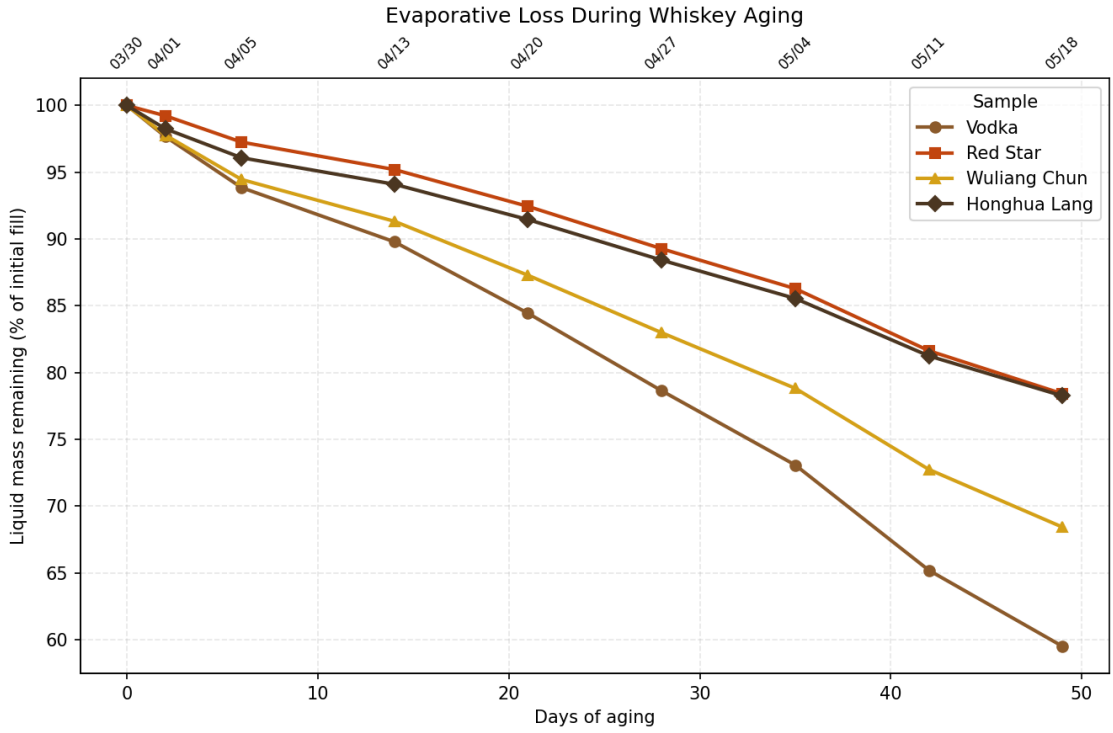


Figure 6.4: Mass loss during barrel aging in the validation trial (Red Star, HongHua Lang, Wuliang Chun, and a vodka control; one barrel per spirit).

Vodka lost the most mass overall (40.5% of net liquid weight), followed by Wuliang Chun (31.6%). Red Star and HongHua Lang lost substantially less, and nearly identical amounts (21.6% and 21.7%; Figure 6.4). This ordering is superficially consistent with the volatility-retention framework proposed above, in which baijiu's matrix of lower-volatility esters, acids, and phenolics might reduce evaporative loss relative to a simpler spirit. It is reported here only as a descriptive observation. Each brand was aged in a single barrel without replication, and alcohol content was not matched across samples. Barrel-to-barrel variation independent of liquid composition was later found to be a large source of mass-loss variance in this system. With one barrel per brand, this trial cannot separate a real compositional effect

from an idiosyncratic barrel effect. The pattern is therefore not treated as evidence for the retention mechanism.

A complementary trial tested the mechanism more directly. A synthetic raw-baijiu matrix was spiked with free C4, C6, C8, and C10 fatty acids at 100–5000 ppm and aged against unspiked controls, with 25 individually barreled replicates. One-way ANOVA found no significant effect of acid type on total mass loss ($F = 0.43$, $p = 0.79$). Acid type explained only 7.9% of total variance, and there was no concentration-dependent trend within any acid. Barrel dry (tare) weight, tested as a proxy for wood density or porosity, was also uncorrelated with mass loss ($r = -0.06$, $p = 0.77$). It did not differ systematically across treatments, so the null treatment effect cannot be attributed to how barrels were assigned. The remaining 92.1% of the variance was not explained by either measured factor. The free organic acids tested are considerably more polar than the ethyl esters that dominate real baijiu volatiles, and they may have partitioned differently within the barrel matrix. With no detectable treatment effect, however, no mechanistic conclusion is drawn from this trial beyond ruling out a simple dose-dependent relationship.

Both trials lead to the same conclusion. In this design, barrel-to-barrel variation was a larger source of mass-loss variance than either liquid composition or fatty acid treatment. This weakens any compositional interpretation of the mass-loss data, including the brand comparison above. Future small-barrel aging studies should therefore treat barrel identity as an explicit factor, for example through replicate barrels per condition or a barrel-level random effect, rather than as residual noise.

6.3.7 Color

Spectrophotometric analysis of color told a different story from the volatile data. Every aged baijiu developed visible color after oak contact, shifting from clear or nearly clear to amber hues that resemble bourbon. Pearson correlation of the absorption spectra (320–668 nm) showed high similarity between aged baijiu and both reference bourbons. Unaged samples, by contrast, correlated poorly with the bourbon spectra and were more similar to vodka

around 320 nm.

Two spectral patterns were observed in the aged samples. Under steady-state conditions, most samples absorbed in a pattern broadly similar to the reference bourbons, highest at 320 nm and decreasing toward 668 nm. Under varying conditions, and for Xifeng and Red Star under both conditions, absorbance peaked at 378 nm rather than 320 nm, rising from the 320 nm value before declining. Absorbance remained detectable at 610 nm instead of falling to zero as it did for the bourbons. Aged vodka gained absorbance over the same range as baijiu, but to a much lower degree.

The color results show that the visual and optical qualities of aged whiskey can be obtained by oak aging of baijiu, even when its volatile profile differs substantially from bourbon. Some pre-existing volatile content appears necessary for color development, given the weaker response of vodka. Beyond that, the particular type and concentration of volatiles had little effect on color.

6.4 Conclusions

Oak aging of Chinese baijiu did not produce a spirit chemically convergent with American bourbon, although the limited replication in this study calls for caution in generalizing. In four of the five varieties examined, one month of oak contact under both regimes lowered total volatile concentration. These were strong-aroma Luzhou Laojiao, sauce-aroma HongHua Lang, light-aroma Red Star, and miscellaneous-aroma Ming River. Aging was dominated by hydrolysis of baijiu's characteristic ester–acid compounds rather than by accumulation of bourbon-like flavor chemistry. The original hypothesis was therefore not supported. Given the duplicate design and the single aging interval completed before volume loss prevented further sampling, these results should be regarded as directional findings that need confirmation in larger, better-replicated studies.

Nevertheless, several findings rest on statistical patterns robust enough to suggest general principles of baijiu aging chemistry. First, the initial volatile composition of the base spirit governs the direction of aging chemistry more strongly than the aging environment does.

PERMANOVA identified liquor type as the dominant source of compositional variation ($F = 5.97$, $p = 0.001$), with a substantially larger effect than aging condition or aging time. The low dispersion associated with aging condition (PERMDISP $p = 0.32$) shows that the barrel environment produces consistent, repeatable shifts. Those shifts, however, act on a chemical trajectory already set by fermentation. At least over the timescales studied, choosing the right baijiu type is a more consequential product-development decision than optimizing the aging environment.

Second, compound volatility acts as a passive selectivity filter during aging. It retains lower-vapor-pressure species and depletes the high-volatility fraction regardless of condition. The nine compounds identified as significant by LME modeling were mainly medium- to long-chain fatty acid esters and alcohols (C11–C16), the compound classes least susceptible to evaporative loss. The pattern held across baijiu types and aging conditions, suggesting a physicochemical constraint of small-barrel aging rather than chemistry specific to any one variety. Pre-aging vapor pressure distribution may therefore predict aging outcome better than total compound richness.

Third, aging time amplifies existing compositional differences between baijiu types rather than driving convergence. The significant PERMDISP effect for aging time ($p = 0.001$), in contrast to the non-significant dispersion effect for aging condition, shows that samples diverged as aging proceeded. Each variety followed a trajectory shaped by its own volatile precursor pool. Aging duration should therefore be modeled as an interaction with liquor type rather than as an independent main effect. Future longitudinal studies should also be powered to detect variety-specific trajectories rather than a single average aging curve.

Beyond these principles, feng-aroma Xifeng was the most promising candidate for further product development. It showed net gains in volatile concentration, new synthesis of bourbon-relevant esters, and a positive response to steady-state aging. These outcomes are consistent with its high-alcohol, high-phenol precursor composition and its favorable position on the esterification equilibrium. A larger study with extended aging and full sensory evaluation is needed before commercial conclusions can be drawn. All aged samples developed amber coloration spectrally consistent with bourbon. The visual character of aged whiskey

can therefore be conferred through oak contact across baijiu types regardless of volatile profile. This finding is robust to the study's replication limits because color development was visually unambiguous and spectrally consistent.

Overall, oak-aged baijiu appears to be a chemically distinct, emerging spirit category whose aging behavior is governed mainly by fermentation biology rather than by the barrel environment. For this dissertation, that conclusion closes the loop on the framework of Chapter 1. Aging acts as a final filter on the chemistry established upstream, and the most productive aging outcomes depend on the precursors supplied by fermentation, such as free alcohols, acids, and medium-chain fatty acids. Future work should use larger barrels to reduce evaporative loss, increase replication to separate true treatment effects from variety-specific idiosyncrasy, and use trained sensory panels to link the chemical patterns identified here to perception and commercial potential.

Chapter 7

Conclusions and Future Work

7.1 Summary of Findings

This dissertation began from the premise, developed in Chapter 1, that traditional baijiu production is best understood as a sequence of enrichment steps rather than as a single fermentation. On this view, each stage imposes selective conditions that favor a particular metabolic function. A liquid-state process could therefore reproduce baijiu-characteristic chemistry by recreating those conditions in sequence instead of copying the solid-state format or its microbial inventory. Chapters 2–6 examined the stages of such a process in turn. Their main findings are summarized below.

Hydrolysis and primary fermentation (Chapters 2 and 3). Grain choice and yeast choice both significantly affected alcohol yield in liquid-state spirit fermentation. For sorghum, waxy varieties gave the highest alcohol concentration and yield (89.65% on average). High-tannin red sorghum gave the lowest, and the fuel-ethanol strain Ethanol Red gave the highest average yield, although the yeast effect was not statistically significant. For maize, blue maize gave the highest alcohol concentration and a yield (about 90%) as high as any variety despite having the highest starch content, and GR-2 was the most efficient yeast on average. The most efficient yeast therefore depends on the grain being fermented. In both grains, the ease with which starch swells and gelatinizes, as measured by RVA and

DSC, was the property most closely linked to conversion efficiency. Yeast strain governed byproduct formation (glycerol) and the higher alcohols and esters in the resulting spirits. Its interaction with grain variety significantly shaped the volatile profile, which makes the yeast–substrate pairing a real design lever for flavor.

Low-energy hydrolysis and coproduct value (Chapter 4). Building on the link between starch swelling and conversion, Chapter 4 showed that partial starch swelling below the gelatinization temperature, combined with granular starch hydrolyzing enzymes, can replace high-temperature liquefaction. Swelling waxy sorghum at 70°C for 30 min gave the highest ethanol concentration (12.02%, v/v) and yield (92.74%) of any treatment, statistically comparable to (and numerically above) conventional 95°C processing. The kafirin proteins recovered from the distillers' grains stayed highly digestible (about 85%), were substantially lighter in color, and showed modified surface hydrophobicity. The hydrolysis stage can therefore be designed to lower energy demand and increase the value of the protein coproduct at the same time.

Chain elongation (Chapter 5). The medium-chain esters that define strong-aroma baijiu appeared only at modest levels in yeast-fermented spirits (Chapter 3). Chapter 5 showed that the missing chain-elongation function of pit mud can be recreated in liquid culture from bovine rumen fluid. Sequential-transfer enrichment produced *Clostridium kluyveri*-dominated consortia. The ethanol-fed lineage Eth-1 sustained hexanoic acid production through reactor operation and reached 4.6 g/L hexanoic acid with ethanol and acetate as substrates. Lactate-fed lineages also produced hexanoate without external ethanol. Community composition and electron balances suggest that lactate-fermenting *Clostridia* supplied *C. kluyveri* with butyrate and hydrogen. These lineages lost activity in gas-purged reactors, which points to interspecies hydrogen transfer and reactor gas management as key control points. Enrichment outcomes were strongly path-dependent because the target organisms were initially very rare.

Maturation (Chapter 6). Oak aging of five commercial baijiu styles in small barrels increased compound richness in every case. It did not, however, make baijiu chemically converge with bourbon. Liquor type, meaning the chemistry established during fermentation, was the dominant source of compositional variation. Aging time amplified differences between baijiu types rather than erasing them. Compound volatility acted as a passive filter, preferentially retaining medium- and long-chain esters. Only feng-aroma Xifeng, which started with an alcohol- and phenol-rich, ester-poor profile, showed net ester synthesis during aging, including ethyl hexanoate and ethyl octanoate. All aged samples nevertheless developed bourbon-like color.

7.2 Synthesis

Taken together, these chapters support the central argument of Chapter 1: the functional stages of baijiu production can be separated, studied, and engineered individually in liquid state. Three themes run across the chapters.

First, *upstream chemistry constrains downstream outcomes.* Starch properties set the efficiency of hydrolysis and fermentation (Chapters 2–4). The substrates delivered by primary fermentation, such as ethanol, lactate, and acetate, determine which chain-elongation pathways can operate (Chapter 5). The precursor pool left after distillation determines whether aging drives esterification or hydrolysis (Chapter 6). Each stage therefore acts on a trajectory established by the stages before it, as the enrichment framework predicts.

Second, *microbial community composition is an outcome of the selective environment, not a fixed input.* This was clearest in Chapter 5. Replicate enrichments from the same rumen inoculum diverged widely, and the reactor environment selected for different communities than the serum bottles did, even under nominally similar feeding. The same principle underlies the strong yeast–substrate interactions seen in Chapters 2 and 3.

Third, *stage separation creates opportunities that a single solid-state vessel does not.* Separating the stages allowed the hydrolysis stage to be optimized for energy and coproduct value (Chapter 4). It allowed the chain-elongation stage to be fed high ethanol and acetate

concentrations that would be incompatible with yeast fermentation in the same vessel (Chapter 5). And it allowed the maturation stage to be chosen for a desired chemical outcome rather than inherited from tradition (Chapter 6).

7.3 Recommendations for Future Work

Several directions follow from this work.

1. **Integrating the stages.** The stages studied here were examined largely in isolation. A logical next step is to couple them. For example, the broth from a GSHE-based primary fermentation of waxy sorghum or blue maize could serve as the feed for an Eth-1-type chain-elongation reactor, followed by esterification and distillation. Such coupling would reveal inhibitory interactions, carry-over effects, and mass-balance constraints that single-stage studies cannot.

2. **Esterification.** Esterification of the medium-chain acids produced by chain elongation was not examined directly in this dissertation. Chemical, enzymatic (lipase or alcohol acyltransferase), and microbial routes to ethyl hexanoate and ethyl octanoate in the liquid process should be compared. In situ product recovery of the acids or esters should also be evaluated.

3. **Robust chain-elongating consortia.** Enrichment outcomes in Chapter 5 were path-dependent because target organisms were initially scarce. Future work should seed enrichments with inocula richer in chain elongators, such as pit mud or previously enriched cultures. It should also measure headspace and dissolved hydrogen directly to test whether lactate fermenters supply *C. kluyveri* with hydrogen in lactate-fed cultures, and design reactor gas management that preserves this exchange.

4. **Techno-economic and life-cycle assessment.** The energy savings from partial starch swelling and the added value of higher-quality distillers' grains (Chapter 4)

should be quantified in a techno-economic analysis. Its scope should cover both fuel-ethanol and spirits production and should include the cost of GSHE.

5. **Sensory evaluation.** Chapters 2, 3, and 6 characterized spirits chemically. Trained sensory panels are needed to link these chemical differences to perceived aroma and flavor, and to judge whether spirits from the staged liquid process are recognizably baijiu-like.

6. **Aging with replication and scale.** The barrel-aging results should be confirmed with larger barrels, replicate barrels per condition, and barrel identity modeled as an explicit factor. Pre-aging vapor-pressure profiles should be tested as predictors of aging outcome, and alternative vessels, including traditional clay and porcelain, should be compared with oak.

7.4 Concluding Remarks

Baijiu has traditionally been produced with a remarkable but opaque combination of solid-state fermentation, spatial heterogeneity, and decades-old microbial ecosystems. This dissertation has shown that its key functions can be understood as a series of engineerable steps. These are the efficient conversion of starch to ethanol, the enrichment of chain-elongating microorganisms, and maturation. Each can be studied and improved in liquid state using grains and resources readily available in the United States. The results provide a foundation for scalable, controllable production of baijiu-style spirits. They also point to new products, such as flavor-forward spirits from specialty grains, higher-value distillers' grains proteins, and oak-aged baijiu, that grow out of the same framework.

Bibliography

[1] X. W. Zheng and B. Z. Han, "Baijiu, Chinese liquor: History, classification and manufacture," *Journal of Ethnic Foods*, vol. 3, no. 1, pp. 19–25, 2016.

[2] J. Li, Q. Zhang, and B. Sun, "Chinese baijiu and whisky: Research reservoirs for flavor and functional food," *Foods*, vol. 12, no. 15, Art. no. 2841, 2023.

[3] L. Qiao, J. Wang, R. Wang, N. Zhang, and F. Zheng, "A review on flavor of baijiu and other world-renowned distilled liquors," *Food Chemistry: X*, vol. 20, Art. no. 100870, 2023.

[4] W. Jiao, F. Xie, L. Gao, L. Du, Y. Wei, J. Zhou, and G. He, "Identification of core microbiota in the fermented grains of a Chinese strong-flavor liquor from Sichuan," *LWT*, vol. 158, Art. no. 113140, 2022.

[5] S. Zhu, X. Lu, K. Ji, K. Guo, Y. Li, C. Wu, and G. Xu, "Characterization of flavor compounds in Chinese liquor Moutai by comprehensive two-dimensional gas chromatography/time-of-flight mass spectrometry," *Analytica Chimica Acta*, vol. 597, no. 2, pp. 340–348, 2007.

[6] N. Ma, F. Yi, and J. Zhu, "Characterization of aroma-active compounds and perceptual interaction between esters and sulfur compounds in Xi baijiu," *European Food Research and Technology*, vol. 246, no. 12, pp. 2517–2535, 2020.

[7] J. Duan, W. Cheng, S. Lv, W. Deng, X. Hu, H. Li, J. Sun, F. Zheng, and B. Sun, "Characterization of key aroma compounds in soy sauce flavor baijiu by molecular sensory science combined with aroma active compounds reverse verification method," *Food Chemistry*, vol. 443, Art. no. 138487, 2024.

[8] Q. Fan, X. Wang, Y. Zhao, F. Zheng, H. Li, F. Zhang, Y. Zhang, and F. Chen, "Characterization of key aroma compounds in Laobaigan Chinese baijiu by GC × GC - TOF / MS and means of molecular sensory science," *Flavour and Fragrance Journal*, vol. 34, no. 6, pp. 514–525, 2019.

[9] E. L. Boothroyd, R. S. T. Linforth, and D. J. Cook, "Effects of ethanol and long-chain ethyl ester concentrations on volatile partitioning in a whisky model system," *Journal of Agricultural and Food Chemistry*, vol. 60, no. 40, pp. 9959–9966, 2012.

[10] L. Ao, K. Guo, X. Dai, W. Dong, X. Sun, B. Sun, J. Sun, G. Liu, A. Li, H. Li, and F. Zheng, "Quick classification of strong-aroma types of base baijiu using potentiometric and voltammetric electronic tongue combined with chemometric techniques," *Frontiers in Nutrition*, vol. 9, Art. no. 977929, 2022.

[11] W. Fan, Y. Xu, and M. C. Qian, "Identification of aroma compounds in Chinese "Moutai" and "Langjiu" liquors by normal phase liquid chromatography fractionation

followed by gas chromatography/olfactometry," in *Flavor Chemistry of Wine and Other Alcoholic Beverages*, ser. ACS Symposium Series. American Chemical Society, 2012, vol. 1104, pp. 303–338.

[12] Z. Xun, X. Guo, X. Ma, L. Huang, M. Wang, Z. Dong, J. He, M. Tan, Z. Liu, and Q. Zhao, "Combined multi-omics analysis revealed the aroma characteristics and the formation mechanism in different grape varieties," *Applied Food Research*, vol. 5, no. 1, Art. no. 100974, 2025.

[13] K. Smith and D. G. Peterson, "Identification of aroma differences in refined and whole grain extruded maize puffs," *Molecules*, vol. 25, no. 9, Art. no. 2261, 2020.

[14] S. M. G. Saerens, F. Delvaux, K. J. Verstrepen, P. Van Dijck, J. M. Thevelein, and F. R. Delvaux, "Parameters affecting ethyl ester production by *Saccharomyces cerevisiae* during fermentation," *Applied and Environmental Microbiology*, vol. 74, no. 2, pp. 454–461, 2008.

[15] S. M. G. Saerens, K. J. Verstrepen, S. D. M. Van Laere, A. R. D. Voet, P. Van Dijck, F. R. Delvaux, and J. M. Thevelein, "The *Saccharomyces cerevisiae EHT1* and *EEB1* genes encode novel enzymes with medium-chain fatty acid ethyl ester synthesis and hydrolysis capacity," *Journal of Biological Chemistry*, vol. 281, no. 7, pp. 4446–4456, 2006.

[16] J. H. Ahn, K. H. Jung, E. S. Lim, S. M. Kim, S. O. Han, and Y. Um, "Recent advances in microbial production of medium chain fatty acid from renewable carbon resources: A comprehensive review," *Bioresource Technology*, vol. 381, Art. no. 129147, 2023.

[17] J. Gao, G. Liu, A. Li, C. Liang, C. Ren, and Y. Xu, "Domination of pit mud microbes in the formation of diverse flavour compounds during Chinese strong aroma-type baijiu fermentation," *LWT*, vol. 137, Art. no. 110442, 2021.

[18] S. Esquivel-Elizondo, C. Bağc, M. Temovska, B. S. Jeon, I. Bessarab, R. B. H. Williams, D. H. Huson, and L. T. Angenent, "The isolate *Caproiciproducens* sp. 7D4C2 produces n-caproate at mildly acidic conditions from hexoses: Genome and rBOX comparison with related strains and chain-elongating bacteria," *Frontiers in Microbiology*, vol. 11, Art. no. 594524, 2020.

[19] B.-C. Kim, B. Seung Jeon, S. Kim, H. Kim, Y. Um, and B.-I. Sang, "*Caproiciproducens galactitolivorans* gen. nov., sp. nov., a bacterium capable of producing caproic acid from galactitol, isolated from a wastewater treatment plant," *International Journal of Systematic and Evolutionary Microbiology*, vol. 65, no. 12, pp. 4902–4908, 2015.

[20] L. J. Chai, W. Qian, X. Z. Zhong, X. J. Zhang, Z. M. Lu, S. Y. Zhang, S. T. Wang, C. H. Shen, J. S. Shi, and Z. H. Xua, "Mining the factors driving the evolution of the pit mud microbiome under the impact of long-term production of strong-flavor baijiu," *Applied and Environmental Microbiology*, vol. 87, no. 17, Art. no. e00885-21, 2021.

[21] Y. Xu, M. Wu, D. Zhao, J. Zheng, M. Dai, X. Li, W. Li, C. Zhang, and B. Sun, "Simulated fermentation of strong-flavor baijiu through functional microbial combination to

realize the stable synthesis of important flavor chemicals," *Foods*, vol. 12, no. 3, Art. no. 644, 2023.

[22] B. Sun, J. Wu, and Y. Yu, *Chinese National Alcohols: Baijiu and Huangjiu*. World Scientific Publishing Company, 2021. [Online]. Available: https://books.google.com/books?id=_nwxEAAAQBAJ

[23] S. Zheng, M. Huang, W. Yang, Z. Wang, Q. Ren, H. Li, J. Wu, N. Meng, J. Li, and B. Wang, "Preparation of Fangxian traditional xiaoqu and its evolution of microbial communities and aroma compounds during fermentation," *Food Research International*, vol. 199, Art. no. 115344, 2025.

[24] Y.-Y. Ma, W. Zhang, H. Tian, T.-T. Meng, S.-B. Yang, X.-J. Zhang, L.-J. Chai, H.-Y. Xu, W.-Q. Zhang, C.-Q. Gao, Z.-M. Lu, and Z.-H. Xu, "Dissecting the division of labor among five jiuqu starters in sesame-flavor baijiu fermentation," *Food Bioscience*, vol. 81, Art. no. 109114, 2026.

[25] S. Arvelli, M. Liu, G. Chen, T. Weiss, Y. Zhang, Y. Li, D. Wang, and Y. Zheng, "Solid-state fermentation of corn to make Chinese liquor: Effect of corn variety and dynamic microbial community variation," *LWT*, vol. 203, Art. no. 116407, 2024.

[26] W. Wei, Y. Shen, W. Cheng, and W. Zhang, "Analysis of microbial diversity and volatile metabolites across different types of pit mud in sauce-flavored baijiu based on nanopore sequencing and metabolomics," *LWT*, vol. 188, Art. no. 115465, 2023.

[27] Z. Suyi, F. Jun, L. Zhongming, Y. Ping, A. Zonghua, T. Feiyong, and L. Yanyang, "Luzhou-flavour liquor and stacking production method thereof," Patent CN102321511A, 2012. [Online]. Available: https://patents.google.com/patent/CN102321511A/en

[28] W. Jia, R. Ma, L. Hu, and H. Mo, "Synergy of physicochemical reactions occurred during aging for harmonizing and improving flavor," *Food Chemistry: X*, vol. 17, Art. no. 100554, 2023.

[29] N. Fitzgerald and J. C. Edwards, "Investigation of solid phase microextraction gas chromatography–mass spectrometry, Fourier transform infrared spectroscopy and ^{1}H qNMR spectroscopy as potential methods for the authentication of baijiu spirits," *Beverages*, vol. 9, no. 1, Art. no. 25, 2023.

[30] T. Guan, Y. Lin, K. Chen, M. Ou, and J. Zhang, "Physicochemical factors affecting microbiota dynamics during traditional solid-state fermentation of Chinese strong-flavor baijiu," *Frontiers in Microbiology*, vol. 11, Art. no. 2090, 2020.

[31] X. W. Zheng, Z. Yan, M. J. Nout, E. J. Smid, M. H. Zwietering, T. Boekhout, J. S. Han, and B. Z. Han, "Microbiota dynamics related to environmental conditions during the fermentative production of Fen-Daqu, a Chinese industrial fermentation starter," *International Journal of Food Microbiology*, vol. 182–183, pp. 57–62, 2014.

[32] Q. Jiang, X. Wu, Y. Xu, Y. Zhang, Z. Wang, L. Shen, W. Yang, J. Sun, and Y. Liu,

"Microbial composition and dynamic succession during the daqu production process of northern Jiang-flavored liquor in China," *3 Biotech*, vol. 11, no. 5, Art. no. 224, 2021.

[33] X.-W. Zheng, M. R. Tabrizi, M. J. R. Nout, and B.-Z. Han, "Daqu—a traditional Chinese liquor fermentation starter," *Journal of the Institute of Brewing*, vol. 117, no. 1, pp. 82–90, 2011.

[34] C. N. Aguilar, "Modeling schemes for control of bed-temperature gradients in solid-state fermentation," *Advances in Biotechnology and Microbiology*, vol. 3, no. 2, Art. no. 555607, 2017.

[35] W. Shi, L.-J. Chai, G.-Y. Fang, J.-L. Mei, Z.-M. Lu, X.-J. Zhang, C. Xiao, S.-T. Wang, C.-H. Shen, J.-S. Shi, and Z.-H. Xu, "Spatial heterogeneity of the microbiome and metabolome profiles of high-temperature daqu in the same workshop," *Food Research International*, vol. 156, Art. no. 111298, 2022.

[36] Y. Yang, M.-S. Niu, H. Yu, W. Shi, L.-J. Chai, Z.-M. Lu, X.-T. Liu, C.-H. Shen, Z.-H. Xu, S.-T. Wang, and J.-S. Shi, "Exploring the contribution of temperature-adapted microbiota to enzyme profile of saccharification in *daqu* using metagenomics and metaproteomics," *LWT*, vol. 197, Art. no. 115916, 2024.

[37] L. Deng, X. Mao, D. Liu, X.-Q. Ning, Y. Shen, B. Chen, H.-F. Nie, D. Huang, and H.-B. Luo, "Comparative analysis of physicochemical properties and microbial composition in high-temperature daqu with different colors," *Frontiers in Microbiology*, vol. 11, Art. no. 588117, 2020.

[38] Y. Wang, Y. Du, X. Jin, Y. Xia, Y. Zhao, Z. Wu, K. Gomi, and W. Zhang, "Temperature-dependent alcohol acyltransferase reactions as the main enzymatic way to produce short-chain (C4–C8) and medium-chain (C9–C13) esters over the whole daqu-making process," *Journal of the Science of Food and Agriculture*, vol. 103, no. 8, pp. 3939–3949, 2023.

[39] X. Hou, M. Hui, Z. Sun, X. Li, X. Shi, R. Xiao, J. Wang, C. Pan, and R. Li, "Comparative analysis of the microbiotas and physicochemical properties inside and outside medium-temperature daqu during the fermentation and storage," *Frontiers in Microbiology*, vol. 13, Art. no. 934696, 2022.

[40] L. Yang, W. Fan, and Y. Xu, "Qu-omics elucidates the formation and spatio-temporal differentiation mechanism underlying the microecology of high temperature daqu," *Food Chemistry*, vol. 438, Art. no. 137988, 2024.

[41] M. Zhu, J. Zheng, J. Xie, D. Zhao, Z.-W. Qiao, D. Huang, and H.-B. Luo, "Effects of environmental factors on the microbial community changes during medium-high temperature daqu manufacturing," *Food Research International*, vol. 153, Art. no. 110955, 2022.

[42] N. Liu, D. Huang, and Z. Li, "Research progress on influencing factors of microbial community succession during fermentation of Nongxiangxingdaqu," *International Journal of New Developments in Engineering and Society*, vol. 7, no. 4, 2023.

[43] Y. Mu, J. Huang, R. Zhou, S. Zhang, H. Qin, H. Tang, Q. Pan, and H. Tang, "Bioaugmented daqu-induced variation in community succession rate strengthens the interaction and metabolic function of microbiota during strong-flavor baijiu fermentation," *LWT*, vol. 182, Art. no. 114806, 2023.

[44] M. Xie, F. Lv, G. Ma, A. Farooq, H. Li, Y. Du, and Y. Liu, "High throughput sequencing of the bacterial composition and dynamic succession in daqu for Chinese sesame flavour liquor," *Journal of the Institute of Brewing*, vol. 126, no. 1, pp. 98–104, 2020.

[45] Y. Xu, H. Huang, H. Lu, M. Wu, M. Lin, C. Zhang, Z. Zhao, W. Li, C. Zhang, X. Li, and B. Sun, "Characterization of an *Aspergillus niger* for efficient fatty acid ethyl ester synthesis in aqueous phase and the molecular mechanism," *Frontiers in Microbiology*, vol. 12, Art. no. 820380, 2022.

[46] D. Fujiwara, H. Yoshimoto, H. Sone, S. Harashima, and Y. Tamai, "Transcriptional co-regulation of *Saccharomyces cerevisiae* alcohol acetyltransferase gene, ATF1 and δ-9 fatty acid desaturase gene, OLE1 by unsaturated fatty acids," *Yeast*, vol. 14, no. 8, pp. 711–721, 1998.

[47] X. Wang, W. Fan, and Y. Xu, "Comparison on aroma compounds in Chinese soy sauce and strong aroma type liquors by gas chromatography–olfactometry, chemical quantitative and odor activity values analysis," *European Food Research and Technology*, vol. 239, no. 5, pp. 813–825, 2014.

[48] Y. Wei, W. Zou, C. H. Shen, and J. G. Yang, "Basic flavor types and component characteristics of Chinese traditional liquors: A review," *Journal of Food Science*, vol. 85, no. 12, pp. 4096–4107, 2020.

[49] C. S. Boruff and L. A. Rittschof, "Whiskey aging, effects of barreling proof on the aging of American whiskeys," *Journal of Agricultural and Food Chemistry*, vol. 7, no. 9, pp. 630–633, 1959.

[50] S. Ye, X. Shang, L. Ao, B. Sun, X. Chen, C.-H. Shen, M. Liu, F. Lin, W. Dong, X. Sun, Y. Xiong, and B. Deng, "Decoding long-chain fatty acid ethyl esters during the distillation of strong aroma-type baijiu and exploring the adsorption mechanism with magnetic nanoparticles," *Journal of Agricultural and Food Chemistry*, vol. 72, no. 39, pp. 21 752–21 762, 2024.

[51] W. Qian, Z.-M. Lu, L.-J. Chai, X.-J. Zhang, Q. Li, S.-T. Wang, C.-H. Shen, J.-S. Shi, and Z.-H. Xu, "Cooperation within the microbial consortia of fermented grains and pit mud drives organic acid synthesis in strong-flavor baijiu production," *Food Research International*, vol. 147, Art. no. 110449, 2021.

[52] S. Yuan, Z. Jin, A. Ali, C. Wang, and J. Liu, "Caproic acid-producing bacteria in Chinese baijiu brewing," *Frontiers in Microbiology*, vol. 13, Art. no. 883142, 2022.

[53] W. R. Harcombe, J. M. Chacón, E. M. Adamowicz, L. M. Chubiz, and C. J. Marx, "Evolution of bidirectional costly mutualism from byproduct consumption," *Proceedings of the National Academy of Sciences*, vol. 115, no. 47, pp. 12 000–12 004, 2018.

[54] K. Tarasava, S. H. Lee, J. Chen, M. Köpke, M. C. Jewett, and R. Gonzalez, "Reverse β-oxidation pathways for efficient chemical production," *Journal of Industrial Microbiology & Biotechnology*, vol. 49, no. 2, Art. no. kuac003, 2022.

[55] H. Yuan, X. Wang, T.-Y. Lin, J. Kim, and W.-T. Liu, "Disentangling the syntrophic electron transfer mechanisms of *Candidatus* Geobacter eutrophica through electrochemical stimulation and machine learning," *Scientific Reports*, vol. 11, no. 1, Art. no. 15140, 2021.

[56] H. B. Machado, Y. Dekishima, H. Luo, E. I. Lan, and J. C. Liao, "A selection platform for carbon chain elongation using the CoA-dependent pathway to produce linear higher alcohols," *Metabolic Engineering*, vol. 14, no. 5, pp. 504–511, 2012.

[57] P. J. Weimer and D. M. Stevenson, "Isolation, characterization, and quantification of *Clostridium kluyveri* from the bovine rumen," *Applied Microbiology and Biotechnology*, vol. 94, no. 2, pp. 461–466, 2012.

[58] C. R. Strachan, C. M. Bowers, B.-C. Kim, T. Movsesijan, V. Neubauer, A. J. Mueller, X. A. Yu, F. C. Pereira, V. Nagl, J. Faas, M. Wagner, Q. Zebeli, P. J. Weimer, P. Candry, M. F. Polz, C. E. Lawson, and E. Selberherr, "Distinct lactate utilization strategies drive niche differentiation between two co-existing *Megasphaera* species in the rumen microbiome," *The ISME Journal*, vol. 19, no. 1, Art. no. wraf147, 2025.

[59] C. Liu, H. Wu, S. Liu, S. Chai, Q. Meng, and Z. Zhou, "Dynamic alterations in yak rumen bacteria community and metabolome characteristics in response to feed type," *Frontiers in Microbiology*, vol. 10, Art. no. 1116, 2019.

[60] H. Wang, B. S. Jeon, A. E. Ortiz-Ardila, and L. T. Angenent, "Steering the chain-elongating microbiome to C8 or C6 production with ethanol and lactate as coelectron donors," *Environmental Science & Technology*, vol. 59, no. 32, pp. 16 947–16 958, 2025.

[61] M. V. Reddy, S. V. Mohan, and Y.-C. Chang, "Sustainable production of medium chain fatty acids (MCFA) with an enriched mixed bacterial culture: microbial characterization using molecular methods," *Sustainable Energy Fuels*, vol. 2, no. 2, pp. 372–380, 2018.

[62] S. Qiu, W. Xia, J. Xu, Z. Li, and S. Ge, "Impacts of 2-bromoethanesulfonic sodium on methanogenesis: Methanogen metabolism and community structure," *Water Research*, vol. 230, Art. no. 119527, 2023.

[63] C. Fernández-Blanco, M. C. Veiga, and C. Kennes, "Effect of pH and medium composition on chain elongation with *Megasphaera hexanoica* producing C4-C8 fatty acids," *Frontiers in Microbiology*, vol. 14, Art. no. 1281103, 2023.

[64] S. Qiu, X. Zhang, W. Xia, Z. Li, L. Wang, Z. Chen, and S. Ge, "Effect of extreme pH conditions on methanogenesis: Methanogen metabolism and community structure," *Science of The Total Environment*, vol. 877, Art. no. 162702, 2023.

[65] P. M. van Bodegom, J. C. M. Scholten, and A. J. M. Stams, "Direct inhibition of

methanogenesis by ferric iron," *FEMS Microbiology Ecology*, vol. 49, no. 2, pp. 261–268, 2004.

[66] Y. Liu, X. Wang, H. Gu, L. Zhao, K. Wang, B. Wang, W. Huang, H. Yang, J. Zhang, and X. Song, "Differential enhancement of chain elongation by nano zero-valent iron and zero-valent iron: Mechanisms, microbial dynamics, and medium-chain fatty acids production," *Journal of Environmental Chemical Engineering*, vol. 13, no. 5, Art. no. 119157, 2025.

[67] Y. Zheng, F. Liang, Y. Wu, S. Ban, H. Huang, Y. Xu, X. Wang, and Q. Wu, "Unraveling multifunction of low-temperature *daqu* in simultaneous saccharification and fermentation of Chinese light aroma type liquor," *International Journal of Food Microbiology*, vol. 397, Art. no. 110202, 2023.

[68] L. Chen, Z.-M. Chi, Z. Chi, and M. Li, "Amylase production by *Saccharomycopsis fibuligera* A11 in solid-state fermentation for hydrolysis of cassava starch," *Applied Biochemistry and Biotechnology*, vol. 162, no. 1, pp. 252–263, 2010.

[69] M. D. Doku, K. S. S. Hlaing, M. Fall, S. Suryoprabowo, Y. Cheng, H. Yu, S. Yuan, Y. Guo, and W. Yao, "Solid-state fermentation of waste bread by *Aspergillus oryzae* and *Rhizopus oryzae*: enzymatic hydrolysis and phenolic release," *Waste Disposal & Sustainable Energy*, vol. 8, no. 2, pp. 281–292, 2026.

[70] J. Xie, B. Wang, Z. He, and L. Pan, "A thermophilic fungal GH36 α-galactosidase from *Lichtheimia ramosa* and its synergistic hydrolysis of locust bean gum," *Carbohydrate Research*, vol. 491, Art. no. 107911, 2020.

[71] X. Huang, J. Liu, H. Luo, and W. Zou, "Research progress on the diversity, physiological and functional characteristics of lactic acid bacteria in the Nongxiangxing baijiu microbiome," *Journal of Food Science*, vol. 90, no. 2, Art. no. e70082, 2025.

[72] G. He, J. Huang, C. Wu, Y. Jin, and R. Zhou, "Bioturbation effect of fortified *daqu* on microbial community and flavor metabolite in Chinese strong-flavor liquor brewing microecosystem," *Food Research International*, vol. 129, Art. no. 108851, 2020.

[73] G. He, J. Huang, R. Zhou, C. Wu, and Y. Jin, "Effect of fortified daqu on the microbial community and flavor in Chinese strong-flavor liquor brewing process," *Frontiers in Microbiology*, vol. 10, Art. no. 56, 2019.

[74] L. J. Chai, Z. M. Lu, X. J. Zhang, J. Ma, P. X. Xu, W. Qian, C. Xiao, S. T. Wang, C. H. Shen, J. S. Shi, and X. Zheng-Hong, "Zooming in on butyrate-producing clostridial consortia in the fermented grains of baijiu via gene sequence-guided microbial isolation," *Frontiers in Microbiology*, vol. 10, Art. no. 1397, 2019.

[75] F. M. F. Elshaghabee, W. Bockelmann, D. Meske, M. de Vrese, H.-G. Walte, J. Schrezenmeir, and K. J. Heller, "Ethanol production by selected intestinal microorganisms and lactic acid bacteria growing under different nutritional conditions," *Frontiers in Microbiology*, vol. 7, Art. no. 47, 2016.

[76] A. H. Sahir, S. Kumar, and S. Kumar, "Modelling of a packed bed solid-state fermentation bioreactor using the N-tanks in series approach," *Biochemical Engineering Journal*, vol. 35, no. 1, pp. 20–28, 2007.

[77] P. O. Saboe, H. R. Monroe, W. E. Michener, L. P. Manker, S. J. Haugen, G. T. Beckham, and E. M. Karp, "In situ product recovery of bio-based ethyl esters via hybrid extraction-distillation," *Green Chemistry*, vol. 21, no. 19, pp. 5306–5315, 2019.

[78] C. M. Spirito, T. N. Lucas, S. Patz, B. S. Jeon, J. J. Werner, L. H. Trondsen, J. J. Guzman, D. H. Huson, and L. T. Angenent, "Variability in n-caprylate and n-caproate producing microbiomes in reactors with in-line product extraction," *mSystems*, vol. 9, no. 8, Art. no. e00416-24, 2024.

[79] M. Balcerek, K. Pielech-Przybylska, and P. Patelski, "The effect of distillation conditions and alcohol content in 'heart' fractions on the concentration of aroma volatiles and undesirable compounds in plum brandies," *Journal of the Institute of Brewing*, vol. 123, no. 3, pp. 452–463, 2017.

[80] F. A. Serafim, C. A. Galinaro, A. A. Da Silva, S. F. Buchviser, E. S. Do Nascimento, F. V. Novaes, and D. W. Franco, "Quantitative chemical profile and multivariate statistical analysis of alembic distilled sugarcane spirit fractions," *Journal of the Brazilian Chemical Society*, vol. 23, no. 8, pp. 1506–1514, 2012.

[81] M. del Alamo-Sanza and I. Nevares, "Recent advances in the evaluation of the oxygen transfer rate in oak barrels," *Journal of Agricultural and Food Chemistry*, vol. 62, no. 35, pp. 8892–8899, 2014.

[82] Y. Feng, Z. Zhang, X. Huang, L. Tang, T. Guo, J. Zhang, S. Chen, and Y. Xu, "Molecular and sensory characterization of Chinese baijiu aged in Jiuhai container and contribution of volatile odorous terpenes to Jiuhai-aroma," *Food Chemistry*, vol. 470, Art. no. 142687, 2025.

[83] Wine Industry Advisor, "A new breed of wine amphoras – measured porosity, oxygen transfer rates and new innovations," https://wineindustryadvisor.com/2019/09/05/a-new-breed-of-wine-amphoras/, 2019.

[84] Y. Deng, A. Xiong, K. Zhao, Y. Hu, B. Kuang, X. Xiong, Z. Yang, Y. Yu, and Q. Zheng, "Mechanisms of the regulation of ester balance between oxidation and esterification in aged baijiu," *Scientific Reports*, vol. 10, no. 1, Art. no. 17169, 2020.

[85] H. Huang, Y. Gao, L. Wang, X. Yu, S. Chen, and Y. Xu, "Maillard reaction intermediates in Chinese baijiu and their effects on Maillard reaction related flavor compounds during aging," *Food Chemistry: X*, vol. 22, Art. no. 101356, 2024.

[86] Jamaica Sugar Experiment Station, *Report on the Experimental Work*. Jamaica Sugar Experiment Station, 1906.

[87] Z. Khan, F. Javed, Z. Shamair, A. Hafeez, T. Fazal, A. Aslam, W. B. Zimmerman, and F. Rehman, "Current developments in esterification reaction: A review on process and

parameters," *Journal of Industrial and Engineering Chemistry*, vol. 103, pp. 80–101, 2021.

[88] H. Xu, Q. Li, Y. Yu, and Q. Zheng, "A thermodynamic and kinetic study on electrochemical esterification in aroma-enhanced distilled liquor (baijiu)," *Catalysts*, vol. 13, no. 3, Art. no. 478, 2023.

[89] Research and Markets, "Alcoholic beverages market share, size, trends, industry analysis report, by type; by distribution channel; by region; segment forecasts, 2021–2028," Research and Markets, Tech. Rep., 2022. [Online]. Available: https://www.researchandmarkets.com/

[90] Statista, "Spirits market," https://www.statista.com/topics/1550/spirits-market/#dossierKeyfigures, 2022. [Online]. Available: https://www.statista.com/topics/1550/spirits-market/#dossierKeyfigures

[91] H. Liu and B. Sun, "Effect of fermentation processing on the flavor of baijiu," *Journal of Agricultural and Food Chemistry*, vol. 66, no. 22, pp. 5425–5432, 2018.

[92] Z. Y. Fan, G. Y. Zuo, and X. Y. Du, "Sorghum materials of different effects on wine of Maotai-flavor liquor," *Journal of Liquor-Making*, vol. 4, pp. 36–41, 2014, in Chinese.

[93] D. Tian, "Influence study of the quality of strong flavour Chinese spirit for different sorghum," Thesis, Chongqing University, Chongqing, China, 2013, in Chinese.

[94] L. Yang, F. Zhang, and X. Guo, "Study on brewing Fenflavour daqu liquor using the different quality of sorghum," *Journal of Anhui Agricultural Sciences*, vol. 35, pp. 129–130, 2015.

[95] X. L. Han, D. L. Wang, W. J. Zhang, and S. R. Jia, "The production of the Chinese baijiu from sorghum and other cereals," *Journal of the Institute of Brewing*, vol. 123, no. 4, pp. 600–604, 2017.

[96] X. Xu, D. Waters, C. Blanchard, and S. H. Tan, "A study on Australian sorghum grain fermentation performance and the changes in Zaopei major composition during solid-state fermentation," *Journal of Cereal Science*, vol. 98, Art. no. 103160, 2021.

[97] K. Szambelan, J. Nowak, A. Szwengiel, and H. Jeleń, "Quantitative and qualitative analysis of volatile compounds in sorghum distillates obtained under various hydrolysis and fermentation conditions," *Industrial Crops and Products*, vol. 155, Art. no. 112782, 2020.

[98] V. Subbiah, B. Zhong, M. A. Nawaz, C. J. Barrow, F. R. Dunshea, and H. A. R. Suleria, "Screening of phenolic compounds in Australian grown berries by LC-ESI-QTOF-MS/MS and determination of their antioxidant potential," *Antioxidants*, vol. 10, no. 1, Art. no. 26, 2021.

[99] M. Pauley and D. Maskell, "Mini-review: The role of *Saccharomyces cerevisiae* in the production of gin and vodka," *Beverages*, vol. 3, no. 1, Art. no. 13, 2017.

[100] S. Yan, X. Wu, S. R. Bean, J. F. Pedersen, T. Tesso, Y. R. Chen, and D. Wang, "Evaluation of waxy grain sorghum for ethanol production," *Cereal Chemistry*, vol. 88, no. 6, pp. 589–595, 2011.

[101] K. Jacques, T. Lyons, and D. Kelsall, *The Alcohol Textbook: A Reference for the Beverage, Fuel and Industrial Alcohol Industries*. Nottingham University Press, 2003. [Online]. Available: https://books.google.com/books?id=jD7yAAAAMAAJ

[102] F. R. Pinu and S. G. Villas-boas, "Rapid quantification of major volatile metabolites in fermented food and beverages using gas chromatography-mass spectrometry," *Metabolites*, vol. 7, no. 3, Art. no. 37, 2017.

[103] J. E. Cremer, L. Liu, S. R. Bean, J.-B. Ohm, M. Tilley, J. D. Wilson, R. C. Kaufman, G. H. Vu, E. K. Gilding, I. D. Godwin, and D. Wang, "Impacts of kafirin allelic diversity, starch content, and protein digestibility on ethanol conversion efficiency in grain sorghum," *Cereal Chemistry*, vol. 91, no. 3, pp. 218–227, 2014.

[104] B. Pang, K. Zhang, I. Kisekka, S. Bean, M. Zhang, and D. Wang, "Evaluating effects of deficit irrigation strategies on grain sorghum attributes and biofuel production," *Journal of Cereal Science*, vol. 79, pp. 13–20, 2018.

[105] X. Wu, R. Zhao, L. Liu, S. Bean, P. A. Seib, J. McLaren, R. Madl, M. Tuinstra, M. Lenz, and D. Wang, "Effects of growing location and irrigation on attributes and ethanol yields of selected grain sorghums," *Cereal Chemistry*, vol. 85, no. 4, pp. 495–501, 2008.

[106] J. Zhao, T. Weiss, Z. Du, S. Hong, S. R. Bean, Y. Li, and D. Wang, "Comparative evaluation of physicochemical and fermentative responses of three sorghum varieties from dryland and irrigated land and the properties of proteins from distillers' grains," *Journal of Cereal Science*, vol. 104, Art. no. 103432, 2022.

[107] X. Wu, R. Zhao, S. R. Bean, P. A. Seib, J. S. McLaren, R. L. Madl, M. Tuinstra, M. C. Lenz, and D. Wang, "Factors impacting ethanol production from grain sorghum in the dry-grind process," *Cereal Chemistry*, vol. 84, no. 2, pp. 130–136, 2007.

[108] X. Wu, B. Jampala, A. Robbins, D. Hays, S. Yan, F. Xu, W. Rooney, G. Peterson, Y.-C. Shi, and D. Wang, "Ethanol fermentation performance of grain sorghums (*Sorghum bicolor*) with modified endosperm matrices," *Journal of Agricultural and Food Chemistry*, vol. 58, no. 17, pp. 9556–9562, 2010.

[109] R. Zhao, X. Wu, B. W. Seabourn, S. R. Bean, L. Guan, Y.-C. Shi, J. D. Wilson, R. Madl, and D. Wang, "Comparison of waxy vs. nonwaxy wheats in fuel ethanol fermentation," *Cereal Chemistry*, vol. 86, no. 2, pp. 145–156, 2009.

[110] D. Wang, S. Bean, J. McLaren, P. Seib, R. Madl, M. Tuinstra, Y. Shi, M. Lenz, X. Wu, and R. Zhao, "Grain sorghum is a viable feedstock for ethanol production," *Journal of Industrial Microbiology and Biotechnology*, vol. 35, no. 5, pp. 313–320, 2008.

[111] S. J. Lee, S. B. Kim, S. W. Kang, S. O. Han, C. Park, and S. W. Kim, "Effect of

crude glycerol-derived inhibitors on ethanol production by *Enterobacter aerogenes*," *Bioprocess and Biosystems Engineering*, vol. 35, no. 1–2, pp. 85–92, 2012.

[112] M. Klein, S. Swinnen, J. M. Thevelein, and E. Nevoigt, "Glycerol metabolism and transport in yeast and fungi: established knowledge and ambiguities," *Environmental Microbiology*, vol. 19, no. 3, pp. 878–893, 2017.

[113] F. Remize, J.-M. Sablayrolles, and S. Dequin, "Reassessment of the influence of yeast strain and environmental factors on glycerol production in wine," *Journal of Applied Microbiology*, vol. 88, no. 3, pp. 371–378, 2000.

[114] N. Deng, H. Du, and Y. Xu, "Cooperative response of *Pichia kudriavzevii* and *Saccharomyces cerevisiae* to lactic acid stress in baijiu fermentation," *Journal of Agricultural and Food Chemistry*, vol. 68, no. 17, pp. 4903–4911, 2020.

[115] M. C. M. Tábua, W. D. Santiago, M. L. Magalhães, V. R. F. Ferreira, R. M. Brandão, M. L. Teixeira, M. P. Pedroso, A. M. de Resende Machado, D. L. Nelson, and M. das Graças Cardoso, "Identification of volatile compounds, quantification of glycerol and trace elements in distilled spirits produced in Mozambique," *Journal of Food Science and Technology*, vol. 57, no. 2, pp. 505–512, 2020.

[116] G. Du, J. Zhan, J. Li, Y. You, Y. Zhao, and W. Huang, "Effect of fermentation temperature and culture medium on glycerol and ethanol during wine fermentation," *American Journal of Enology and Viticulture*, vol. 63, no. 1, pp. 132–138, 2012.

[117] J. Wei, H. Du, H. Zhang, Y. Nie, and Y. Xu, "Mannitol and erythritol reduce the ethanol yield during Chinese *baijiu* production," *International Journal of Food Microbiology*, vol. 337, Art. no. 108933, 2021.

[118] Z. Song, H. Du, Y. Zhang, and Y. Xu, "Unraveling core functional microbiota in traditional solid-state fermentation by high-throughput amplicons and metatranscriptomics sequencing," *Frontiers in Microbiology*, vol. 8, Art. no. 1294, 2017.

[119] D. Porro, M. M. Bianchi, L. Brambilla, R. Menghini, D. Bolzani, V. Carrera, J. Lievense, C. L. Liu, B. M. Ranzi, L. Frontali, and L. Alberghina, "Replacement of a metabolic pathway for large-scale production of lactic acid from engineered yeasts," *Applied and Environmental Microbiology*, vol. 65, no. 9, pp. 4211–4215, 1999.

[120] V. Tilloy, A. Ortiz-Julien, and S. Dequin, "Reduction of ethanol yield and improvement of glycerol formation by adaptive evolution of the wine yeast *Saccharomyces cerevisiae* under hyperosmotic conditions," *Applied and Environmental Microbiology*, vol. 80, no. 8, pp. 2623–2632, 2014.

[121] D. Marquina, A. Santos, and J. M. Peinado, "Biology of killer yeasts," *International Microbiology*, vol. 5, no. 2, pp. 65–71, 2002.

[122] V. Kostik, B. Gjorgeska, B. Angelovska, and I. Kovacevska, "Determination of some volatile compounds in fruit spirits produced from grapes (*Vitis vinifera* L.) and plums (*Prunus domestica* L.) cultivars," *Science Journal of Analytical Chemistry*, vol. 2, no. 4,

pp. 41–46, 2014.

[123] B. J. Sun, J. Wu, and M. Huang, "Recent advances of flavor chemistry in Chinese liquor spirits (baijiu)," *Journal of Chinese Institute of Food Science and Technology*, vol. 15, pp. 1–8, 2015.

[124] Statista, "Vodka industry – statistics & facts," https://www.statista.com/topics/3741/vodka-industry/, 2022. [Online]. Available: https://www.statista.com/topics/3741/vodka-industry/

[125] R. J. Arnold, A. Ochoa, C. R. Kerth, R. K. Miller, and S. C. Murray, "Assessing the impact of corn variety and Texas terroir on flavor and alcohol yield in new-make bourbon whiskey," *PLOS ONE*, vol. 14, no. 8, Art. no. e0220787, 2019.

[126] J.-I. Chen, "Spirit beverage development in the Asia-China region," in *Whisky and Other Spirits (Third Edition)*, I. Russell, G. G. Stewart, and J. Kellershohn, Eds. Academic Press, 2022, pp. 41–61.

[127] X. Wu, R. Zhao, D. Wang, S. R. Bean, P. A. Seib, M. R. Tuinstra, M. Campbell, and A. O'Brien, "Effects of amylose, corn protein, and corn fiber contents on production of ethanol from starch-rich media," *Cereal Chemistry*, vol. 83, no. 5, pp. 569–575, 2006.

[128] R. Agu, T. Bringhurst, and J. Brosnan, "Production of grain whisky and ethanol from wheat, maize and other cereals," *Journal of the Institute of Brewing*, vol. 112, no. 4, pp. 314–323, 2006.

[129] S. Siyuan, L. Tong, and R. Liu, "Corn phytochemicals and their health benefits," *Food Science and Human Wellness*, vol. 7, no. 3, pp. 185–195, 2018.

[130] N. Vanbeneden, F. Gils, F. Delvaux, and F. R. Delvaux, "Formation of 4-vinyl and 4-ethyl derivatives from hydroxycinnamic acids: Occurrence of volatile phenolic flavour compounds in beer and distribution of Pad1-activity among brewing yeasts," *Food Chemistry*, vol. 107, no. 1, pp. 221–230, 2008.

[131] Association of Official Analytical Chemists, *Changes in Official Methods of Analysis.* Arlington, VA: Association of Official Analytical Chemists, 1989.

[132] ASAE, "D241.4: Density, specific gravity, and mass-moisture relationships of grain for storage," in *ASAE Standards 2000.* St. Joseph, MI: American Society of Agricultural Engineers, 2000, pp. 504–506.

[133] T. Weiss, J. Zhao, R. Hu, M. Liu, Y. Li, Y. Zheng, G. Smith, and D. Wang, "Production of distilled spirits using grain sorghum through liquid fermentation," *Journal of Agriculture and Food Research*, vol. 9, Art. no. 100314, 2022.

[134] J. D. Hunter, "Matplotlib: A 2D graphics environment," *Computing in Science & Engineering*, vol. 9, no. 3, pp. 90–95, 2007.

[135] A. Nankar, L. Grant, P. Scott, and R. C. Pratt, "Agronomic and kernel compositional traits of blue maize landraces from the Southwestern United States," *Crop Science*,

vol. 56, no. 5, pp. 2663–2674, 2016.

[136] A. Nankar, F. O. Holguin, M. P. Scott, and R. C. Pratt, "Grain and nutritional quality traits of Southwestern U.S. blue maize landraces," *Cereal Chemistry*, vol. 94, no. 6, pp. 950–955, 2017.

[137] K. Szambelan, J. Nowak, A. Szwengiel, H. Jeleń, and G. Łukaszewski, "Separate hydrolysis and fermentation and simultaneous saccharification and fermentation methods in bioethanol production and formation of volatile by-products from selected corn cultivars," *Industrial Crops and Products*, vol. 118, pp. 355–361, 2018.

[138] S. A. Watson and P. E. Ramstad, Eds., *Corn: Chemistry and Technology*. St. Paul, MN: American Association of Cereal Chemists, 1987.

[139] Australian Home Brewing, "How to use glycerine to make smoother, better spirits," https://www.australianhomebrewing.com.au/blogs/learn/use-glycerine-to-make-spirits, n.d.

[140] D. Hartanto, P. A. Handayani, A. Sutrisno, V. W. Anugrahani, A. Mustain, and I. Khoiroh, "Isopropyl alcohol purification through extractive distillation using glycerol as an entrainer: Technical performances simulation and design," *Jurnal Bahan Alam Terbarukan*, vol. 8, no. 2, pp. 133–143, 2019.

[141] J. Twidell and T. Weir, *Renewable Energy Resources*, 2nd ed. London: Routledge, 2006.

[142] S. A. Shahir, H. H. Masjuki, M. A. Kalam, A. Imran, and A. M. Ashraful, "Performance and emission assessment of diesel-biodiesel-ethanol/bioethanol blend as a fuel in diesel engines: a review," *Renewable and Sustainable Energy Reviews*, vol. 48, pp. 62–78, 2015.

[143] L. Myat and G. H. Ryu, "Effect of thermostable α-amylase injection on mechanical and physiochemical properties for saccharification of extruded corn starch," *Journal of the Science of Food and Agriculture*, vol. 94, no. 2, pp. 288–295, 2014.

[144] L. H. Lim, D. G. Macdonald, and G. A. Hill, "Hydrolysis of starch particles using immobilized barley α-amylase," *Biochemical Engineering Journal*, vol. 13, pp. 53–62, 2003.

[145] G. H. Robertson, D. W. S. Wong, C. C. Lee, K. Wagschal, M. R. Smith, and W. J. Orts, "Native or raw starch digestion: a key step in energy efficient biorefining of grain," *Journal of Agricultural and Food Chemistry*, vol. 54, no. 2, pp. 353–365, 2006.

[146] B. A. Cinelli, L. R. Castilho, D. M. G. Freire, and A. M. Castro, "A brief review on the emerging technology of ethanol production by cold hydrolysis of raw starch," *Fuel*, vol. 150, pp. 721–729, 2015.

[147] Z. Li, L. Cai, Z. Gu, and Y.-C. Shi, "Effects of granule swelling on starch saccharification by granular starch hydrolyzing enzyme," *Journal of Agricultural and Food Chemistry*, vol. 62, no. 32, pp. 8114–8119, 2014.

[148] U. Uthumporn, Y. N. Shariffa, and A. A. Karim, "Hydrolysis of native and heat-treated starches at sub-gelatinization temperature using granular starch hydrolyzing enzyme," *Applied Biochemistry and Biotechnology*, vol. 166, no. 5, pp. 1167–1182, 2012.

[149] P. Wang, V. Singh, L. Xu, D. B. Johnston, K. D. Rausch, and M. E. Tumbleson, "Comparison of enzymatic (E-mill) and conventional dry-grind corn processes using a granular starch hydrolyzing enzyme," *Cereal Chemistry*, vol. 82, no. 6, pp. 734–738, 2005.

[150] P. Wang, V. Singh, H. Xue, D. B. Johnston, K. D. Rausch, and M. E. Tumbleson, "Comparison of raw starch hydrolyzing enzyme with conventional liquefaction and saccharification enzymes in dry-grind corn processing," *Cereal Chemistry*, vol. 84, no. 1, pp. 10–14, 2007.

[151] Z. Tong, T. Tong, and Y. C. Shi, "Partial swelling of granules enables high conversion of normal maize starch to glucose catalyzed by granular starch hydrolyzing enzyme," *Industrial Crops and Products*, vol. 140, Art. no. 111626, 2019.

[152] W. Białas, A. Czerniak, and D. Szymanowska-Powałowska, "Kinetic modeling of simultaneous saccharification and fermentation of corn starch for ethanol production," *Acta Biochimica Polonica*, vol. 61, no. 1, pp. 153–162, 2014.

[153] Y. N. Shariffa, A. A. Karim, A. Fazilah, and I. S. M. Zaidul, "Enzymatic hydrolysis of granular native and mildly heat-treated tapioca and sweet potato starches at sub-gelatinization temperature," *Food Hydrocolloids*, vol. 23, no. 2, pp. 434–440, 2009.

[154] G. Bhatia, A. Juneja, D. Johnston, K. Rausch, M. E. Tumbleson, and V. Singh, "Characterization of amylose lipid complexes and their effect on the dry grind ethanol process," *Starch – Stärke*, vol. 73, no. 7–8, Art. no. 2100069, 2021.

[155] R. H. Mumm, P. D. Goldsmith, K. D. Rausch, and H. H. Stein, "Land usage attributed to corn ethanol production in the United States: sensitivity to technological advances in corn grain yield, ethanol conversion, and co-product utilization," *Biotechnology for Biofuels*, vol. 7, no. 1, Art. no. 61, 2014.

[156] K. Zhang, G. Zheng, K. Saul, Y. Jiao, Z. Xin, and D. Wang, "Evaluation of the multi-seeded (msd) mutant of sorghum for ethanol production," *Industrial Crops and Products*, vol. 97, pp. 345–353, 2017.

[157] G. Buonaiuto, A. Palmonari, F. Ghiaccio, G. Visentin, D. Cavallini, L. Campidonico, A. Formigoni, and L. M. E. Mammi, "Effects of complete replacement of corn flour with sorghum flour in dairy cows fed Parmigiano Reggiano dry hay-based ration," *Italian Journal of Animal Science*, vol. 20, no. 1, pp. 826–833, 2021.

[158] S. Liu, Z. Li, B. Yu, S. Wang, Y. Shen, and H. Cong, "Recent advances on protein separation and purification methods," *Advances in Colloid and Interface Science*, vol. 284, Art. no. 102254, 2020.

[159] S. Khalid, S. A. Hassan, A. B. Altemimi, K. Chaudhary, S. Raana, H. Javaid,

M. Naeem, Z. F. Bhat, and R. M. Aadil, "Recovery of valuable substances from food waste by ohmic heating assisted extraction – a step towards sustainable production," *Future Foods*, vol. 9, Art. no. 100365, 2024.

[160] S. Khalid, K. Chaudhary, H. Aziz, S. Amin, H. M. Sipra, S. Ansar, H. Rasheed, M. Naeem, and H. Onyeaka, "Trends in extracting protein from microalgae *Spirulina platensis*, using innovative extraction techniques: mechanisms, potentials, and limitations," *Critical Reviews in Food Science and Nutrition*, vol. 65, no. 22, pp. 4293–4309, 2024.

[161] H. Agrawal, R. Joshi, and M. Gupta, "Isolation and characterisation of enzymatic hydrolysed peptides with antioxidant activities from green tender sorghum," *LWT – Food Science and Technology*, vol. 84, pp. 608–616, 2017.

[162] S. Xu, Y. Shen, G. Chen, S. Bean, and Y. Li, "Antioxidant characteristics and identification of peptides from sorghum kafirin hydrolysates," *Journal of Food Science*, vol. 84, no. 8, pp. 2065–2076, 2019.

[163] S. Xu, Y. Shen, J. Xu, G. Qi, G. Chen, W. Wang, X. Sun, and Y. Li, "Antioxidant and anticancer effects in human hepatocarcinoma (HepG2) cells of papain-hydrolyzed sorghum kafirin hydrolysates," *Journal of Functional Foods*, vol. 58, pp. 374–382, 2019.

[164] K. G. Duodu, J. R. N. Taylor, P. S. Belton, and B. R. Hamaker, "Factors affecting sorghum protein digestibility," *Journal of Cereal Science*, vol. 38, pp. 117–131, 2003.

[165] N. J. de Mesa-Stonestreet, S. Alavi, and S. R. Bean, "Sorghum proteins: the concentration, isolation, modification, and food applications of kafirins," *Journal of Food Science*, vol. 75, no. 5, pp. R90–R104, 2010.

[166] K. G. Duodu, A. Nunes, I. Delgadillo, M. L. Parker, E. N. C. Mills, P. S. Belton, and J. R. N. Taylor, "Effect of grain structure and cooking on sorghum and maize in vitro protein digestibility," *Journal of Cereal Science*, vol. 35, pp. 161–174, 2002.

[167] AACC International, *Approved Methods of Analysis, Method 76-13.01: Total Starch Assay Procedure (Megazyme Amyloglucosidase/alpha-Amylase Method)*, 11th ed. St. Paul, MN: Cereals & Grains Association, 1999.

[168] AOAC International, *Official Methods of Analysis, Method 920.39*, 18th ed. Gaithersburg, MD: AOAC International, 2005.

[169] ——, *Official Methods of Analysis, Method 962.09*. Gaithersburg, MD: AOAC International, 2010.

[170] ——, *Official Methods of Analysis, Method 942.05*. Gaithersburg, MD: AOAC International, 1995.

[171] S. R. Bean, O. K. Chung, M. R. Tuinstra, J. F. Pedersen, and J. Erpelding, "Evaluation of the single kernel characterization system (SKCS) for measurement of sorghum grain attributes," *Cereal Chemistry*, vol. 83, no. 1, pp. 108–113, 2006.

[172] Y. Xu and D. Wang, "Integrating starchy substrate into cellulosic ethanol production to boost ethanol titers and yields," *Applied Energy*, vol. 195, pp. 196–203, 2017.

[173] H. W. Hsu, D. L. Vavak, L. Satterlee, and G. A. Miller, "A multienzyme technique for estimating protein digestibility," *Journal of Food Science*, vol. 42, no. 5, pp. 1269–1273, 1977.

[174] T. Tinus, M. Damour, V. Van Riel, and P. A. Sopade, "Particle size-starch–protein digestibility relationships in cowpea (*Vigna unguiculata*)," *Journal of Food Engineering*, vol. 113, pp. 254–264, 2012.

[175] X. Tang, Y. Shen, Y. Zhang, M. W. Schilling, and Y. Li, "Parallel comparison of functional and physicochemical properties of common pulse proteins," *LWT – Food Science and Technology*, vol. 146, Art. no. 111594, 2021.

[176] A. Chatzifragkou, O. Kosik, P. C. Prabhakumari, A. Lovegrove, R. A. Frazier, P. R. Shewry, and D. Charalampopoulos, "Biorefinery strategies for upgrading distillers' dried grains with solubles (DDGS)," *Process Biochemistry*, vol. 50, no. 12, pp. 2194–2207, 2015.

[177] A. E.-M. M. R. Afify, H. S. El-Beltagi, S. M. Abd El-Salam, and A. A. Omran, "Protein solubility, digestibility and fractionation after germination of sorghum varieties," *PLoS ONE*, vol. 7, no. 2, Art. no. e31154, 2012.

[178] T. H. Vu, S. Bean, C. F. Hsieh, and Y. C. Shi, "Changes in protein and starch digestibility in sorghum flour during heat–moisture treatments," *Journal of the Science of Food and Agriculture*, vol. 97, no. 14, pp. 4770–4779, 2017.

[179] W. Zhang, S. Liu, Y. Wang, L. Zheng, F. Liu, X. Han, and J. Wan, "A study of the in vitro protein digestibility of indica and japonica cultivars," *Food Chemistry*, vol. 122, pp. 1199–1204, 2010.

[180] I. Correia, A. Nunes, A. S. Barros, and I. Delgadillo, "Comparison of the effects induced by different processing methods on sorghum proteins," *Journal of Cereal Science*, vol. 51, pp. 146–151, 2010.

[181] R. Zhao, S. R. Bean, B. P. Ioerger, D. Wang, and D. L. Boyle, "Impact of mashing on sorghum proteins and its relationship to ethanol fermentation," *Journal of Agricultural and Food Chemistry*, vol. 56, no. 3, pp. 946–953, 2008.

[182] S. Adhikari, M. Schop, I. J. M. de Boer, and T. Huppertz, "Protein quality in perspective: a review of protein quality metrics and their applications," *Nutrients*, vol. 14, no. 5, Art. no. 947, 2022.

[183] Y. Wang, X. S. Sun, and D. Wang, "Effects of preheating treatment on thermal property and adhesion performance of soy protein isolates," *Journal of Adhesion Science and Technology*, vol. 21, no. 15, pp. 1469–1481, 2007.

[184] R. S. Walnofer, N. S. Hettiarachchy, and R. Horax, "Effects of heating on hydrophobicity, viscosity, and gelling properties of soy products," *Discovery: The*

Student Journal of Dale Bumpers College of Agricultural, Food and Life Sciences, vol. 6, pp. 38–44, 2005. [Online]. Available: https://scholarworks.uark.edu/discoverymag/vol6/iss1/9

[185] J. Semwal and M. S. Meera, "In situ thermal modification of kafirin using infrared radiations and microwaves," *Journal of the Science of Food and Agriculture*, vol. 102, no. 5, pp. 1903–1911, 2022.

[186] S. M. Zhu, S. L. Lin, H. S. Ramaswamy, Y. Yu, and Q. T. Zhang, "Enhancement of functional properties of rice bran proteins by high pressure treatment and their correlation," *Food and Bioprocess Technology*, vol. 10, no. 2, pp. 317–327, 2017.

[187] Y. Chen, S. Hong, and Y. Li, "Pea protein composition, functionality, modification, and food applications: a review," *Advances in Food and Nutrition Research*, vol. 101, pp. 71–127, 2022.

[188] J. Espinosa-Ramírez and S. O. Serna-Saldívar, "Functionality and characterization of kafirin-rich protein extracts from different whole and decorticated sorghum genotypes," *Journal of Cereal Science*, vol. 70, pp. 57–65, 2016.

[189] Y. Wang, M. Tilley, S. Bean, X. S. Sun, and D. Wang, "Comparison of methods for extracting kafirin proteins from sorghum distillers dried grains with solubles," *Journal of Agricultural and Food Chemistry*, vol. 57, no. 18, pp. 8366–8372, 2009.

[190] U. Shah, D. Dwivedi, M. Hackett, H. Al-Salami, R. P. Utikar, C. Blanchard, A. Gani, M. R. Rowles, and S. K. Johnson, "Physicochemical characterization of kafirins extracted from sorghum grain and dried distillers grain with solubles related to their biomaterial functionality," *Scientific Reports*, vol. 11, no. 1, Art. no. 15204, 2021.

[191] P. Musigakun and M. Thongngam, "Characteristics and functional properties of sorghum protein (kafirin)," *Kasetsart Journal (Natural Science)*, vol. 41, pp. 313–318, 2007.

[192] W. Buckel and R. K. Thauer, "Flavin-based electron bifurcation, ferredoxin, flavodoxin, and anaerobic respiration with protons (Ech) or NAD+ (Rnf) as electron acceptors: A historical review," *Frontiers in Microbiology*, vol. 9, Art. no. 401, 2018.

[193] H. Wang, W. Zhou, J. Gao, C. Ren, and Y. Xu, "Revealing the characteristics of glucose- and lactate-based chain elongation for caproate production by *Caproicibacterium lactatifermentans* through transcriptomic, bioenergetic, and regulatory analyses," *mSystems*, vol. 7, no. 5, Art. no. e00534-22, 2022.

[194] Y. Yin, Y. Zhang, D. B. Karakashev, J. Wang, and I. Angelidaki, "Biological caproate production by *Clostridium kluyveri* from ethanol and acetate as carbon sources," *Bioresource Technology*, vol. 241, pp. 638–644, 2017.

[195] A. Detman, D. Mielecki, A. Chojnacka, A. Salamon, M. K. Baszczyk, and A. Sikora, "Cell factories converting lactate and acetate to butyrate: *Clostridium butyricum* and microbial communities from dark fermentation bioreactors," *Microbial Cell Factories*,

vol. 18, no. 1, Art. no. 36, 2019.

[196] S. Schoberth and G. Gottschalk, "Considerations on the energy metabolism of *Clostridium kluyveri*," *Archiv für Mikrobiologie*, vol. 65, no. 4, pp. 318–328, 1969.

[197] P. Candry, T. Van Daele, K. Denis, Y. Amerlinck, S. J. Andersen, R. Ganigué, J. B. A. Arends, I. Nopens, and K. Rabaey, "A novel high-throughput method for kinetic characterisation of anaerobic bioproduction strains, applied to *Clostridium kluyveri*," *Scientific Reports*, vol. 8, no. 1, Art. no. 9724, 2018.

[198] K. N. Joblin, G. E. Naylor, and A. G. Williams, "Effect of *Methanobrevibacter smithii* on xylanolytic activity of anaerobic ruminal fungi," *Applied and Environmental Microbiology*, vol. 56, no. 8, pp. 2287–2295, 1990.

[199] S. Yu, Y. Chen, P. Huang, B. Zhang, Z. Li, L. Peng, and Y. Zhou, "Selective carbon sources influence the microbial community, metabolic pathways, and intracellular carbon storage preference of purple phototrophic bacteria culture," *Chemical Engineering Journal*, vol. 508, Art. no. 161046, 2025.

[200] K. Choi, B. S. Jeon, B.-C. Kim, M.-K. Oh, Y. Um, and B.-I. Sang, "In situ biphasic extractive fermentation for hexanoic acid production from sucrose by *Megasphaera elsdenii* NCIMB 702410," *Applied Biochemistry and Biotechnology*, vol. 171, no. 5, pp. 1094–1107, 2013.

[201] K. Pradhan and R. Hemken, "Utilization of ethanol and its effect on fatty acid patterns in ruminants," *Journal of Dairy Science*, vol. 53, no. 12, pp. 1739–1746, 1970.

[202] X. Zhu, Y. Zhou, Y. Wang, T. Wu, X. Li, D. Li, and Y. Tao, "Production of high-concentration n-caproic acid from lactate through fermentation using a newly isolated *Ruminococcaceae* bacterium CPB6," *Biotechnology for Biofuels*, vol. 10, no. 1, Art. no. 102, 2017.

[203] X. Peng, S. E. Wilken, T. S. Lankiewicz, S. P. Gilmore, J. L. Brown, J. K. Henske, C. L. Swift, A. Salamov, K. Barry, I. V. Grigoriev, M. K. Theodorou, D. L. Valentine, and M. A. O'Malley, "Genomic and functional analyses of fungal and bacterial consortia that enable lignocellulose breakdown in goat gut microbiomes," *Nature Microbiology*, vol. 6, no. 4, pp. 499–511, 2021.

[204] Y.-T. Zhang, C. Chuan, X.-T. Wang, D.-F. Xing, N.-Q. Ren, and L. Zhao, "Synergistic acetate-butyrate co-utilization enhances caproate production by *Clostridium kluyveri* CICC 24509 under high substrate loads," *Journal of Environmental Management*, vol. 394, Art. no. 127599, 2025.

[205] T. Silvetti, S. Morandi, and M. Brasca, "Growth factors affecting gas production and reduction potential of vegetative cell and spore inocula of dairy-related *Clostridium* species," *LWT*, vol. 92, pp. 32–39, 2018.

[206] M. Atasoy and Z. Cetecioglu, "Butyric acid dominant volatile fatty acids production: Bio-augmentation of mixed culture fermentation by *Clostridium butyricum*," *Journal*

of Environmental Chemical Engineering, vol. 8, no. 6, Art. no. 104496, 2020.

[207] S. Shrestha, S. Xue, and L. Raskin, "Competitive reactions during ethanol chain elongation were temporarily suppressed by increasing hydrogen partial pressure through methanogenesis inhibition," *Environmental Science & Technology*, vol. 57, no. 8, pp. 3369–3379, 2023.

[208] W. T. Scott, S. Rockx, Q. Mariën, A. Regueira, P. Candry, R. Ganigué, J. J. Koehorst, and P. J. Schaap, "Implementation of a *Clostridium luticellarii* genome-scale model for upgrading syngas fermentations," *Computational and Structural Biotechnology Journal*, vol. 27, pp. 649–660, 2025.

[209] D. P. P. Gomes, T. Santos, F. Motteran, M. T. Kato, L. Florencio, S. M. Santos, O. Menezes, and S. Gavazza, "Biological production of n-caproic acid by different anaerobic inocula: Chain elongation performance, kinetics, and changes in microbial community composition," *Biomass and Bioenergy*, vol. 200, Art. no. 108044, 2025.

[210] L. Li, C. Liu, L. Xu, H. Zhuang, J. He, Q. He, and J. Zhang, "Acclimation of anaerobic fermentation microbiome with acetate and ethanol for chain elongation and the biochemical response," *Chemosphere*, vol. 320, Art. no. 138083, 2023.

[211] C. Zhang, H. Liu, P. Wu, J. Li, and J. Zhang, "*Clostridium kluyveri* enhances caproate production by synergistically cooperating with acetogens in mixed microbial community of electro-fermentation system," *Bioresource Technology*, vol. 369, Art. no. 128436, 2023.

[212] F. Zamora, "Barrel aging; types of wood," in *Red Wine Technology*, A. Morata, Ed. Academic Press, 2019, pp. 125–147.

[213] J. M. Conner, A. Paterson, L. Birkmyre, and J. R. Piggott, "Role of organic acids in maturation of distilled spirits in oak casks," *Journal of the Institute of Brewing*, vol. 105, no. 5, pp. 287–291, 1999.

[214] J. M. Conner, A. Paterson, and J. R. Piggott, "Changes in wood extractives from oak cask staves through maturation of scotch malt whisky," *Journal of the Science of Food and Agriculture*, vol. 62, no. 2, pp. 169–174, 1993.

[215] J. Gollihue, M. Richmond, H. Wheatley, V. G. Pook, M. Nair, I. A. Kagan, and S. DeBolt, "Liberation of recalcitrant cell wall sugars from oak barrels into bourbon whiskey during aging," *Scientific Reports*, vol. 8, no. 1, Art. no. 15899, 2018.

[216] C. Xiao, L. Wang, Y.-G. Zhang, T.-Y. Tu, S.-T. Wang, C.-H. Shen, H.-W. Yuan, and X.-Z. Zhong, "A comparison of microbial communities and volatile compounds in wheat Qu from different geographic locations," *LWT*, vol. 148, Art. no. 111752, 2021.

[217] B. Öcal and A. Yüksel, "Liquefaction of oak wood using various solvents for bio-oil production," *ACS Omega*, vol. 8, no. 43, pp. 40 944–40 959, 2023.

[218] M. J. Delgado-González, M. M. Sánchez-Guillén, M. V. García-Moreno, M. C. Rodríguez-Dodero, C. García-Barroso, and D. A. Guillén-Sánchez, "Study of a

laboratory-scaled new method for the accelerated continuous ageing of wine spirits by applying ultrasound energy," *Ultrasonics Sonochemistry*, vol. 36, pp. 226–235, 2017.

[219] B. Li, "The impact of climate change on the United States whiskey industry," Plan II Honors Theses, The University of Texas at Austin, 2021.

[220] J. D. E. Jeffery and K. A. Berglund, "Extraction of wood constituents from non-conventional, small whiskey barrels," *Journal of Food Processing & Beverages*, vol. 4, no. 1, pp. 1–7, 2016.

[221] J. D. E. Jeffery, "Aging of whiskey spirits in barrels of non-traditional volume," Ph.D. dissertation, Michigan State University, 2012.

[222] M. Balcerek, K. Pielech-Przybylska, U. Dziekońska-Kubczak, P. Patelski, and E. Strąk, "Changes in chemical composition of plum distillate during maturation in the presence of oak chips under different conditions," *Food Technology and Biotechnology*, vol. 55, no. 3, pp. 333–359, 2017.

[223] G. H. Reazin, "Chemical mechanisms of whiskey maturation," *American Journal of Enology and Viticulture*, vol. 32, no. 4, pp. 283–289, 1981.

[224] M. Luo, D. Cui, J. Li, P. Zhou, C. Duan, Y. Lan, and G. Wu, "Factors in modulating the potential aromas of oak whisky barrels: Origin, toasting, and charring," *Foods*, vol. 12, no. 23, Art. no. 4266, 2023.

[225] K. Babič, L. Strojnik, A. Ćirić, and N. Ogrinc, "Optimization and validation of an HS-SPME/GC-MS method for determining volatile organic compounds in dry-cured ham," *Frontiers in Nutrition*, vol. 11, Art. no. 1342417, 2024.

[226] X. Yin, Y. Yoshizaki, S. Kurazono, M. Sugimachi, H. Takeuchi, X.-L. Han, K. Okutsu, T. Futagami, H. Tamaki, and K. Takamine, "Characterization of flavor compounds in rice-flavor baijiu, a traditional Chinese distilled liquor, compared with Japanese distilled liquors, awamori and kome-shochu," *Food Science and Technology Research*, vol. 26, no. 3, pp. 411–422, 2020.

[227] H. Wijngaard and E. Arendt, "Optimisation of a mashing program for 100% malted buckwheat," *Journal of the Institute of Brewing*, vol. 112, no. 1, pp. 57–65, 2006.

[228] A. Wanikawa, "Flavors in malt whisky: A review," *Journal of the American Society of Brewing Chemists*, vol. 78, no. 4, pp. 260–278, 2020.

[229] A. Rodríguez, E. Espinosa, J. Domínguez-Robles, R. Sánchez, I. Bascón, and A. Rosal, "Different solvents for organosolv pulping," in *Pulp and Paper Processing*. IntechOpen, 2018.

[230] N. d. T. d. Toro, F. F. Casas, J. A. Rial, M. C. P. González, H. C. Sariol, J. N. Campa, J. Yperman, D. Vandamme, and R. Carleer, "Boltzmann-based empirical model to calculate volume loss during spirit ageing," *Beverages*, vol. 5, no. 4, Art. no. 60, 2019.

[231] A. Versari, N. Natali, M. T. Russo, and A. Antonelli, "Analysis of some Italian lemon

liquors (Limoncello)," *Journal of Agricultural and Food Chemistry*, vol. 51, no. 17, pp. 4978–4983, 2003.

[232] M. Kashif, M. E. Keating, and H. J. Byrne, "Raman spectroscopic monitoring of multiproduct chemical reaction kinetics; the case of ester hydrolysis," *Analyst*, vol. 151, no. 7, pp. 2024–2036, 2026.

[233] Y.-S. Lee, E.-A. Cho, Y.-H. Cha, D.-W. Yoon, D.-H. Im, B.-G. Choi, and J.-H. Jeon, "Comparisons of flavor ingredients changes according to whisky types and maturation period," *The Korean Journal of Food and Nutrition*, vol. 24, no. 3, pp. 471–479, 2011.